เนื้อหางานวิจัย

Part I: Molecular cloning of *Penaeus monodon* Tudor staphylococcal nuclease and its involvement in RNA interference

Part II: Protein-protein interaction between *Penaeus monodon* Tudor staphylococcal nuclease and RNAi machineries; Argonaute proteins

Part III: Transcriptional profiling of *Marsupenaeus japonicus* in response to MjTSN and MjArgonaute-1 knockdown

Part IV: Identification and characterization of *Penaeus monodon* Tudor staphylococcal nuclease interacting protein, laminin receptor

Part V: Molecular cloning and characterization of *Penaeus monodon* Argonaute-3

Part I: Molecular cloning of *Penaeus monodon* Tudor staphylococcal nuclease and its involvement in RNA interference

Abstract

RNA interference (RNAi) plays an important role in an antiviral defense in shrimp. RNAi technology has been extensively used for inhibition of viral replication and studying gene function. However, the mechanism of shrimp RNAi pathway is still poorly understood. In this study, we identified and characterized an additional protein in the RNAi pathway, tudor staphylococcal nuclease from *Penaeus monodon* (PmTSN). The full-length cDNA of PmTSN is 2897 bp, with an open reading frame encoding a putative protein of 889 amino acids. Phylogenetic analysis and domain structure comparison revealed that PmTSN is more closely related to vertebrate TSN by sharing the amino acid sequence identity of 57% with TSN of zebrafish. This represents a new type of TSN proteins by exhibiting the four tandem repeat of staphylococcal nuclease-like domain (SN), followed by a Tudor and a partially truncated C-terminal SN domain. Knockdown of *PmTSN* by dsRNA targeting SN3 domain resulted in the impairment of dsRNA targeting *PmRab7* gene to silence *PmRab7* expression. In addition, the efficiency of dsRNA targeting *YHV-protease* gene inhibiting yellow head virus replication was decreased in the *PmTSN*-knockdown shrimps. Our results imply that PmTSN is involved in dsRNA-mediated gene silencing in shrimp and thus we identified the additional protein involved in shrimp RNAi pathway.

Keywords: RISC, RNAi, double-stranded RNA, black tiger shrimp

1. Introduction

Eukaryotes possess a conserved post-transcriptional gene regulation mechanism known as RNA interference (RNAi) [1-2]. In this phenomenon, small RNA duplexes including short-interfering RNA (siRNA) and micro RNA (miRNA) trigger the silencing of the target mRNA in a sequence specific manner by mRNA degradation or translational repression. The ability of RNAi to silence the expression of a specific gene is a potential tool for analyzing gene function in eukaryotes [3]. In addition, RNAi acts as an antiviral immune defense which can be considered as a new promising therapeutic modality to combat viral diseases [4].

In penaeid shrimp, RNAi technology was employed as a powerful tool for studying gene function *in vivo* [5]. In addition, double-stranded RNA (dsRNA) is a potent trigger in the RNAi pathway and can induce both sequence-dependent and sequence-independent antiviral immunity in penaeid shrimp [6]. Therefore, RNAi technology was applied to prevent or cure viral infection in shrimp [7-9]. An understanding of the molecular mechanism of RNAi and identifying the proteins involved in the shrimp RNAi pathway will be essential before using RNAi as a tool for viral protective immunity or studying gene function in this economically important species.

Very little is known about the RNAi machineries in shrimp. Recently, the key proteins of the shrimp RNAi pathway have been identified including Dicer [10-12] and Argonaute [13-15]. In addition, the Dicer-interacting protein, the TAR-RNA binding protein (TRBP) has been identified in the Chinese shrimp, *Fenneropenaeus chinensis* [16]. However, other proteins that involved in the shrimp RNAi pathway are remained unknown. A number of the associated proteins in the RNA-induced silencing complex (RISC) such as dFXR, VIG and Tudor staphylococcal nuclease were indentified in *C. elegans, Drosophila* and human [17-18], whether these RNAi machineries play important roles in the shrimp RNAi pathway remains to be elucidated. Therefore, the purpose of this study is to clone and characterize one of the RNAi machineries, Tudor staphylococcal nuclease from black tiger shrimp, *Penaeus monodon.*

Tudor staphylococcal nuclease (TSN, also known as SND1 and P100) is a highly conserved protein ranging from yeasts to humans [19]. This protein contains five staphylococcal nuclease-like (SN) domains and a Tudor domain [20]. Biochemical purification of the RISC revealed that TSN is one of the components in the silencing complex [17]. Knockdown of *tsn-1* expression impairs RNAi in *Caenorhabditis elegans*, indicating the requirement of TSN for the proper function of the RISC [17]. TSN was first identified in human as a transcriptional coactivator of Epstein-Barr virus nuclear antigen 2 (EBNA2) [21]. It interacts with several transcription factors and chromatin remodeler to enhance their activities, such as STAT5 [22], STAT6 and RNA polymerase II [23], and CREB-binding protein [24]. In addition, TSN interacts with small nuclear ribonucleoproteins (snRNP) and functions in spliceosome assembly and pre-mRNA splicing [25]. TSN was shown to bind and promote the cleavage of hyper-edited inosine-containing dsRNA [26]. Whether such diverse functions of TSN exist in shrimp remain to be elucidated.

In this study, we cloned and characterized the full-length cDNA encoding TSN from *P. monodon (PmTSN)*. We further demonstrated that RNAi knockdown of PmTSN expression diminished the efficiency of RNAi, suggesting the involvement of PmTSN in dsRNA-mediated gene silencing in shrimp.

2. Experimental Procedures

2.1. Animals

Black tiger shrimps, *Penaeus monodon* (4 - 5 g) were purchased from the commercial shrimp farms in Thailand. They were reared in the laboratory tanks with continuous aerated sea water (10 ppt) for 3 days before processing to allow acclimatization. Shrimps were fed *ab libitum* with commercial shrimp feed. Apparently healthy looking shrimp were picked and used in all experiments.

2.2. Virus stock and experimental infection

Yellow head virus (YHV) stock was kindly prepared by Dr. Witoon Tirasophon, Mahidol University. The YHV viral titer (~$3x10^9$ infectious virions ml^{-1}) was determined according to the method described by Assavalapsakul et al. [27]. The YHV stock was diluted to 10^7 fold and 50 µl of the diluted YHV stock was used to inject into shrimp [28].

2.3. RNA extraction and cDNA synthesis

The tissue samples were homogenized in TRI-REAGENT® or TRI-LS® (Molecular Research Center). Total RNA was extracted according to manufacturer's instruction. The RNA concentration was determined by NanoDrop ND-1000 spectrophotometer (Nanodrop Technologies). The absorbance ratio of A260 and A280 was 1.8 to 2.0, indicated that the RNA samples were relatively pure. Total RNA (1 µg) was used for cDNA synthesis. Reverse transcription was performed by using Improm-II™ reverse transcriptase (Promega), following the manufacturer's instruction with PRT-oligo-dT_{12} primer (Table 1).

2.4. Cloning of PmTSN cDNA

A partial *PmTSN* cDNA fragment was first amplified by RT-PCR with gene specific primers. Briefly, total RNA (5 µg) extracted from gills was primed with PRT-oligo-dT_{12} primer and reverse transcribed with SuperScript® III reverse transcriptase (Invitrogen). PCR was performed using TuF1 and TuR1 primers, following the condition: denaturation at 94°C for 5 min, followed by 30 cycles of 94°C for 30 s, 50°C for 30 s, and 72°C for 1 min. The final extension was carried out at 72°C for 7 min. The amplified fragments were purified from the gel using QIAquick gel extraction kit (Qiagen). Purified PCR products were cloned into pGEM®-T Easy vector (Promega) and subsequently subjected for DNA sequencing by First Base Co., Ltd. (Malaysia).

2.4.1. Amplification of the 5' and 3' end sequences

Rapid amplification of cDNA ends (5' and 3' RACE) were used for identifying the 5' and 3' end sequences. Primers for RACE were designed from a partial sequence of *PmTSN* cDNA fragment. For 3' RACE, PCR was performed using TuF2 primer and an adaptor primer, PM1. Subsequently, the nested PCR was performed with 3RF1 and PM1 primers. For 5' RACE, a poly-A tail was added to the 3'-end of cDNA using terminal deoxynucleotidyl transferase (TdT) (Promega) and

purified by QIAquick PCR purification kit (Qiagen). A-tailed cDNA was subsequently used for PCR with Tu5R and PRT- oligo-dT_{12} primers. The nested PCR was performed using TuN5R and PRT- oligo-dT_{12} primers. Identification of the remaining 5'end sequences was performed using 5'-Full Race Core Set (Takara) according to manufacturer's instruction. Briefly, cDNA was synthesized using 5' end-phosphorylated primer, P-5RACE and was subsequently circularized by T4 RNA ligase (Takara). Then, PCR was performed by using S1 and AS1 primers. The nested PCR was subsequently performed with S2 and AS2 primers. All primers used for cloning were ordered from Pacific Science Co., Ltd. (Thailand) and were listed in Table 1. PCR products were purified, cloned and subjected for sequencing as described above.

Table 1 Sequences for primers used in this study

Primers	Sequence (5'-3')	Purposes
PRT-oligo-dT	CCGGAATTCAAGCTTCTAGAGGATCCTTTTTTTTTTTTTTT	Reverse transcription
TuF1	GAAGCTGTGGTGGAATTTGTT	RT-PCR
TuR1	GTATTCACTCACCACAGTCTG	RT-PCR
PM1	CCGGAATTCAAGCTTCTAGAGGATCC	5' and 3'RACE
TuF2	CGGGAAGTTGAGATTGAGGTG	3'RACE
3RF1	CCAGCATTGGAACAGCTGAT	3'RACE
Tu5R	TGCTGAGGTTGAGTGCTTCCT	5'RACE
TuN5R	TCCAGATGCAACAAATTCCAC	5'RACE, Multiplex RT-PCR
P-5RACE	GACTCCTCGGATACTCTCC	Reverse transcription
S1	AGTAGAGAATTCTTGCGGAA	5'RACE
AS1	CATAAGGCTCATCCACTG	5'RACE
S2	ACTTCAACTGGTCGAGAATATG	5'RACE
AS2	GTGTTGGGTGAGACGCAG	5'RACE
CDS-F	ATGGCTGCGTCTCACCCAA	RT-PCR
CDS-R	GCTTCTCCATCAGCTGTTCC	RT-PCR
TSN-F1	GCTGCACAGTCAAGATTGGA	Multiplex RT-PCR
Actin-F	GACTCGTACGTCGGGCGACGA	Multiplex RT-PCR
Actin-R	AGCAGCGGTGGTCATCACCTG	Multiplex RT-PCR
SN3-FT7	TAATACGACTCACTATAGGCTGGCAAGGTCATAGAAGTCG	Preparation of dsRNA
SN3-R	CACGCTGGTCATCATCTTGT	Preparation of dsRNA
SN3-F	CTGGCAAGGTCATAGAAGTCG	Preparation of dsRNA
SN3-RT7	TAATACGACTCACTATAGGCACGCTGGTCATCATCTTGT	Preparation of dsRNA
qTSN-F3	TAAGCCCTCTGGTCCTAAGATTGC	Real-time PCR
qTSN-R3	CTCTGGTAGCCTGGGTGGTCTTAT	Real-time PCR
qRab7-F2	CTGGAGAATAGGGCGGTATCAACG	Real-time PCR
qRab7-R2	CGAGCAATGGTCTGGAAGGCTAAC	Real-time PCR
EF1a-F	GAACTGCTGACCAAGATCGACAGG	Real-time PCR
EF1a-R	GAGCATACTGTTGGAAGGTCTCCA	Real-time PCR
YHV-helF	CAAGGACCACCTGGTACCGGTAAGAC	Multiplex RT-PCR
YHV-helR	GCGGAAACGACTGACGGCTACATTCAC	Multiplex RT-PCR

2.4.2. Amplification of the full-length coding sequences of PmTSN

To amplify the coding region of *PmTSN* cDNA, RT-PCR was performed using VENT® DNA polymerase (New Englang Biolabs) with CDS-F and CDS-R primers, following the condition: denaturation at 95°C for 3 min, followed by 30 cycles of 95°C for 30 s, 55°C for 30 s, and 72°C for 3 min. The final extension was carried out at 72°C for 7 min. PCR product was purified, cloned and subjected for sequencing as described above.

2.5. Sequence and phylogenetic analysis

The nucleotide and deduced amino acid sequences of *PmTSN* were compared with other known TSN sequences available in the GenBank database using BLAST search program [29]. The protein domain features of PmTSN were predicted by using ScanProsite [30] and Conserved Domain Architecture Retrieval Tool (CDART) [31]. Molecular weight and isoelectric point of the protein were predicted by tools in the Expasy website (www.expasy.org). For multiple sequence alignment and phylogenetic analysis, TSN sequences from several species were retrieved from the GenBank database. Multiple sequence alignment was performed by using ClustalW [32] and phylogenetic analysis was performed by using MEGA 4.1 program [33] based on the neighbor-joining methods [34]. Bootstrap values of 1000 replicates were calculated for each node of the consensus tree.

2.6. Tissue distribution study

Multiplex RT-PCR was employed to study the expression of *PmTSN* in various shrimp tissues. hemolymph, gill, lymphoid organ, hepatopancreas, stomach, testis, abdominal muscle, pleopods and thoracic ganglia were dissected out from male brood stock shrimps. Total RNA from different tissues were extracted and reverse transcribed to cDNA. To determine the expression of *PmTSN*, multiplex RT-PCR was performed. The *PmTSN* primers were TSN-F1 and TuN5R, and the *β-actin* primers were Actin-F and Actin-R (Table 1). The multiplex PCR was performed under the following condition: denaturation at 94°C for 5 min, followed by 5 cycles of 94°C for 30 s, 59°C for 30 s (-1°C/cycle) and 72°C for 40 s, and 23 cycles of 94°C for 30 s, 54°C for 30 s, and 72°C for 40 s. The final extension was carried out at 72°C for 7 min. PCR products were analyzed on 1.2% agarose gel electrophoresis, stained with ethidium bromide and visualized under ultraviolet light.

2.7. Preparation of double-stranded RNA (dsRNA)

The dsRNA specific to SN3-like domain of *PmTSN* (dsSN3) was synthesized by *in vitro* transcription using RiboMAX® Large Scale RNA Production System (Promega) following the manufacturer's protocol. Briefly, sense and anti-sense DNA template strands were synthesized by PCR with the primers that contained T7 promoter sequences (Table 1) using VENT® DNA polymerase (New England Biolabs). Five micrograms of each purified PCR product was used for *in vitro* transcription. After the reaction, DNA template was removed by incubating with RQ1 DNase (Promega) (1 unit per μg of DNA template) at 37°C for 15 min. The *in vitro* transcribed RNA product was annealed to produce dsRNA by incubating at 95°C for 2 min. The temperature was decreased to 25°C at the rate of 0.1°C s^{-1} and hold at 25°C for 30 min. The left-over single-stranded RNA (ssRNA) was degraded by adding 10 ng of Ribonuclease A (RNase A) (New Englang Biolabs) and incubated at 37°C for 10 min. dsSN3 was further purified by TRI-LS® (Molecular Research Center) according to manufacturer's protocol.

The dsRNA specific to *PmRab7*, *gfp* and *YHV-protease* (dsRab7, dsGFP and dsYHV) were produced by *in vivo* bacterial expression [35]. The quality of dsRNAs was determined by ribonuclease digestion assay using RNase A and RNase III (New England Biolabs).

2.8. Knockdown of PmTSN expression

To knockdown *PmTSN* transcript, shrimps (size 4-5 g, 6 shrimps per group) were intramuscularly injected with 5 μg g^{-1} shrimp of dsSN3. Shrimps injected with dsGFP were used as a control group. To determine the earliest time point for complete *PmTSN* knockdown, hemolymph was individually collected at 0, 1, 3, 5 and 7 days post injection. To examine the expression of *PmTSN*, multiplex RT-PCR was performed as described above. The PCR products were analyzed on 1.5% agarose gel electrophoresis, stained with ethidium bromide and visualized under ultraviolet light. The intensity of each band was quantified by Scion image analysis program. The relative expression level of *PmTSN* was normalized against *β-actin* and expressed in arbitrary units.

2.9. Functional assay of PmTSN in dsRNA-mediated gene silencing

Shrimps (size 4-5 g, 6 shrimp per group) were intramuscularly injected with dsSN3 or dsGFP (5 μg g^{-1} shrimp) for 48 h prior to injecting with dsRab7 (0.63 μg g^{-1} shrimp). Hemolymph was individually collected at 48 h post dsRab7 injection. Shrimps injected with 150 mM NaCl or dsRab7 alone were used as control groups. Total RNA (1 μg) was used for cDNA synthesis. The expression of *PmTSN* and *PmRab7* was determined by quantitative real-time PCR (qRT-PCR) analysis.

qRT-PCR was performed in an ABI 7500 real-time detection system (Applied Biosystems) using KAPA™ SYBR® FAST master mix (2X) ABI Prism™ (KAPA Biosystems). The primers for *PmTSN* were qRTSN-F3and qRTSN-R3, and the primers for *PmRab7* were qRab7-F2 and qRab7-R2. The primers for an internal control gene, *EF1-α* were EF1a-F and EF1a-R. All primers used for qRT-PCR are listed in Table 1. qRT-PCR was carried out in triplicates for each sample in a 20-μl reaction containing 10 μl of 2X KAPA™ SYBR® FAST master mix, 5 μl of 1:50 diluted cDNA, 0.25 μl of 10 μM of each primer and 4.5 μl of sterile water. PCR amplification was performed under the following conditions: enzyme activation at 95°C for 3 min, followed by 40 cycles of 95°C for 3 s and 60°C for 31 s. The specificity of primers was determined by melting curve analysis from the ABI Prism 7500 detection system. The cycle threshold (Ct) value for the *PmTSN* and *PmRab7* target genes and the internal control *EF1-α* gene were determined for each sample. The expression levels of *PmTSN* and *PmRab7* in each treatment group relative to NaCl-injected group were then determined by comparative Ct method ($2^{-\Delta\Delta Ct}$) [36].

2.10. Cumulative mortality assay

Shrimps (size 4-5 g, 9 – 15 shrimp per group) were injected with 5 μg g^{-1} shrimp of dsSN3, dsGFP or 150 mM NaCl for 48 h prior to injecting with a mixture of dsYHV (2.5 μg g^{-1} shrimp) and 50 μl of the 10^7 fold diluted YHV stock. Shrimps injected with 150 mM NaCl or YHV alone were used as control groups. Shrimp mortality was recorded twice a day for 10 days after the second injection. Expression of YHV was detected from gill tissues of death shrimps by using multiplex RT-PCR [37]. Only the death shrimp that can be detected YHV expression was used to calculate the cumulative percent mortality.

2.11. Statistical analysis

The data were expressed as mean ± standard error (SEM). The statistical analysis of the mean ± SEM was performed by using ANOVA in the Sigma Stat 3.5 program. A measurement of $P<0.05$ was accepted as statistically significant.

3. Results

3.1. Cloning and sequence analysis of P. monodon Tudor staphylococcal nuclease

The full-length cDNA encoding TSN from *P. monodon* (*PmTSN*) was cloned by PCR approach. A 1043-bp fragment of *PmTSN* corresponding to SN4 and Tudor domains was obtained by RT-PCR with TuF1 and TuR1 primers. A BLAST search of the nucleotide and deduced amino acid sequences revealed that the product shared high sequence similarity with TSN from other species. This partial sequence was used to design gene specific primers to clone the 3′ and 5′ ends of this gene by RACE. Amplification of the full-length *PmTSN* coding region was used to confirm the sequence. The full-length of *PmTSN* cDNA consisted of 2897 bp, containing 44 bp in the 5'untranslated region (UTR), 2670 bp in an open reading frame (ORF), and 183 bp in the 3'UTR with a poly A-tail (Fig. 1). The translation initiation sequence (nucleotides 42-47, CAAC*ATG*G) was in an agreement with the Kozak's consensus sequence. In addition, atypical polyadenylation signal (AATTAAA) was found to reside 10 bp upstream of the poly (A) tail. The nucleotide sequence of *PmTSN* cDNA was submitted in the GenBank database under the accession number EF_429696.

The ORF of *PmTSN* encoded a polypeptide of 889 amino acids with an estimated molecular weight of 99.7 kDa and a predicted isoelectric point of 8. The deduced amino acid sequence of *PmTSN* was compared to TSN sequences from other known species. Sequence alignment showed that PmTSN had higher identities (54-57%) to vertebrate TSN. Among these, PmTSN showed the highest (57%) amino acid sequence identity to TSN of *D. rerio* (GenBank ID: NP_878285). In addition, PmTSN showed 50%, 51% and 54% amino acid sequence identities with TSN of *C. elegans* (GenBank ID: NP_494839), *A. gambiae* (GenBank ID: XP_315689) and *D. melanogaster* (GenBank ID: NP_612021), respectively, while it exhibited lower identities of 29-34% with plants, fungi and slime mold.

Phylogenetic analysis based on a bootstrapped NJ tree indicated that TSN proteins could be divided into four clusters, including vertebrates, other invertebrates, plants, and fungi (Fig. 2). Interestingly, PmTSN clustered on a separated branch from vertebrate and other invertebrate clusters. Similar tree was obtained from the analysis based on Maximum Parsimony method (data not shown). In addition, the domain structures of TSN proteins from shrimp and several organisms including *H. sapiens* (GenBank ID: NP_055205), *C. elegans*, *D. melanogaster*, *A. thaliana* (GenBank ID: NP_200986), *A. fumigatus* (GenBank ID: XP_753714), and *S. pombe* (GenBank ID: NP_588117) were compared (Fig. 3). PmTSN contained four SN domains at the N-terminus, followed by a Tudor and a partially truncated SN domain. A severely truncated SN5 domain was found in TSN of *H. sapiens*, whereas a SN5 domain of TSN of *C. elegans* and *D. melanogaster* overlapped with a Tudor domain. A SN5 domain was totally absent in TSN of *S. pombe*. In addition, a partially truncated SN5 domain was also found in TSN of *A. thaliana* and *A. fumigatus*, but distinct from PmTSN in term of amino acid sequence identities (26% identities, supplementary Table 1).

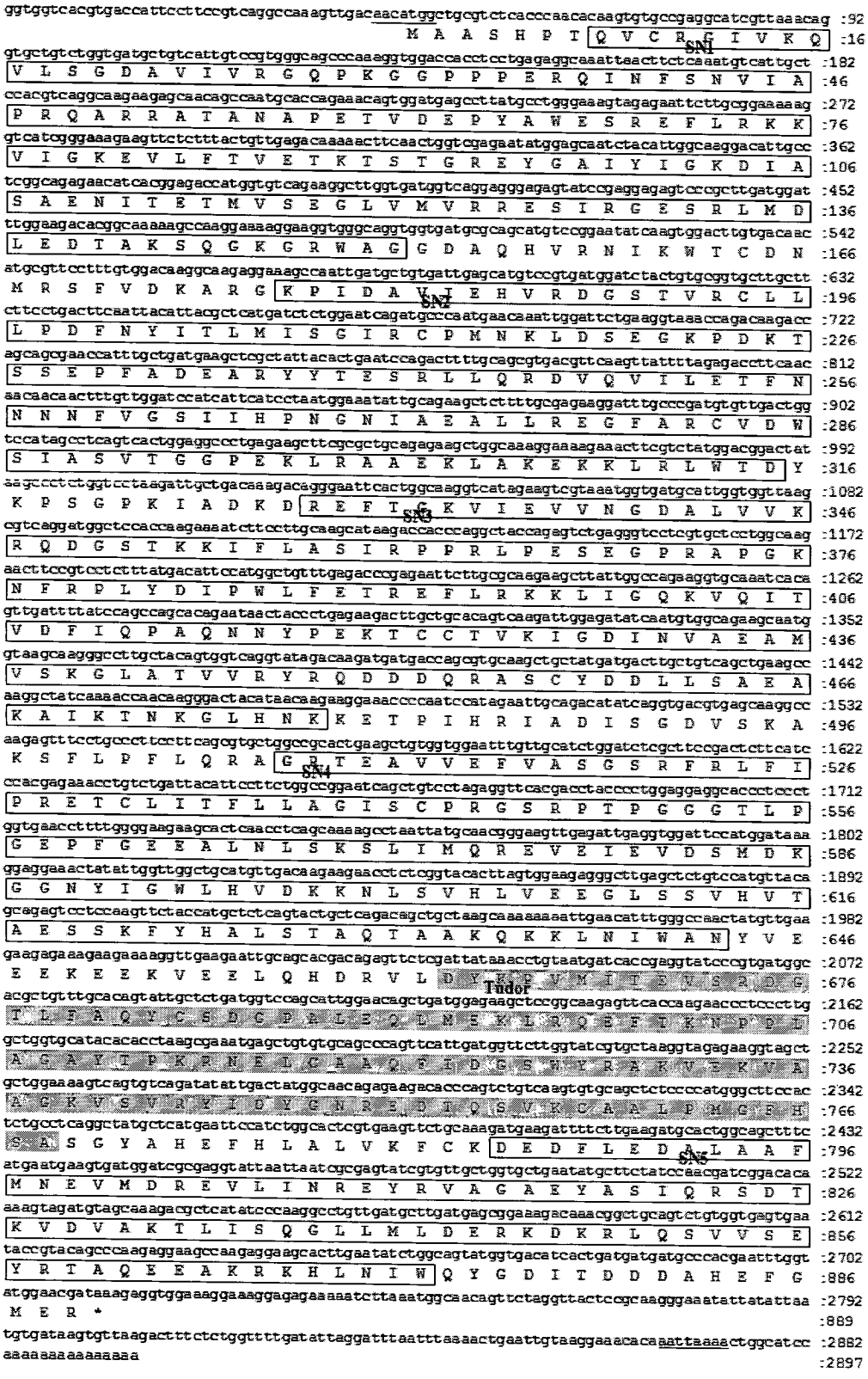

Fig. 1 The nucleotide and deduced amino acid sequences of *PmTSN* cDNA. Kozak's sequence and polyadenylation signal are underlined. The deduced amino acid sequence of *PmTSN* is shown in a single letter under the respective codon. Staphylococcal nuclease-like domains (SN) are boxed and a Tudor domain is shaded. The asterisk represents the stop codon. This nucleotide sequence is available in the GenBank database under the accession number EF_429696.

A

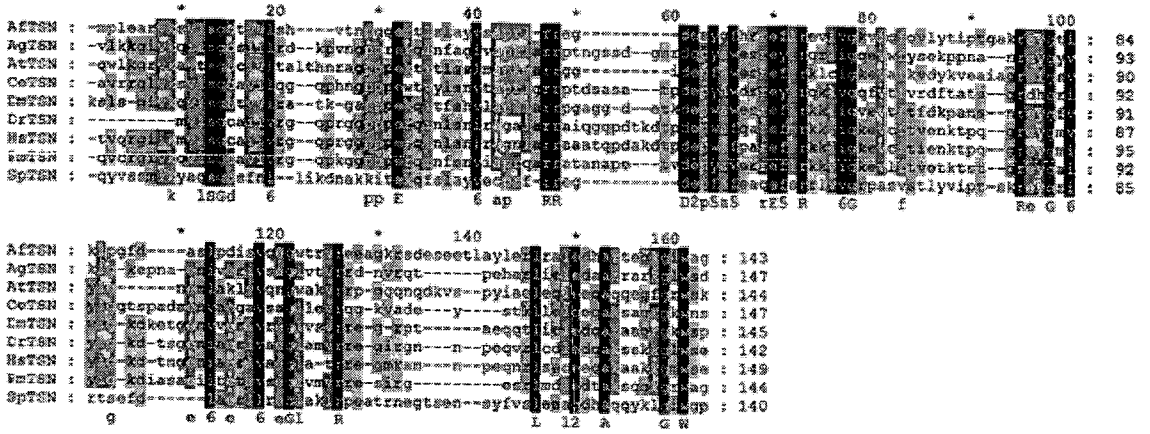

B

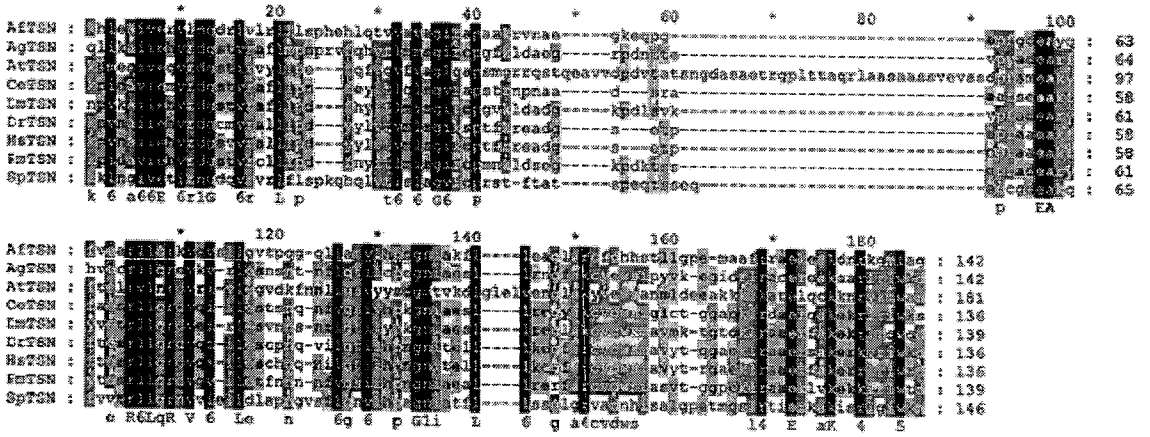

C

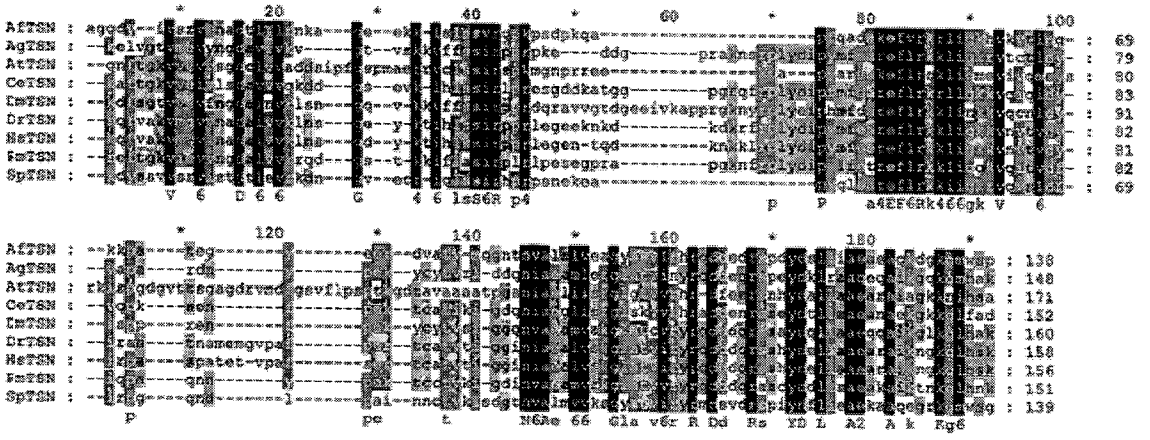

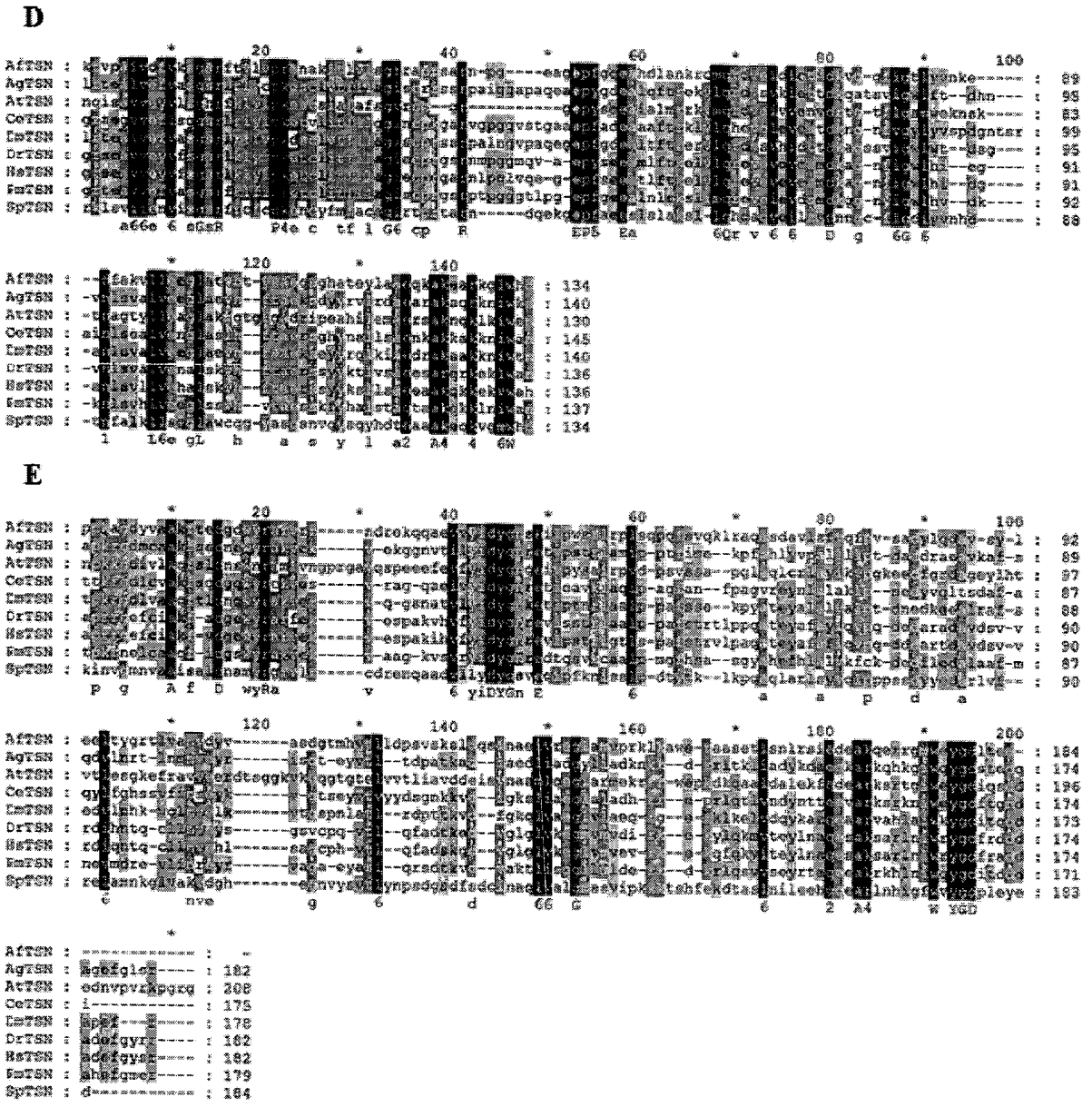

Supplementary Fig. 1 Multiple sequence alignments of the conserved domains in TSN protein of *P. monodon* with that of other species. *P. monodon* (PmTSN, GenBank ID: JF_429696); *A. fumigatus* (AfTSN, GenBank ID: XP_753714); *A. gambiae* (AgTSN, GenBank ID: XP_315689); *A. thailiana* (AtTSN, GenBank ID: NP_200986); *C. elegans* (CeTSN, GenBank ID: NP_494839); *D. melanogaster* (DmTSN, GenBank ID: NP_612021), *D. rerio* (DrTSN, GenBank ID: NP_878285); *H. sapiens* (HsTSN, GenBank ID: NP_0055205); *S. pombe* (SpTSN, GenBank ID: NP_588117). Identical amino acids are shown in black and similar amino acids are shown in dark grey. Panels: A, SN1 domain; B, SN2 domain; C, SN3 domain; D, SN4 domain; E, Tudor and SN5 domain.

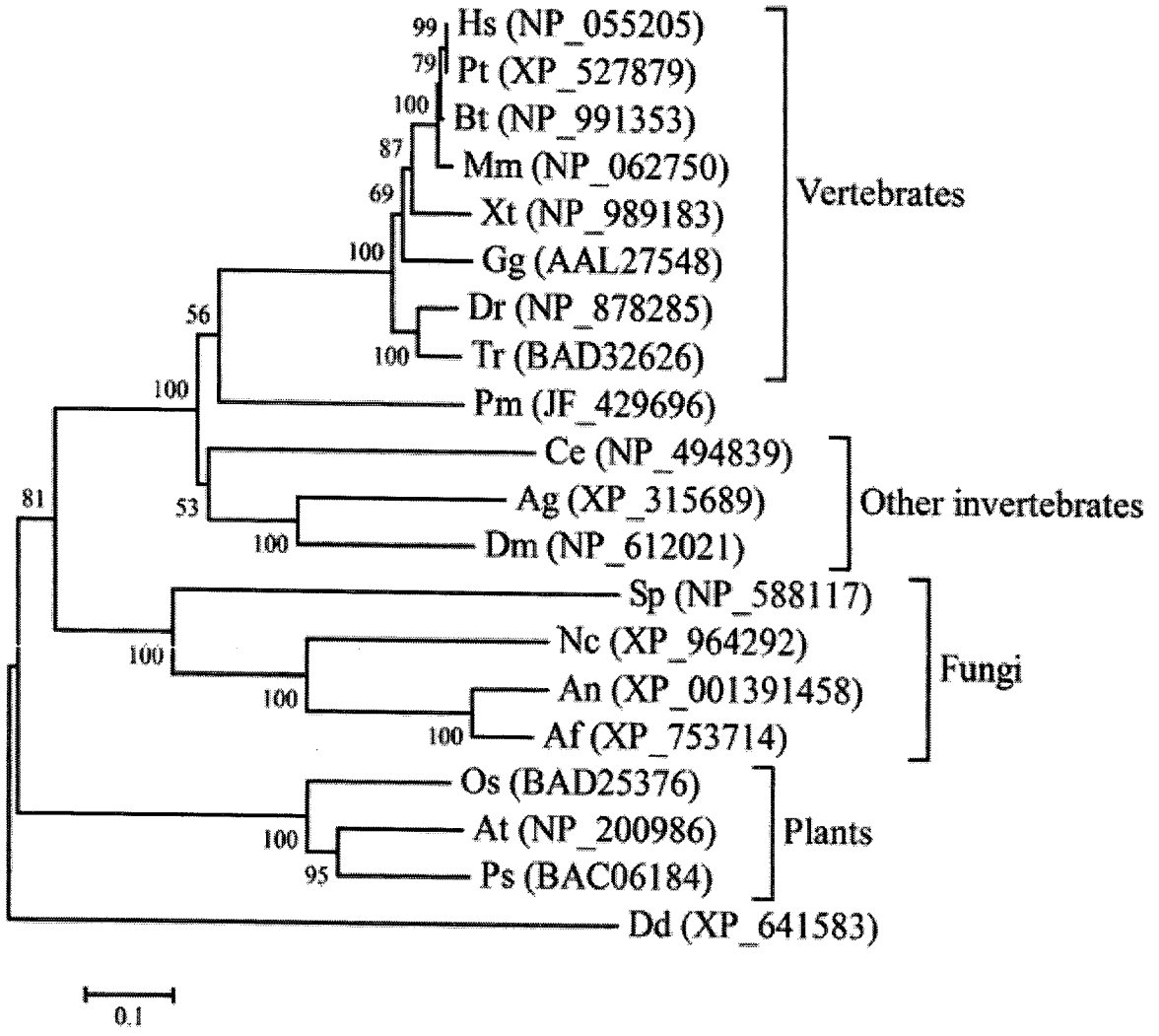

Fig. 2 Phylogenetic relationship of TSN on the basis of amino acid sequence using neighbor-joining distance analysis. *Hs, Homo sapiens*; *Pt, Pan troglodytes*; *Bt, Bos Taurus*; *Mm, Mus musulus*; *Gg, Gallus gallus*; *Xt, Xenopus tropicalis*; *Dr, Danio rerio*; *Tr, Takifugu rupripes*; *Pm, Penaeus monodon*; *Ce, Caenorhabditis elegans*; *Dm, Drosophila melanogaster*; *Ag, Anopheles gambiae*; *Os, Oryza sativa*; *At, Arabidopsis thaliana*; *Ps, Pisum sativum*; *Sp, Schizosaccharomyces pombe*; *Nc, Neurospora crassa*; *An, Aspergillus niger*; *Af, Aspergillus fumigatus* and *Dd, Dictyostelium discoideum.* The GenBank accession number of TSN from each species was shown in the parenthesis. Bootstrap values from 1000 replicates are indicated at the nodes.

Supplementary Table 1 Percent amino acid sequence identity comparing between conserved domains of PmTSN with that of other species.

Species	% Amino acid sequence identity					
	Full-length	SN1	SN2	SN3	SN4	Tudor-SN5
A. fumigatus (XP_753714)	34	40	33	38	41	26
S. pombe (NP_588117)	29	29	32	40	37	19
A. thaliana (NP_200986)	34	45	34	37	42	26
C. elegans (NP_494839)	50	50	60	56	55	41
A. gambiae (XP_315689)	51	53	59	56	54	44
D. melanogaster (NP_612021)	54	50	67	59	57	46
D. rerio (NP_878285)	57	64	67	59	57	46
H. sapiens (NP_0055205)	55	60	62	61	64	42

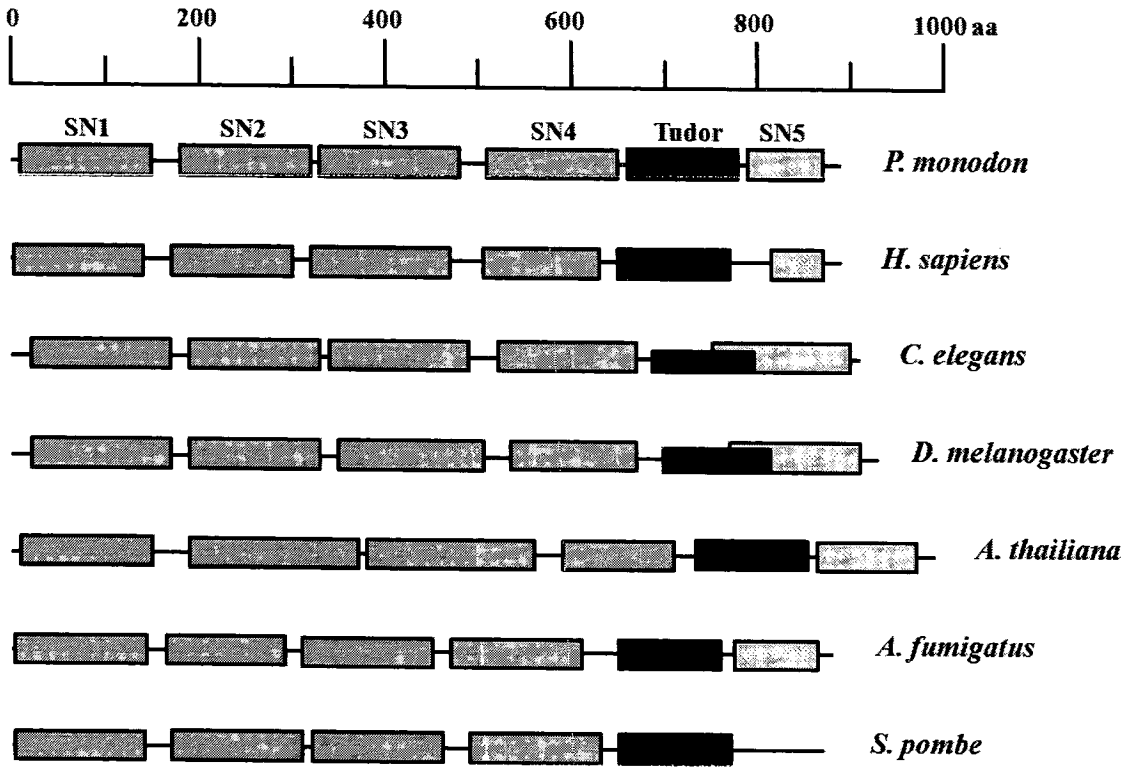

Fig. 3 Schematic diagram representation of the predicted domain structure of PmTSN (GenBank ID: JF_429696) and comparison with the predicted structure of TSN proteins of *H. sapiens* (GenBank ID: NP_0055205); *C. elegans* (GenBank ID: NP_494839); *D. melanogaster* (GenBank ID: NP_612021); *A. thaliana* (GenBank ID: NP_200986); *A. fumigatus* (GenBank ID: XP_753714) and *S. pombe* (GenBank ID: NP_588117). The locations of six functional domains are indicated: SN, staphylococcal nuclease-like domain; Tudor, Tudor domain.

3.2. Tissue distribution study

The expression of *PmTSN* in various tissues of shrimp was determined by multiplex RT-PCR. The result in Fig. 4 revealed that *PmTSN* was ubiquitously expressed in all examined tissues including hemolymph, lymphoid, gill, thoracic ganglia, testis, stomach, hepatopancreas, abdominal muscle and pleopod.

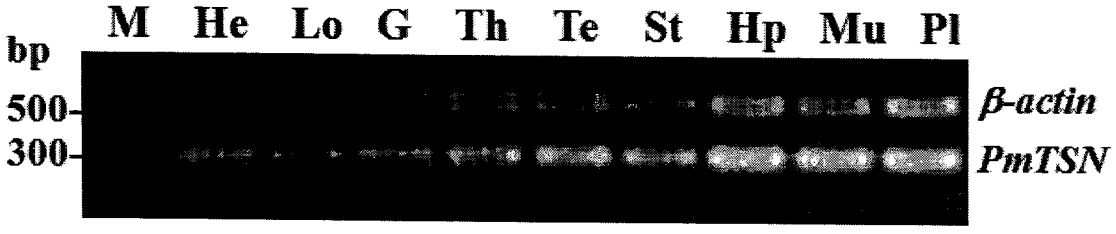

Fig. 4 Tissue distribution study of *PmTSN* expression in *P. monodon*. A representative gel represents RT-PCR products of *PmTSN* and *β-actin*. M, 1kb+DNA ladder; He, hemolymph; Lo, lymphoid organ; G, gill; Th, thoracic ganglia; Te, testis; St, stomach; Hp, hepatopancreas; Mu, abdominal muscle; and Pl, pleopods.

3.3. *Knockdown of PmTSN in vivo using dsRNA*

The dsRNA targeting the SN3 domain of *PmTSN* (dsSN3) was used to knockdown the expression of *PmTSN in vivo* (Fig. 5A). Shrimps were intramuscularly injected with 5 μg g^{-1} shrimp of dsSN3. Shrimps injected with dsGFP (5 μg g^{-1} shrimp) were used as a control group. The knockdown effect of dsSN3 on *PmTSN* expression was shown in Fig. 5B and 5C. Injection of dsSN3 significantly decreased ($P < 0.05$) the *PmTSN* transcript approximately 86% at 1 day post dsSN3 injection. The knockdown effect of *PmTSN* persisted at least 7 days. However, injection of dsGFP, an unrelated dsRNA had no effect on the level of *PmTSN* transcript. This result suggested the sequence-specific inhibition of *PmTSN* by dsSN3.

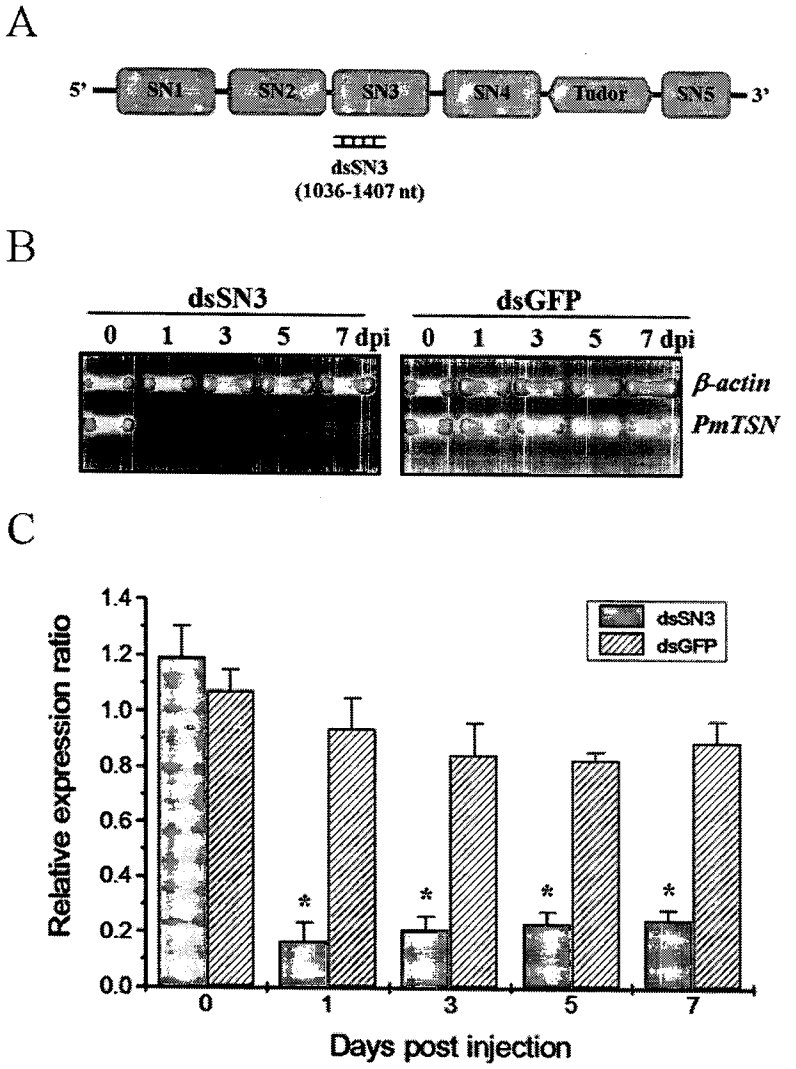

Fig. 5 RNAi knockdown of *PmTSN* transcript in *P. monodon* hemolymph. (A) Schematic diagram representation of *PmTSN* and the target region of dsSN3. (B) A representative gel of RT-PCR products showing *PmTSN* expression at 0, 1, 3, 5 and 7 days post dsSN3 or dsGFP injection. *β-actin* was used as an internal control. (C) Relative expression of *PmTSN* normalized with *β-actin*. Bars represent mean ± SEM ($n = 6$). The asterisks represent the significant difference ($P < 0.05$) between before and 1, 3, 5 or 7 days after dsRNA injection.

3.4. The effect of PmTSN knockdown on dsRNA-mediated gene silencing in shrimp

To examine the involvement of *PmTSN* in the shrimp RNAi pathway, dsRNA-mediated gene silencing approach was used to knock down the expression of *PmTSN in vivo*. Subsequently, the ability of dsRab7 in inhibition of *PmRab7* expression was determined. The knockdown effect of *PmTSN* and *PmRab7* were determined by qRT-PCR. The representative amplification plots of *PmTSN*, *PmRab7* and *EF-1α* were shown in Supplementary Fig. 2. The result in Fig. 6 showed that similar reduction of *PmRab7* transcript at 85.5% and 85% was observed in shrimps injected with dsRab7 alone (NaCl→dsRab7) and with dsGFP followed by dsRab7 (dsGFP→dsRab7), respectively. In contrast, only 68.3% reduction of *PmRab7* transcript was observed in *PmTSN*-knockdown shrimps (85.6% knockdown of *PmTSN*). The results showed a significant increase of the *PmRab7* transcript ($P < 0.05$) in *PmTSN*-knockdown shrimps when compared to the NaCl→dsRab7 and dsGFP→dsRab7 groups which had normal transcript levels of PmTSN. This result indicated that the ability of dsRab7 to knock down *PmRab7* was partially diminished in *PmTSN*-knockdown shrimp.

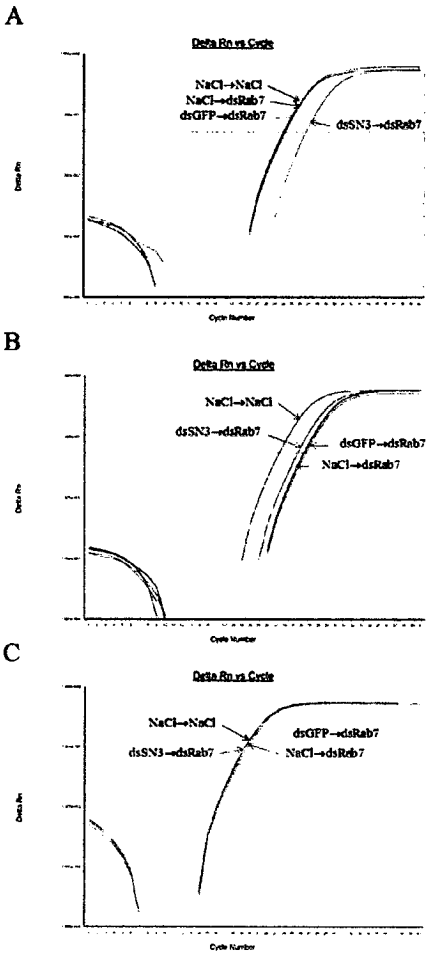

Supplementary Fig. 2 Efficiency of RNAi in *PmTSN*-knockdown shrimp. Quantitative real-time PCR was performed with specific primers for *PmTSN* and *PmRab7*. *EF1-α* was used as an internal control for normalization. The representative amplification plots of *PmTSN* (A), *PmRab7* (B) and *EF-1α* (C) are shown.

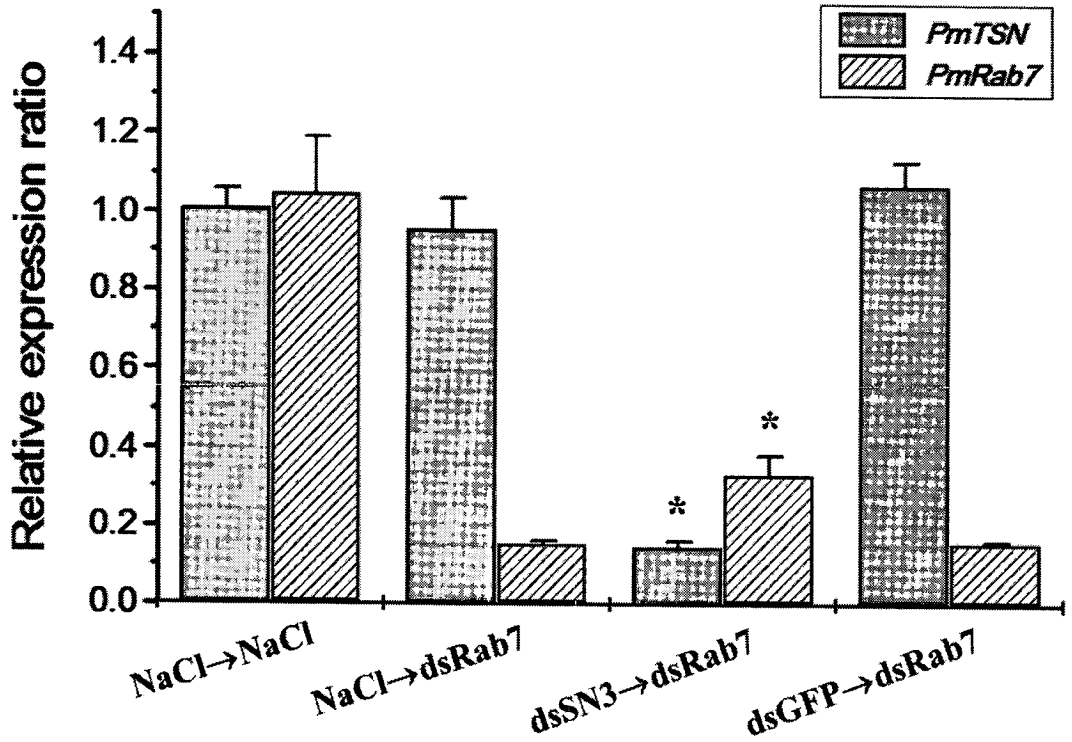

Fig. 6 Efficiency of RNAi in *PmTSN*-knocked down shrimp. Quantitative real-time PCR was performed with specific primers for *PmTSN* and *PmRab7*. *EF1-α* was used as an internal control for normalization. The relative expression of *PmTSN* and *PmRab7* was calculated by comparative Ct method ($2^{-\Delta\Delta Ct}$). Bars represent means ± SEM ($n = 6$). The asterisks (*) represent the significant difference ($P < 0.05$) of the relative *PmTSN* and *PmRab7* expression among dsSN3→dsRab7 group and other groups.

3.5. Cumulative mortality assay

To further examine the involvement of PmTSN in the shrimp RNAi pathway, the effect of *PmTSN* knockdown on the ability of dsYHV in inhibition of YHV replication was determined by cumulative mortality assay (Fig. 7). The *PmTSN*-knockdown shrimp (dsSN3→dsYHV+YHV) had a cumulative mortality of 35% at 10 days post YHV challenge, whilst the mortalities of shrimps in the NaCl→dsYHV+YHV and dsGFP→dsYHV+YHV groups was 12% and 9%, respectively. The significant increase in shrimp mortality ($P < 0.05$) was observed in the *PmTSN*-knockdown shrimps. The multiplex RT-PCR analysis of *PmTSN* expression in survival shrimps showed that the knockdown effect was still observed in *PmTSN*-knockdown shrimps (Supplementary Fig. 3).

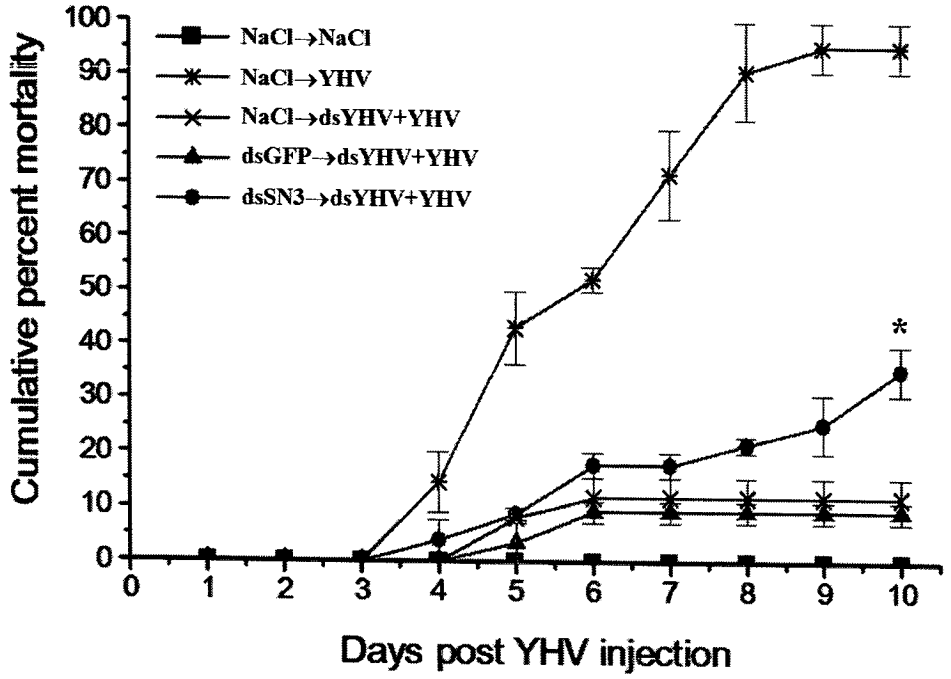

Fig. 7 Increase in cumulative mortality upon YHV challenge in *PmTSN*-knocked down shrimp. Cumulative percent mortality in each treatment group (9-15 shrimps/group) is presented as means ± SEM. Two independent experiments were performed. An asterisk (*) represents the significant difference ($P > 0.05$) among *PmTSN*-knocked down shrimp (dsSN3→dsYHV+YHV) and other groups.

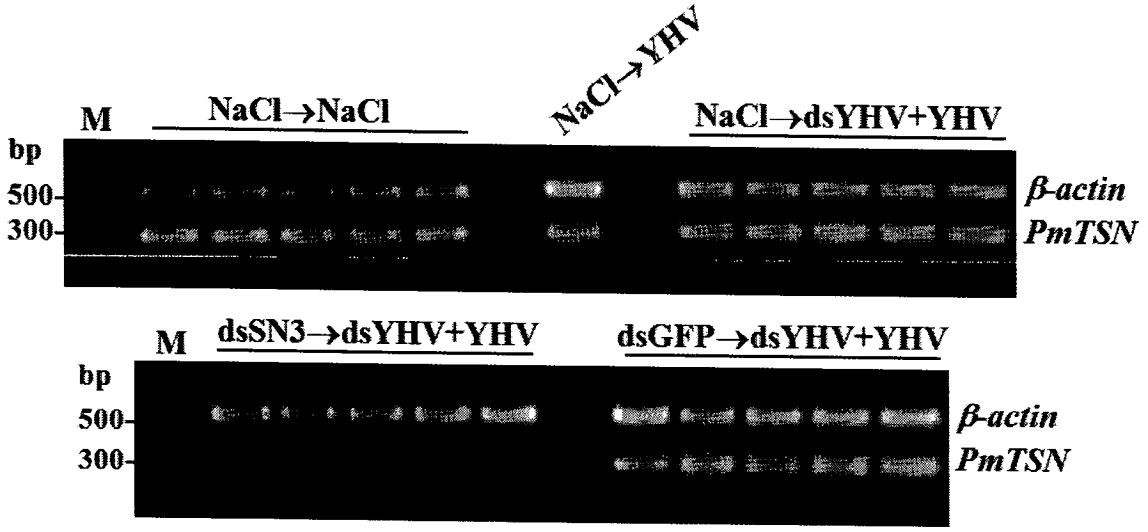

Supplementary Fig. 3 The expression of *PmTSN* in survival shrimps from cumulative mortality assay. Gills were collected from survival shrimps at 10 days-post YHV injection. Each lane shows representative RT-PCR products of *PmTSN* and *β-actin*. The PCR products was resolved by using 1.5% agarose gel electrophoresis and visualized by ethidium bromide staining. M is 1 kb+DNA ladder.

4. Discussion

In this study, we have cloned and characterized a Tudor staphylococcal nuclease (TSN) gene from black tiger shrimp, *P. monodon*. To our knowledge, this is the first report of TSN in crustacean. The full-length cDNA of *PmTSN* is 2897 bp, encoding a protein of 889 amino acids with a predicted molecular weight of 99.7 kDa. Analysis of the deduced amino acid sequence of *PmTSN* revealed that the PmTSN showed the domain organization similar to that seen in other organisms by exhibiting the four tandem repeats of SN domains followed by a Tudor and SN5 domain. Based on phylogenetic analysis and the characteristics of SN5 domain, TSN could be divided into five categories [38]. Our analysis showed that PmTSN contains a partially truncated SN5 domain, but distinct from higher plant and fungal types in term of amino acid sequence similarities. Interestingly, phylogenetic analysis revealed that PmTSN was more closely related to vertebrate TSN by sharing the highest sequence identity of 57% with TSN of *D. rerio*, and PmTSN clustered on a separated branch from vertebrate and other invertebrate clusters on the bootstrapped NJ tree. From these results, we proposed that PmTSN represents a new type of TSN, a crustacean type. Further identification of the crustacean TSN will provide a better understanding of the evolutionary relatedness of this protein. Tissue distribution study revealed the expression of *PmTSN* in all examined tissues with the similar level of transcript. Given the fact that TSN involves in a variety of cellular processes, a ubiquitous distribution of *PmTSN* indicated that this protein may involve in one or more cellular processes common to all cell types in shrimp. In human, TSN exists in a wide range of organs and tissues, especially in epithelial cells [39].

In this study, knockdown of *PmTSN* diminished the efficiency of dsRNA-mediated gene silencing in shrimp. A partially impaired *PmRab7* silencing was observed in *PmTSN*-knockdown shrimps. However, it was not observed in shrimps injected with NaCl and dsGFP, suggesting the involvement of PmTSN in dsRNA-mediated gene silencing. In *C. elegans*, knockdown of *tsn-1* expression was also found to impair the efficiency of RNAi [17]. In shrimp, knockdown of the core RNAi machinery, *Pem-ago1* led to the impairment of RNAi to silence the endogenous gene in primary lymphoid cell culture [13]. In this study, we also found that knockdown of *PmTSN* resulted in a decrease of the ability of dsYHV in inhibition of YHV replication. An increase of the cumulative percent mortaliy was observed
The multiplex RT-PCR analysis of *PmTSN* expression in the survival shrimps showed that the knockdown effect is still observed in shrimps injected with dsSN3. Previous study reported that knockdown of PmDicer (*PmDcr-1)* enhanced the susceptibility of gill-associated virus infection [11]. In our study, knockdown of *PmTSN* did not increase the susceptibility of shrimp to YHV infection. The level of *PmTSN* transcript in hemolymph did not change significantly after YHV challenge (data not shown). This indicated that the decrease of the ability of dsYHV is the result of *PmTSN* knockdown. These results suggested that PmTSN involved in dsRNA-mediated gene silencing in shrimp.

Silencing of RNAi components resulted in a general loss of RNAi mechanism [40]. In *D. melanogaster*, *r2d2* and *loqs* mutants showed impaired silencing triggered by injection of exogenous dsRNA or by artificial and natural expression of endogenous dsRNA [41]. Knockdown of MOV10, a putative DExD-box helicase and TNRC6B, a marker of mRNA-degrading cytoplasmic processing bodies (P-bodies) resulted in failure of miRNA-guide mRNA cleavage in HeLa cells [42]. However, knockdown of some additional components which play a minor role in RNAi, such as dFXR and VIG

were found to partially diminish RNAi activity in *Drosophila* [18]. It is noteworthy that knockdown of *PmTSN* expression did not substantially reduce the efficiency of dsRNA-mediated gene silencing in shrimp. We speculate that PmTSN may function as a minor component which affect the efficiency of RISC, but not absolutely required for RNAi in shrimp. However, we could not completely knockdown the expression of *PmTSN*. Therefore, the possibility that the residual PmTSN can function in the shrimp RNAi pathway cannot be ruled out. This effect may interfere us for observing the greater effect of *PmTSN* knockdown on dsRNA-mediated gene silencing in shrimp.

In conclusion, we provide the first description of the crustacean TSN from *P. monodon*. Our findings suggest that PmTSN involves in dsRNA-mediated gene silencing in shrimp. However, the mode of action of PmTSN in the shrimp RNAi pathway is still unknown. Therefore, identification of the PmTSN-interacting proteins will be essential for better understanding of the RNAi mechanism in the penaeid shrimp.

Acknowledgements

The authors thank Asst. Prof. Dr. Witoon Tirasophon for the viral stock, Ms. Chaweewan Chimwai and Ms. Pensri Hongthong for technical assistance. This work is supported by grants from the Thailand Research Fund (TRF), the Office of the Higher Education Commission (CHE) and Mahidol University under the National Research University Initiatives. A student fellowship granted to A.P. by the Royal Golden Jubilee Ph.D. Program.

References

[1] Carthew RW, Sontheimer EJ. Origins and Mechanisms of miRNAs and siRNAs. Cell. 2009;136:642-55.

[2] Fire A, Xu S, Montgomery MK, Kostas SA, Driver SE, Mello CC. Potent and specific genetic interference by double-stranded RNA in *Caenorhabditis elegans*. Nature. 1998;391:806-11.

[3] Castanotto D, Rossi JJ. The promises and pitfalls of RNA-interference-based therapeutics. Nature. 2009;457:426-33.

[4] Lopez-Fraga M, Wright N, Jimenez A. RNA interference-based therapeutics: new strategies to fight infectious disease. Infect Disord Drug Targets. 2008;8:262-73.

[5] Hirono I, Fagutao FF, Kondo H, Aoki T. Uncovering the Mechanisms of Shrimp Innate Immune Response by RNA Interference. Mar Biotechnol (NY). 2010. doi:10.1007/s10126-010-9292-0.

[6] Robalino J, Bartlett T, Shepard E, Prior S, Jaramillo G, Scura E, et al. Double-stranded RNA induces sequence-specific antiviral silencing in addition to nonspecific immunity in a marine shrimp: convergence of RNA interference and innate immunity in the invertebrate antiviral response? J Virol. 2005;79:13561-71.

[7] Attasart P, Kaewkhaw R, Chimwai C, Kongphom U, Namramoon O, Panyim S. Inhibition of *Penaeus monodon* densovirus replication in shrimp by double-stranded RNA. Arch Virol. 2010;155:825-32.

[8] Ongvarrasopone C, Chomchay E, Panyim S. Antiviral effect of PmRab7 knock-down on inhibition of Laem-Singh virus replication in black tiger shrimp. Antiviral Res. 2010;88:116-8.

[9] Xu J, Han F, Zhang X. Silencing shrimp white spot syndrome virus (WSSV) genes by siRNA. Antiviral Res. 2007;73:126-31.

[10] Chen YH, Jia XT, Zhao L, Li CZ, Zhang S, Chen YG, et al. Identification and functional characterization of Dicer2 and five single VWC domain proteins of *Litopenaeus vannamei*. Dev Comp Immunol. 2011. doi:10.1016/j.dci.2011.01.010.

[11] Su J, Oanh DT, Lyons RE, Leeton L, van Hulten MC, Tan SH, et al. A key gene of the RNA interference pathway in the black tiger shrimp, *Penaeus monodon*: identification and functional characterisation of Dicer-1. Fish Shellfish Immunol. 2008;24:223-33.

[12] Yao X, Wang L, Song L, Zhang H, Dong C, Zhang Y, et al. A Dicer-1 gene from white shrimp *Litopenaeus vannamei*: expression pattern in the processes of immune response and larval development. Fish Shellfish Immunol. 2010;29:565-70.

[13] Dechklar M, Udomkit A, Panyim S. Characterization of Argonaute cDNA from *Penaeus monodon* and implication of its role in RNA interference. Biochem Biophys Res Commun. 2008;367:768-74.

[14] Labreuche Y, Veloso A, de la Vega E, Gross PS, Chapman RW, Browdy CL, et al. Non-specific activation of antiviral immunity and induction of RNA interference may engage the same pathway in the Pacific white leg shrimp *Litopenaeus vannamei*. Dev Comp Immunol. 2010. doi:10.1016/j.dci.2010.06.017.

[15] Unajak S, Boonsaeng V, Jitrapakdee S. Isolation and characterization of cDNA encoding Argonaute, a component of RNA silencing in shrimp (*Penaeus monodon*). Comp Biochem Physiol B Biochem Mol Biol. 2006;145:179-87.

[16] Wang S, Liu N, Chen AJ, Zhao XF, Wang JX. TRBP homolog interacts with eukaryotic initiation factor 6 (eIF6) in *Fenneropenaeus chinensis*. J Immunol. 2009;182:5250-8.

[17] Caudy AA, Ketting RF, Hammond SM, Denli AM, Bathoorn AM, Tops BB, et al. A micrococcal nuclease homologue in RNAi effector complexes. Nature. 2003;425:411-4.

[18] Caudy AA, Myers M, Hannon GJ, Hammond SM. Fragile X-related protein and VIG associate with the RNA interference machinery. Genes Dev. 2002;16:2491-6.

[19] Tsuchiya N, Ochiai M, Nakashima K, Ubagai T, Sugimura T, Nakagama H. SND1, a component of RNA-induced silencing complex, is up-regulated in human colon cancers and implicated in early stage colon carcinogenesis. Cancer Res. 2007;67:9568-76.

[20] Callebaut I, Mornon JP. The human EBNA-2 coactivator p100: multidomain organization and relationship to the staphylococcal nuclease fold and to the tudor protein involved in *Drosophila melanogaster* development. Biochem J. 1997;321 (Pt 1):125-32.

[21] Tong X, Drapkin R, Yalamanchili R, Mosialos G, Kieff E. The Epstein-Barr virus nuclear protein 2 acidic domain forms a complex with a novel cellular coactivator that can interact with TFIIE. Mol Cell Biol. 1995;15:4735-44.

[22] Paukku K, Yang J, Silvennoinen O. Tudor and nuclease-like domains containing protein p100 function as coactivators for signal transducer and activator of transcription 5. Mol Endocrinol. 2003;17:1805-14.

[23] Yang J, Aittomaki S, Pesu M, Carter K, Saarinen J, Kalkkinen N, et al. Identification of p100 as a coactivator for STAT6 that bridges STAT6 with RNA polymerase II. EMBO J. 2002;21:4950-8.
[24] Valineva T, Yang J, Palovuori R, Silvennoinen O. The transcriptional co-activator protein p100 recruits histone acetyltransferase activity to STAT6 and mediates interaction between the CREB-binding protein and STAT6. J Biol Chem. 2005;280:14989-96.
[25] Yang J, Valineva T, Hong J, Bu T, Yao Z, Jensen ON, et al. Transcriptional co-activator protein p100 interacts with snRNP proteins and facilitates the assembly of the spliceosome. Nucleic Acids Res. 2007;35:4485-94.
[26] Scadden AD. The RISC subunit Tudor-SN binds to hyper-edited double-stranded RNA and promotes its cleavage. Nat Struct Mol Biol. 2005;12:489-96.
[27] Assavalapsakul W, Smith DR, Panyim S. Propagation of infectious yellow head virus particles prior to cytopathic effect in primary lymphoid cell cultures of *Penaeus monodon*. Dis Aquat Organ. 2003;55:253-8.
[28] Posiri P, Ongvarrasopone C, Panyim S. Improved preventive and curative effects of YHV infection in *Penaeus monodon* by a combination of two double stranded RNAs. Aquaculture. 2011;314:34-38.
[29] Altschul SF, Gish W, Miller W, Myers EW, Lipman DJ. Basic local alignment search tool. J Mol Biol. 1990;215:403-10.
[30] Gattiker A, Gasteiger E, Bairoch A. ScanProsite: a reference implementation of a PROSITE scanning tool. Appl Bioinformatics. 2002;1:107-8.
[31] Geer LY, Domrachev M, Lipman DJ, Bryant SH. CDART: protein homology by domain architecture. Genome Res. 2002;12:1619-23.
[32] Chenna R, Sugawara H, Koike T, Lopez R, Gibson TJ, Higgins DG, et al. Multiple sequence alignment with the Clustal series of programs. Nucleic Acids Res. 2003;31:3497-500.
[33] Kumar S, Nei M, Dudley J, Tamura K. MEGA: a biologist-centric software for evolutionary analysis of DNA and protein sequences. Brief Bioinform. 2008;9:299-306.
[34] Saitou N, Nei M. The neighbor-joining method: a new method for reconstructing phylogenetic trees. Mol Biol Evol. 1987;4:406-25.
[35] Ongvarrasopone C, Chanasakulniyom M, Sritunyalucksana K, Panyim S. Suppression of PmRab7 by dsRNA inhibits WSSV or YHV infection in shrimp. Mar Biotechnol (NY). 2008;10:374-81.
[36] Pfaffl MW. A new mathematical model for relative quantification in real-time RT-PCR. Nucleic Acids Res. 2001;29:e45.
[37] Tirasophon W, Yodmuang S, Chinnirunvong W, Plongthongkum N, Panyim S. Therapeutic inhibition of yellow head virus multiplication in infected shrimps by YHV-protease dsRNA. Antiviral Res. 2007;74:150-5.
[38] Abe S, Sakai M, Yagi K, Hagino T, Ochi K, Shibata K, et al. A Tudor protein with multiple SNc domains from pea seedlings: cellular localization, partial characterization, sequence analysis, and phylogenetic relationships. J Exp Bot. 2003;54:971-83.
[39] Saarikettu J, Ovod V, Vuoksio M, Grönholm J, Yang J, Silvennoinen O. Monoclonal Antibodies Against Human Tudor-SN. Hybridoma. 2010;29:231-6.
[40] Kuehbacher A, Urbich C, Zeiher AM, Dimmeler S. Role of Dicer and Drosha for endothelial microRNA expression and angiogenesis. Circ Res. 2007;101:59-68.

[41] Marques JT, Kim K, Wu PH, Alleyne TM, Jafari N, Carthew RW. Loqs and R2D2 act sequentially in the siRNA pathway in *Drosophila*. Nat Struct Mol Biol. 2009;17:24-30.

[42] Meister G, Landthaler M, Peters L, Chen PY, Urlaub H, Luhrmann R, et al. Identification of novel argonaute-associated proteins. Curr Biol. 2005;15:2149-55.

Part II: Protein-protein interaction between *Penaeus monodon* Tudor staphylococcal nuclease and RNAi machineries; Argonaute proteins

Abstract

RNA interference (RNAi) plays a crucial role as an antiviral defense in several organisms including plants and invertebrates. An understanding of RNAi machineries especially protein components of the RNA-induced silencing complex (RISC) is essential for prior to applying RNAi as a tool for viral protective immunity in shrimp. Tudor staphylococcal nuclease (TSN) is an evolutionarily conserved protein and is one of the RISC components. In previous study, suppression of *Penaeus monodon* TSN (*PmTSN*) by double-stranded RNA (dsRNA) resulted in decreasing dsRNA-mediated gene silencing activity. To elucidate the functional significance of PmTSN in shrimp RNAi pathway, interactions between PmTSN and three Argonaute proteins (PmAgo) were characterized by yeast two-hybrid and *in vitro* pull-down assays. The results demonstrated that PmTSN interacted with PmAgo1, but not with PmAgo2 or PmAgo3. The interaction between PmAgo and PmTSN was mediated through the N-terminal domain of PmAgo1 and the SN1-2 domains of PmTSN. Analysis of the nuclease activity of the recombinant PmTSN indicated that PmTSN possessed calcium-dependent nuclease activity specific to single-stranded RNA (ssRNA), but not dsRNA and DNA. Knockdown of *PmAgo1* and *PmTSN* diminished the ability of dsRNA-Rab7 to knockdown *PmRab7* expression, indicating the involvement of PmAgo1 and PmTSN in shrimp RNAi pathway. Taken together, the results imply that PmTSN is one of the components of PmAgo1-RISC, thus providing new insights in the RNAi-based mechanism in shrimp.

Keywords: RISC; RNAi; *in vitro* pull-down; yeast two-hybrid system; black tiger shrimp

1. Introduction

Invertebrates employ RNAi as a major host-defense mechanism against viruses [1]. In *Drosophila melanogaster*, the dsRNA-replicative intermediate of viruses is recognized and cleaved by Dicer, generating viral-derived small RNA which is subsequently incorporated into RISC, and mediated the degradation of viral RNA [1-3]. In addition, mutation of the core RNAi machineries such as Dicer-2, Ago2, and R2D2 substantially increases susceptibility of the mutant flies to viruses, indicating the crucial role of RNAi as an antiviral immunity in invertebrates [4-7]. A number of evidences emphasized that dsRNA triggered an antiviral response in shrimp in both sequence-independent [8] and sequence-specific manners [9-12]. Even though, there are several evidences revealing the existence of RNAi, the mechanism by which the RNAi operates in shrimp cells is not yet completely understood. An understanding of the RNAi machineries especially the components of RISC will provide insights into an innate antiviral immunity and the host-viral interaction in this economically important species. Tudor staphylococcal nuclease (TSN, also known as SND1 or p100) is an evolutionarily conserved protein which is composed of four tandem repeats of staphylococcal nuclease-like domains (SN), followed by Tudor and C-terminal SN domains. It is a multifunctional protein involved in a variety of cellular processes. For example, TSN can interact with several transcription factors to modulate their activities such as a transcriptional co-activator of Epstein-Barr virus nuclear antigen 2 (EBNA2), STAT5, STAT6, c-Myb, and Pim-1 [13-16]. In RNA splicing, TSN regulates small nuclear ribonucleoprotein (snRNP) assembly by interacting with SmB/B' and SmD1/D3, the core proteins of snRNP complex [17]. In addition, cleavage of TSN by caspase-3 is important for the execution of apoptosis in plant and human [18]. Despite its roles in several biological processes as described above, Caudy et al., 2003 revealed that TSN also involved in RNAi pathway in *Caenorhabditis elegans*, *D. melanogaster*, and mammals. Biochemical fractionation of RISC from these organisms revealed that TSN was co-purified with other proteins of RISC including Ago, VIG, and FMRP, and also resided in miRNA-ribonucleoprotein complex (miRNP) [19]. In addition, suppression of *TSN* expression impaired the RNAi activity indicating the importance of this protein in the RNAi mechanism [19-21].

In previous study, we identified and characterized a TSN gene from the black tiger shrimp, *Penaeus monodon*. The *P. monodon* TSN gene (*PmTSN*) encoded a polypeptide of 889 amino acids with an estimated molecular weight of 99.7 kDa. It contained the four tandem repeats of SN domains followed by a Tudor and a partially truncated C-terminal SN domain. Silencing of *PmTSN* expression by dsRNA resulted in diminishing of the dsRNA-mediated gene silencing in shrimp [22]. In this study, to elucidate the functional insights of PmTSN as one of the components of RISC, we characterized the interaction between PmTSN and the catalytic engine of RNAi, PmAgo by using yeast two-hybrid (Y2H) and *in vitro* pull-down assays. In addition, the nuclease activity of the recombinant PmTSN was also investigated.

2. Materials and Methods

2.1. Shrimp

The black tiger shrimps, *Penaeus monodon* (~10 g body weight) were purchased from the commercial shrimp farms in Thailand. They were reared in the laboratory tanks with continuous aerated artificial sea water (10 ppt) for 2-3 days before

processing to allow acclimatization, and were fed *ad libitum* with commercial shrimp feed. Apparently healthy shrimp free of yellow head virus (YHV) and white spot syndrome virus (WSSV) were selected and used in all experiments.

2.2. Plasmid construction

The plasmids pGEM-T containing coding regions of PmTSN (GenBank acc. no. JF429696), PmAgo1 (GenBank acc. no. DQ663629), PmAgo2 (kindly provided by Dr. Apinunt Udomkit, Mahidol University, Thailand), and PmAgo3 (GenBank acc. no. JX845575) were used as templates for PCR. VENT® DNA polymerase (New England Biolabs) was used for all PCR amplifications. For Y2H assay, the DNA fragment of PmTSN (amino acid residues 1-889) was amplified and cloned into *Nde*I/*Sal*I sites of pGBKT7 to create plasmid expressing GAL4-DNA binding domain fusion protein (BD-TSN). To generate plasmids expressing GAL4-activation domain fusion protein of PmAgo (AD-Ago), the DNA fragments of PmAgo1 (amino acids residues 1-939) and PmAgo2 (amino acid residues 1-810) were amplified and cloned into *Nde*I/*Xho*I sites, and PmAgo3 (amino acid residues 1-825) was amplified and cloned into *Eco*RI/*Xho*I sites of pGADT7, respectively.
For *in vitro* pull-down assay, the DNA fragments of TSN (amino acid residues 1-889), SND (amino acid residues 1-660) and SN34 (amino acid residues 320-889) were amplified and cloned into *Xma*I/*Xho*I sites of pGEX-5X-1 to generate N-terminal GST-fusion constructs of PmTSN and its deletion mutants. For N-terminal His_6-tagged constructs, the DNA fragments of PmAgo1 (amino acid residues 1-939), NTD-Ago1 (amino acid residues 1-291), NPAZ-Ago1 (amino acid residues 1-409), PAZ-Ago1 (amino acid residues 274-409), PIWI-Ago1 (amino acid residues 402-939), PmAgo2 (amino acid residues 1-810), and PmAgo3 (amino acid residues 1-825) were amplified and cloned into *Eco*RI/*Xho*I sites of pET-28a(+). All primers used for cloning are listed in Table 1. All constructs were subsequently sequenced to confirm gene sequences and correct reading frames.

2.3. Yeast two-hybrid assay

Matchmaker GAL4 Two-hybrid System 3 (Clontech) was used for yeast two-hybrid studies, according to the manufacturer's protocol. *Saccharomyces cerevisiae* strains Y187 and AH109 were kindly provided by Dr. Saengchan Senapin (Biotec, Thailand). The yeast strain Y187 harboring pGBKT7-TSN was used for mating with the yeast strain AH109 harboring pGADT7-Ago1, -Ago2, or -Ago3. The mated cultures were selected on synthetic double dropout medium (SD/-L/-W). Protein interaction was further indicated on synthetic quadruple dropout medium (SD/-L/-W/-H/-A) containing X-α-Gal (40 μg/ml). Yeast harboring pGBKT7-TSN and pGADT7-Laminin receptor (AD-Lamr) served as a positive control whereas yeast harboring pGBKT7-TSN and empty pGADT7 served as a negative control. Preparation of yeast protein extracts was performed according to Yeast Protocol Handbook (Clontech). Expression of BD-TSN and AD-Ago in yeasts were confirmed before performing two-hybrid experiments using anti-c-Myc antibody and anti-HA antibody (US Biological), respectively.

2.4. Protein expression and purification

All GST-fusion and His_6-tagged constructs were expressed in *Escherichia coli* Rossetta (DE3) (Novagen). The recombinant GST-TSN, GST-SND, and GST-SN34

were expressed by using auto-induction approach [23]. Briefly, overnight cultures in non-inducing media ZYP-505 (1% N-Z-amine, 0.5% yeast extract, 50 mM Na_2HPO_4, 50 mM KH_2PO_4, 25 mM $(NH_4)_2SO_4$, 2 mM $MgSO_4$, 0.5% glycerol, and 0.05 % glucose) were inoculated in auto-inducing media ZYZ-5052 (1% N-Z-amine, 0.5% yeast extract, 50 mM Na_2HPO_4, 50 mM KH_2PO_4, 25 mM $(NH_4)_2SO_4$, 2 mM $MgSO_4$, 0.5% glycerol, 0.05 % glucose, and 0.2% lactose) containing ampicillin (100 μg/ml) and chloramphenicol (34 μg/ml) and incubated at 37°C with shaking until A_{600} reached ~1.0. The cultures were then incubated at 18°C for 20 hours with shaking. For GST-fusion protein purification, cells were collected by centrifugation, resuspended in lysis buffer (PBS, pH 7.4, 0.2% Triton X-100, 1 mM DTT, 1 mM PMSF, and 100 μg/ml lysozyme) and lysed by sonication. Following centrifugation, the clear cell lysates containing GST-fusion proteins were filtrated and applied to the GSTrap FF column (GE Healthcare) for affinity purification. GST-TSN and GST-SN34 were further purified by anion-exchange chromatography using HiTrap Q column (GE Healthcare). On the other hand, GST-SND was further purified by cation-exchange chromatography using HiTrap SP column (GE Healthcare). The purified proteins were dialyzed against binding buffer (25 mM HEPES, pH 7.5, 150 mM NaCl, 1 mM DTT, 0.2% Triton X-100, 10% glycerol, 1 mM PMSF), concentrated by Vivaspin 6 (GE Healthcare), and determined the concentration by Bradford's assay.

Expression of His_6-tagged fusion proteins were induced by the addition of Isopropyl-β-D-thiogalactopyranoside (IPTG) to a final concentration of 0.2 mM at A_{600} ~ 0.6 and proceeded for 6 hours for His-Ago1 and its deletion mutants, or 20 hours for His-Ago2 and His-Ago3 at 18°C with shaking. Following centrifugation, the cells were resuspended in binding buffer at the ratio of 100 OD per ml, lysed by sonication, and centrifuged at 48,000xg for 30 min at 4°C to separate inclusion bodies and cell debris. The clear cell lysates containing His_6-tagged proteins were then divided into small aliquots, flash frozen with liquid nitrogen, and stored at -80°C until used.

2.5. In vitro pull-down assay

In vitro pull-down assay was performed according to Adachi et al. with some modifications [24]. Ten micrograms of the purified GST-fusion proteins or GST alone were immobilized on 30 μl of 50% (v/v) glutathione-agarose resin (Sigma) for 2 hours at 4°C with rotating. The resins were then washed three times with washing buffer (25 mM HEPES, pH 7.5, 150 mM NaCl, 1 mM DTT, 1% Triton X-100, 10% glycerol, 0.2 mM PMSF). Subsequently, the resins were incubated with the lysates of *E. coli* expressing His_6-tagged proteins for 4 hours at 4°C with rotating. After incubation, the resins were washed four times with washing buffer. The protein complex was eluted from the beads by boiling in SDS-loading buffer. The complex was separated on SDS-PAGE and subsequently transferred to nitrocellulose membrane. The presence of His_6-tagged proteins was detected by western blot with anti-His antibody (GE Healthcare). For detection GST-fusion proteins, bound proteins were diluted 10 fold, separated on SDS-PAGE, and blotted with anti-GST antibody (Sigma).

2.6. Nuclease activity assay

The recombinant GST-TSN was evaluated for its ability to cleave both RNA and DNA. The luciferase (luc) oligonucleotide substrates with ~400 nucleotides in length (nucleotides 619-1000) were synthesized by using plasmid pGL3-Basic

(Promega) as a template. The luc-ssRNA and luc-dsRNA substrates were synthesized by *in vitro* transcription using RiboMAX® Large Scale RNA Production System (Promega), according to the manufacturer's protocol. The luc-DNA was synthesized by PCR and purified from the gel using QIAquick gel extraction kit (Qiagen). To assay the nuclease activity of the recombinant GST-TSN, 2 pmol of luc-ssRNA, luc-dsRNA, or luc-DNA were incubated with 10 pmol of the purified GST-TSN or GST in 20-µl reaction containing 20 mM Tris, pH 7.0, 1 mM DTT, 100 mM NaCl, 2 mM $MgCl_2$, 2 mM $CaCl_2$ and 2 mM $MnCl_2$ at 37°C for 4 hours. The reactions were analyzed on 6% non-denaturing polycrylamide gel for reactions containing luc-dsRNA and luc-DNA, or 6% denaturing polyacrylamide for reactions containing luc-ssRNA. The presence of oligonucleotide substrate was visualized by ethidium bromide staining. In the assays, RQ1 DNase (Promega), RNase A (US Biological), and RNase III (New England Biolabs) were included as controls.

2.7. Preparation of double-stranded RNA

The double-stranded RNA (dsRNA) targeting PAZ domain of *PmAgo1* (kindly provided by Dr. Apinunt Udomkit, Mahidol University, Thailand), *PmRab7* [25], and *gfp* (kindly provided by Dr. Witoon Tirasophon, Mahidol University, Thailand) were produced in bacterial expression system [26]. Briefly, the plasmid pET-17b-stAgo1, pET-17b-stRab7 and pET-3a-stGFP were transformed into *E. coli* HT115 (DE3). The induction of dsRNA expression was carried out by the addition of IPTG to the final concentration of 0.1 mM (for dsRNA-Ago1 and dsRNA-Rab7) or 0.4 mM (for dsRNA-GFP) at $A_{600} \sim 0.6$ and proceeded for 4 hours at 37°C with shaking. Extraction and purification of dsRNA was performed as previously described [27]. For preparation of dsRNA targeting *PmTSN*, *in vitro* transcription was performed as previously described [22]. The concentration of the dsRNA was measured by Nanodrop ND-1000 spectrophotometer (Nanodrop technologies) and gel electrophoresis. The quality of dsRNA was determined by RNase A and RNase III digestion assay.

2.8. In vivo gene knockdown and RNAi against RNAi assay

To knockdown *PmAgo* and *PmTSN* expression, 50 µg of dsRNA-Ago1 or dsRNA-TSN was injected into shrimps (~10 g body weight) via intramuscular injection. Shrimps injected with dsRNA-GFP were used as negative control. Hemolymph was individually collected before and after dsRNA injection (1, 2 and 4 days). Total RNA was extracted from hemolymph using TRI Reagent® LS (Molecular Research Center, Inc.). Transcription levels of *PmAgo1* and *PmTSN* were determined by RT-PCR.
The effects of *PmAgo1* and *PmTSN* knockdown on RNAi in shrimp were determined by using RNAi against RNAi assay, as previously described [22, 28]. Briefly, shrimps (n = 6) were injected with dsRNA-Ago1, dsRNA-TSN or dsRNA-GFP as described above. Two days later, shrimps were injected with 6.3 µg of dsRNA-Rab7. Hemolymph was individually collected 2 days after the second injection. Transcription level of *PmRab7* was observed by quantitative real-time PCR (qRT-PCR) [22]. The data obtained from qRT-PCR were analyzed by comparative Ct method ($2^{-\Delta\Delta Ct}$) [29]. The data were expressed as mean ± standard error of mean (SEM) and analyzed by using one-way ANOVA in the Sigma Stat 3.5 program. A measurement of $P < 0.05$ was accepted as statistically significant. All primers used for RT-PCR and qRT-PCR are listed in Table 1.

Table 1. Primers used in this study. Nucleotides that are underlined indicate restriction sites or T7 promoter sequences.

Primers	Sequence (5'→3')	Purposes
HisAgo1-F	CCGGAATTCATGTACCCTGTCGGGCAGC	Protein expression of
HisAgo1-R	GCCGCTCGAGTTAAGCAAAGTACATGACTCTGT	His-Ago1
HisAgo2-F	CCGGAATTCATGGACGCAGCAAAGGGAAG	Protein expression of
HisAgo2-R	GCCGCTCGAGTTAACTCTCTTGTATATTTA	His-Ago2
HisAgo3-F	CCGGAATTCATGCCTTGGATATCAGAAGTC	Protein expression of
HisAgo3-R	CGGTGCTCGAGTTTACCCTTCTTCCCTTTGCTCGTAT	His-Ago3
NTD-F	GCATTGGAATTCATGTACCCTGTCGGGCAGCC	Protein expression of
NTD-R	CAATGCCTCGAGTTATAACACTTCACACAT AAACTC	NTD-Ago1
NTD-F	GCATTGGAATTCATGTACCCTGTCGGGCAGCC	Protein expression of
PAZ-R	CAATGCCTCGAGTTATAGTTTCTTGATGCATCGTTG	NPAZ-Ago1
PAZ-F	GCATTGGAATTCGCTACAGCATTCTACAAGGC	Protein expression of
PAZ-R	CAATGCCTCGAGTTATAGTTTCTTGATGCATCGTTG	PAZ-Ago1
PIWI-F	GCATTGGAATTCGGACAACGATGCATCAAGAAAC	Protein expression of
PIWI-R	CAATGCCTCGAGTTAAGCAAAGTACATGACTCT GTTTG	PIWI-Ago1
YAgo1-F	GCCAGTCATATGTACCCTGTCGGGCAGC	Y2H: AD-Ago1
YAgo1-R	CTGCAGCTCGAGCAAAGTACATGACTCTGT	
YAgo2-F	GCCAGTCATATGGACGCAGCAAAGGGAAG	Y2H: AD-Ago2
YAgo2-R	CTGCAGCTCGAGCACTCTCTTGTATATTTA	
YAgo3-F	GCCAGTGAATTCATGCCTTGGATATCAGAAGTC	Y2H: AD-Ago3
YAgo3-R	CTGCAGCTCGAGCCCCTTCTTCCCTTTGCTCGTAT	
YTSN-F	GGGAATTCCATATGGCTGCGTCTCACCCAAC	Y2H: BD-TSN
YTSN-R	GGACGCGTCGACGTCGTTCCATACCAAATTCG	
GSTTSN-F	TCCCCCGGGTATGGCTGCGTCTCACCCAAC	Protein expression of
GSTTSN-R	GCCGCTCGAGTTATCGTTCCATACCAAATTCG	GST-TSN
GSTTSN-F	TCCCCCGGGTATGGCTGCGTCTCACCCAAC	Protein expression of
GSTSND-R	GCCGCTCGAGTTATCTGTCGTGCTGCAATTCTT	GST-SND
GST34-F	TCCCCCGGGTGGTCCTAAGATTGCTGACAAAG	Protein expression of
GSTTSN-R	GCCGCTCGAGTTATCGTTCCATACCAAATTCG	GST-SN34
TSN-F1	GCTGCACAGTCAAGATTGGA	Multiplex RT-PCR
TuN5R	TCCAGATGCAACAAATTGCAC	
Actin-F	GACTCGTACGTCGGGCGACGA	Multiplex RT-PCR
Actin-R	AGCAGCGGTGGTCATCACCTG	
Ago1-F	CAAGAATTTGGTCTGACGAT	RT-PCR
Ago1-R	AGTGTCACCCACACGCTTCAC	
qRab7-F2	CTGGAGAATAGGGCGGTATCAACG	qRT-PCR
qRab7-R2	CGAGCAATGGTCTGGAAGGCTAAC	
EF1a-F	GAACTGCTGACCAAGATCGACAGG	qRT-PCR
EF1a-R	GAGCATACTGTTGGAAGGTCTCCA	
Luci-F	GGTGTCGCTCTGCCTCATAG	*In vitro* transcription
Luci-R	GCAGATGGAACCTCTTGGC	
Luci-FT7	TAATACGACTCACTATAGGGGTGTCGCTCTGCCTCATAG	
Luci-RT7	TAATACGACTCACTATAGGGCAGATGGAACCTCTTGGC	
PRT oligo	CCGGAATTCAAGCTTCTAGAGGATCCTTTTTTTTTTTTTTT	cDNA synthesis

3. Results

3.1 Interaction between PmTSN and three PmAgo proteins

TSN was identified as one of the components of RISC in *C. elegans*, *Drosophila*, and mammals [19, 30]. In previous study, identification and characterization of a TSN gene from *P. monodon* (*PmTSN*) demonstrated the involvement of PmTSN in the shrimp RNAi pathway [22]. To investigate whether PmTSN was one of the components of RISC in shrimp, the yeast two-hybrid assay (Y2H) was performed to study the interaction between PmTSN and the core component of RISC, PmAgo. PmTSN was fused with GAL4-DNA-binding domain (BD-TSN), and the three PmAgo proteins including PmAgo1, PmAgo2, and PmAgo3 were fused with GAL4-activation domain (AD-Ago). The expression of BD-TSN and AD-Ago proteins in yeasts were confirmed before Y2H was performed with anti-c-Myc and anti-HA antibodies, respectively. The results showed that western blotting with anti-c-Myc antibody could detect the expression of BD-TSN at the expected band of 120 kDa. Expression of AD-Ago1, AD-Ago2, and AD-Ago3 could be detected by anti-HA antibody and showed the expected bands of 118 kDa, 105 kDa, and 107 kDa, respectively (Fig. 1A). By using Y2H, the diploids harboring BD-TSN and AD-Ago1 showed the positive interaction observed by the growth and blue color on the quadruple dropout medium (SD/-W/-L/-H/-A/X-α-gal), similar to the results observed in the diploids harboring BD-TSN and AD-Laminin receptor (AD-Lamr) which were used as a positive control. The positive interaction was not observed in the diploids harboring BD-TSN and AD-Ago2 or AD-Ago3. In addition, no sign of the interaction was observed in the negative control diploids harboring BD-TSN and Empty pGADT7. Therefore, this data confirmed that the interaction of BD-TSN and AD-Ago1 was not the result of an auto-activation of the reporter genes.

The interaction between PmTSN and PmAgo1 was further confirmed by using *in vitro* pull-down assay. PmTSN was expressed as a GST-fusion protein (GST-TSN) by an auto-induction approach and showed an expected band of 126 kDa in both soluble and insoluble fractions when compared to the non-induced condition. After purification by chromatographic techniques, the purified protein was confirmed by western blotting with anti-GST antibody (Fig. 2A). The expression of His-Ago proteins were observed in both soluble and insoluble fractions by using western blotting with anti-His antibody. The expected bands of His-Ago1, His-Ago2, and His-Ago3 were shown at 105, 92, and 94 kDa, respectively. In addition, no band was observed in the *E. coli* harboring the empty pET-28a(+) (Fig. 2B). *In vitro* pull-down assay was performed by incubating immobilized GST-TSN with cell lysate from *E. coli* expressing His-Ago1, His-Ago2 or His-Ago3. The presence of GST- and His_6-tagged proteins was detected by western blotting with anti-GST and anti-His antibody, respectively. The results demonstrated that GST-TSN could interact with His-Ago1, but not interact with His-Ago2 or His-Ago3, confirming the results of Y2H (Fig. 2C). In addition, GST alone could not interact with all three His-Ago proteins, indicating the specific interaction between GST-TSN and His-Ago1. Taken together, by using both Y2H and *in vitro* pull-down assay, the results demonstrated that PmTSN specifically interacts with PmAgo1, suggesting that PmTSN is one of the components of PmAgo1-RISC.

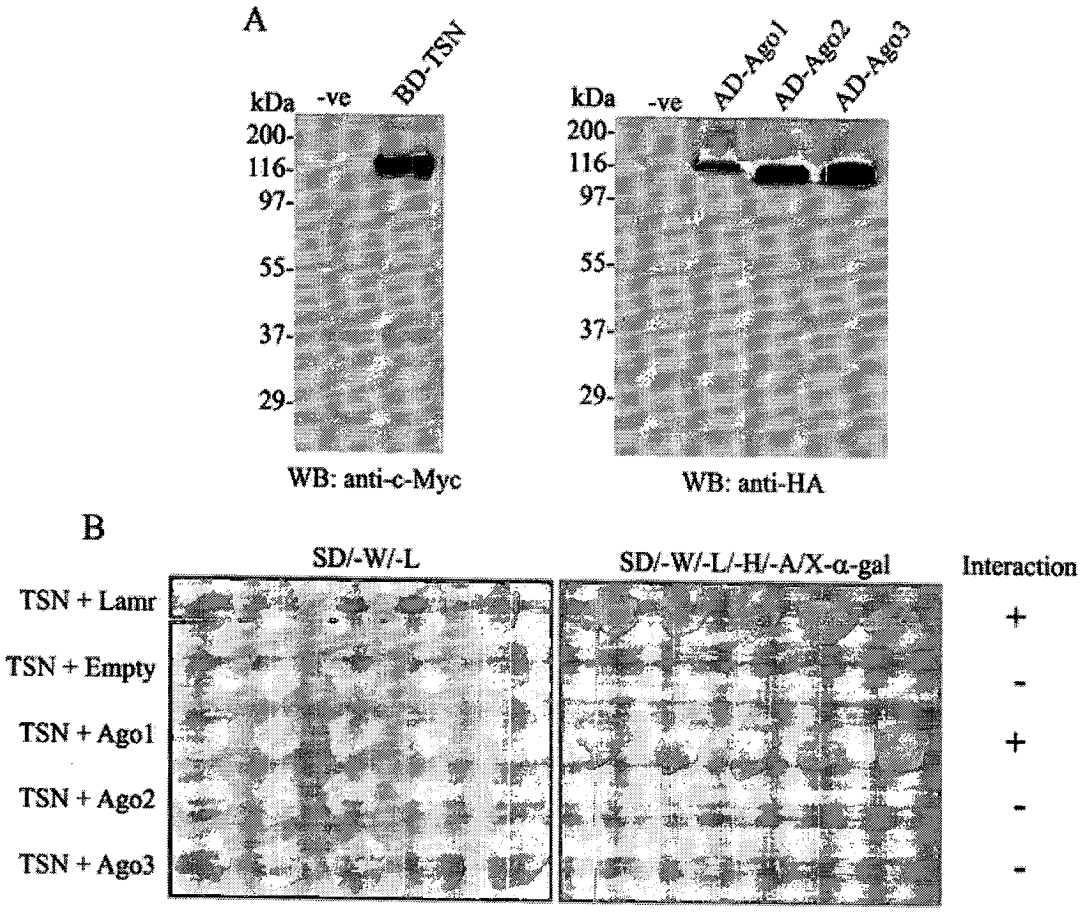

Fig. 1 PmTSN interacts with PmAgo1 in Y2H assay. (A) Western blot analysis of BD-TSN and AD-Ago expression in yeasts confirmed by using anti-c-Myc and anti-HA antibodies, respectively. Lane -ve represents untransformed yeasts. (B) Y2H assay showing the interaction between PmTSN and PmAgo1. *S. cerevisiae* Y187 expressing BD-TSN was mated with *S. cerevisiae* AH109 expressing AD-Ago1, AD-Ago2, or AD-Ago3, respectively. The mated cultures were selected on SD/-W/-L medium and subsequently confirmed on SD/-W/-L/-H/-A/X-α-gal medium. Yeast expressing BD-TSN and AD-Lamr served as a positive control whereas yeast harboring pGBKT7-TSN and empty pGADT7 served as a negative control. (+) and (-) represent the presence and absence of the interaction.

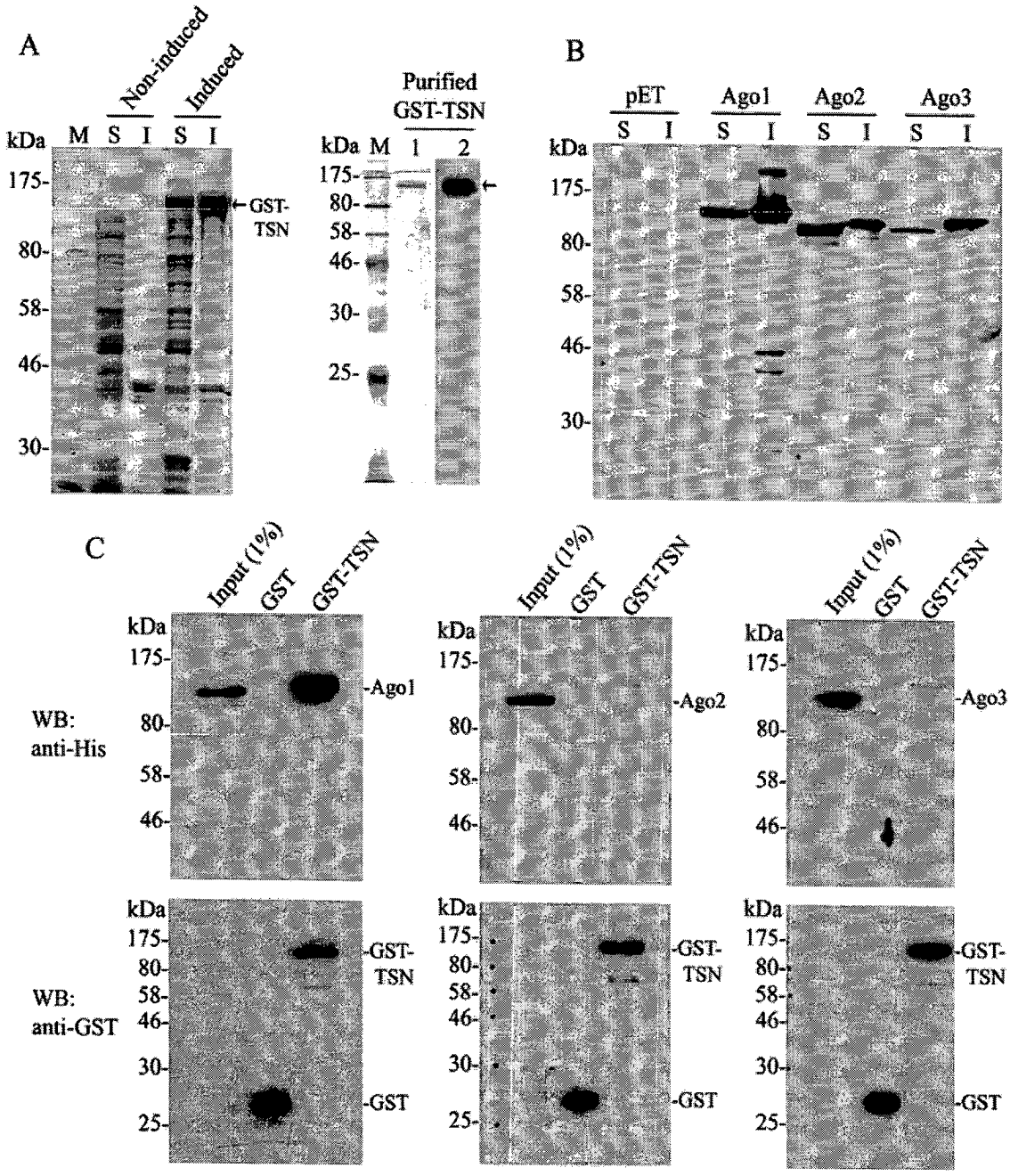

Fig. 2 *In vitro* pull-down assay confirming PmAgo1-PmTSN interaction. (A) Expression and purification of the recombinant GST-TSN using auto-induction approach and further purified by chromatographic techniques. Lane M, pre-stained protein marker; lane S, soluble fraction; lane I, insoluble fraction; lane 1, coomassie blue staining; lane 2, western blot analysis detected with anti-GST antibody. The arrows indicate GST-TSN. (B) Western blot analysis using anti-His antibody to detect the expression of His-Ago1 (105 kDa), His-Ago2 (92 kDa), and His-Ago3 (94 kDa) in *E. coli* Rosetta (DE3). Lane pET shows soluble and insoluble fractions from *E. coli* harboring empty pET-28a(+). (C) *In vitro* pull-down assay showing PmTSN-PmAgo1 interaction analyzed by western blotting with anti-His and anti-GST antibodies.

3.2. Mapping of PmAgo1-PmTSN interaction

To identify the PmTSN-binding site of PmAgo1, a variety of His-Ago1 deletion mutants, including N-terminal domain (NTD), NTD and PAZ domains (NPAZ), PAZ domain, and MID-PIWI domains (PIWI) was generated and used for *in vitro* pull-down assay with GST-TSN. Western blotting with anti-His antibody revealed the expected bands of His-NTD, His-NPAZ, His-PAZ, and His-PIWI at 29, 48, 19, and 61 kDa in both soluble and insoluble fractions, respectively. In addition, no band was observed in the *E. coli* harboring the empty pET-28a(+) (Fig. 3A and B). The full-length His-Ago1 (FL) was also included in pull-down experiments as a positive control. The results of an *in vitro* pull-down assay demonstrated that FL, NTD and NPAZ were able to interact with GST-TSN, but PAZ and PIWI were not (Fig. 4A). In addition, no interaction was observed in the pull-down reactions containing GST. These results suggest that NTD of PmAgo1 serves as an interacting domain for PmAgo1 to interact with PmTSN, and PAZ and PIWI are not involved in the interaction between these two proteins.

The PmAgo1-binding site of PmTSN was further characterized. The GST-fusion proteins of PmTSN-deletion mutants including GST-SND (contains SN1-SN4 domains) and GST-SN34 (contains SN3, SN4, Tudor, and C-terminal SN5 domains) (Fig. 3C) were expressed by an auto-induction approach and showed the expected bands of 100 and 90 kDa in both soluble and insoluble fraction, respectively, compared to a non-induced condition. Both GST-fusion proteins were purified by chromatographic techniques and were subsequently confirmed by western blotting with anti-GST antibody (Fig. 3D and E). The PmTSN deletion mutant containing Tudor and SN5 domains (GST-Tud) was also generated. Unfortunately GST-Tud was expressed as inclusion bodies. Attempts to refold the recombinant protein were unsuccessful. Therefore GST-Tud was not included in this experiment (data not shown). To identify the PmAgo1-binding site of PmTSN, His-NTD was used to perform *in vitro* pull-down assay with GST-TSN and its deletion mutants. The results showed that His-NTD could be pulled-down with GST-TSN and GST-SND. A faint band of His-NTD was also observed in the GST-SN34 reaction. However, this minor interaction of His-NTD with GST-SN34 was possibly at the background level when compared to the control reaction containing GST only (Fig. 4B). Similar results were observed with His-FL instead of His-NTD for *in vitro* pull-down assay. His-FL could be pulled-down by GST-TSN and GST-SND, but not GST-SN34 (Fig. 4C). These results suggest that SN1 and SN2 domains are required for PmTSN to interact with the N-terminal domain of PmAgo1, and SN3, SN4, Tudor and SN5 domains are not involved in PmTSN-PmAgo1 interaction.

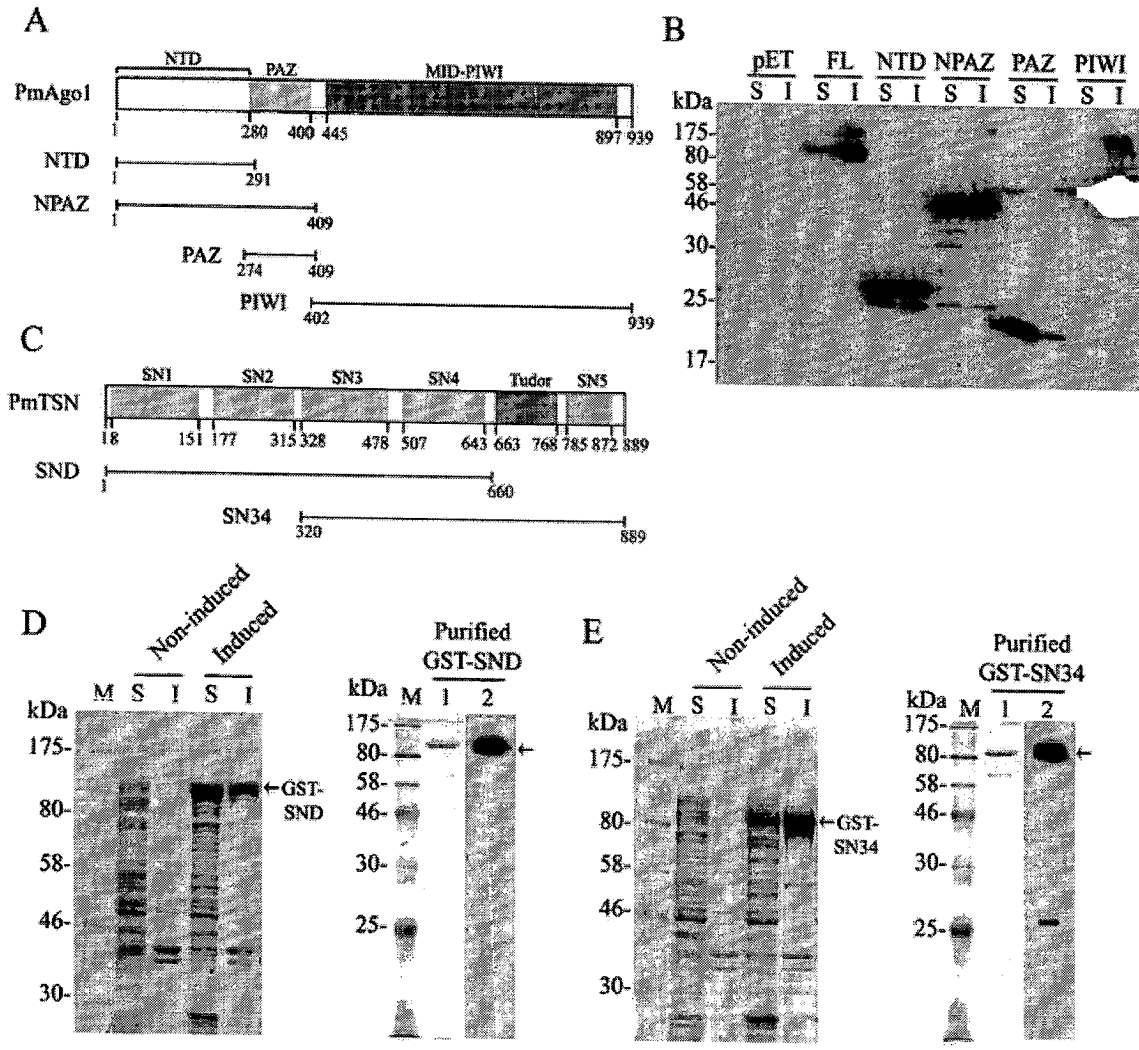

Fig. 3 Expression of the deletion mutant proteins used for mapping of PmTSN-PmAgo1 interaction. (A) Schematic diagram showing PmAgo1-deletion mutants used to map the PmTSN-interacting domain. The positions of amino acid residues at various domain junctions are indicated. (B) Western blot analysis using anti-His antibody to detect the expression of His-Ago1 (FL, 105 kDa) and its deletion mutants, including His-NTD (29 kDa), His-NPAZ (48 kDa), His-PAZ (19 kDa), and His-PIWI (61 kDa) in *E. coli* Rosetta (DE3). Lane pET shows soluble and insoluble fractions from *E. coli* harboring empty pET-28a(+); lane S and I represent soluble and insoluble fractions. (C) Schematic diagram showing PmTSN-deletion mutants used to map the PmAgo1-interacting domain. The positions of amino acid residues at various domain junctions are indicated. Expression and purification of the recombinant GST-SND (D) and -SN34 (E) in *E. coli* Rosetta (DE3). The recombinant GST-SND (100 kDa) and GST-SN34 (90 kDa) were expressed by auto-induction approach and further purified by chromatographic techniques. The arrows indicate GST-SND and GST-SN34. Lane M, pre-stained protein marker; lane 1, coomassie blue staining; lane 2, western blot analysis with anti-GST antibody.

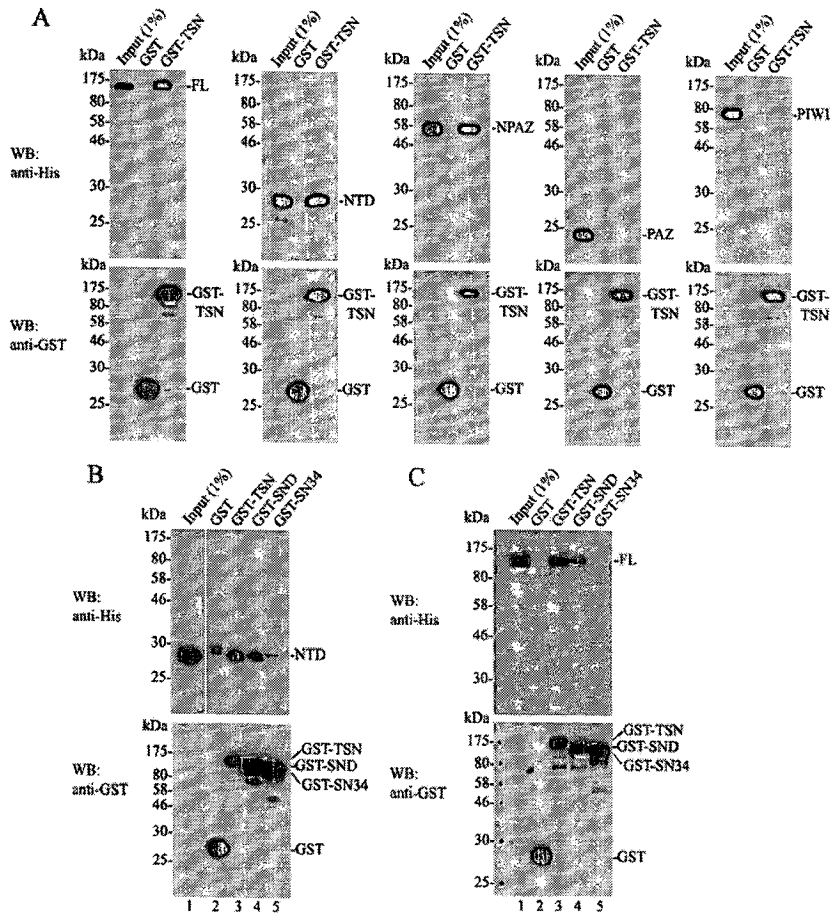

Fig. 4 Mapping of PmTSN-PmAgo1 interaction. (A) Mapping of PmTSN-binding site of PmAgo1. Full-length (FL) and deletion mutants of His-Ago1 were analyzed their abilities to interact with the immobilized GST-TSN using *in vitro* pull-down assay. (B and C) Mapping of PmAgo1-binding site of PmTSN. The immobilized GST-TSN, GST-SND, and GST-SN34 were used for *in vitro* pull-down assay with His-NTD or His-FL. The immobilized GST was used as a negative control in all experiments. The presence of GST- and His-tagged proteins was analyzed by western blotting with anti-GST and anti-His antibody, respectively.

3.3. Nuclease activity assay of the recombinant GST-TSN

The nuclease activity of TSN has been reported in *Drosophila* [19], parasites [31], human, and plant [18]. To investigate whether PmTSN possessed the nuclease activity, purified GST-TSN was incubated with luc-DNA, luc-ssRNA and luc-dsRNA. The results showed that only GST-TSN could cleave luc-ssRNA, while the cleavages of luc-DNA and luc-dsRNA were not observed (Fig. 5A), indicating that PmTSN was a single-stranded RNase. The effect of metal ion on PmTSN RNase activity was further determined. The GST-TSN was incubated with luc-ssRNA in the presence or absence of Ca^{2+}, Mg^{2+}, or Mn^{2+}. The RNase activity of the recombinant protein was strongly inhibited in the absence of Ca^{2+} (Fig. 5B, lane 3, 4, 7, and 8), indicating the calcium-dependent RNase activity of PmTSN.

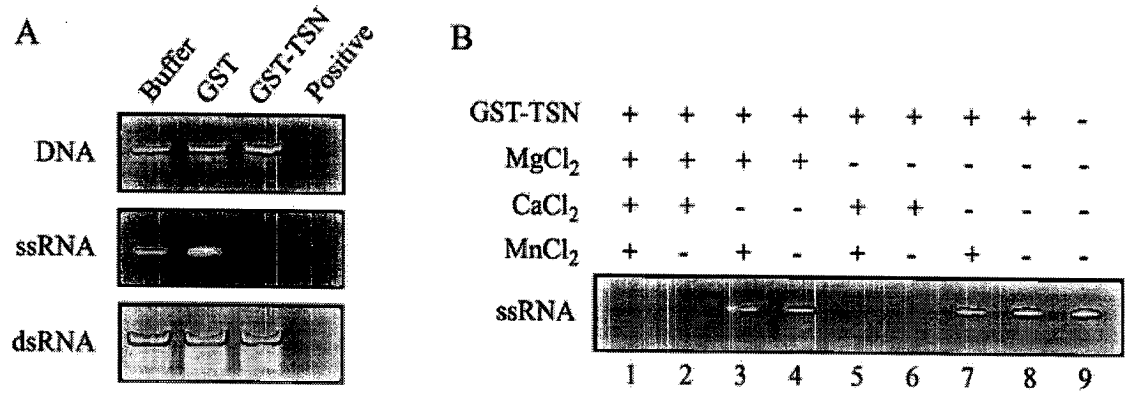

Fig. 5 Nuclease activity of the recombinant GST-TSN. (A) Purified GST-TSN (10 pmol) was incubated with various nucleic acids (2 pmol). The reactions were incubated at 37°C for 4 hours. Purified GST was used as a negative control. The commercial DNase, RNase A, and RNase III were included as positive controls. (B) GST-TSN exhibits calcium-dependent nuclease activity. Purified GST-TSN was incubated with Luc-ssRNA in the presence of Ca^{2+}, Mg^{2+}, or Mn^{2+}. (+) and (-) indicate the presence and absence of the divalent cations.

3.4. PmAgo1 and PmTSN are involved in dsRNA-mediated gene silencing

According to the results from Y2H and *in vitro* pull-down assay, the interaction between PmAgo1 and PmTSN indicates that PmTSN is one of the components of PmAgo1-RISC. Therefore, the roles of PmAgo1 and PmTSN in shrimp RNAi pathway were further investigated. The dsRNA corresponding to *PmAgo1* and *PmTSN* were synthesized and used for gene knockdown *in vivo*. Injection of dsRNA-Ago1 or dsRNA-TSN could significantly knockdown the transcripts of *PmAgo1* or *PmTSN* in shrimp, respectively. The transcription levels of *PmAgo1* and *PmTSN* were substantially reduced approximately 80% and 83% after 2 days dsRNA injection, respectively. In addition, injection of dsRNA-GFP had no effect on the transcripts of *PmAgo1* and *PmTSN* (Fig. S1). Two-fold increase of the dosage of dsRNA did not completely knockdown *PmAgo1* and *PmTSN* (data not shown). We speculated that PmAgo1 and PmTSN are indispensable for RNAi in shrimp.

The effects of suppression *PmAgo1* and *PmTSN* on the abilities of dsRNA-Rab7 to knockdown *PmRab7* expression were determined by qRT-PCR (Fig. 6, Fig. S2 and Fig. S3). Shrimps injected with dsRNA-Rab7 alone (NaCl→dsRab7) and dsRNA-GFP followed by dsRNA-Rab7 (dsGFP→dsRab7) showed similar reduction in *PmRab7* transcripts approximately 91% and 96%, respectively. *PmRab7* transcripts were significantly increased ($P < 0.05$) in *PmAgo1*-knockdown (dsAgo1→dsRab7) and *PmTSN*-knockdown groups (dsTSN→dsRab7) when compared to the NaCl→dsRab7 and dsGFP→dsRab7 groups, as they showed 58% and 76% knockdown of *PmRab7*, respectively. These results indicated that PmAgo1 and PmTSN are involved in dsRNA-mediated gene silencing in shrimp.

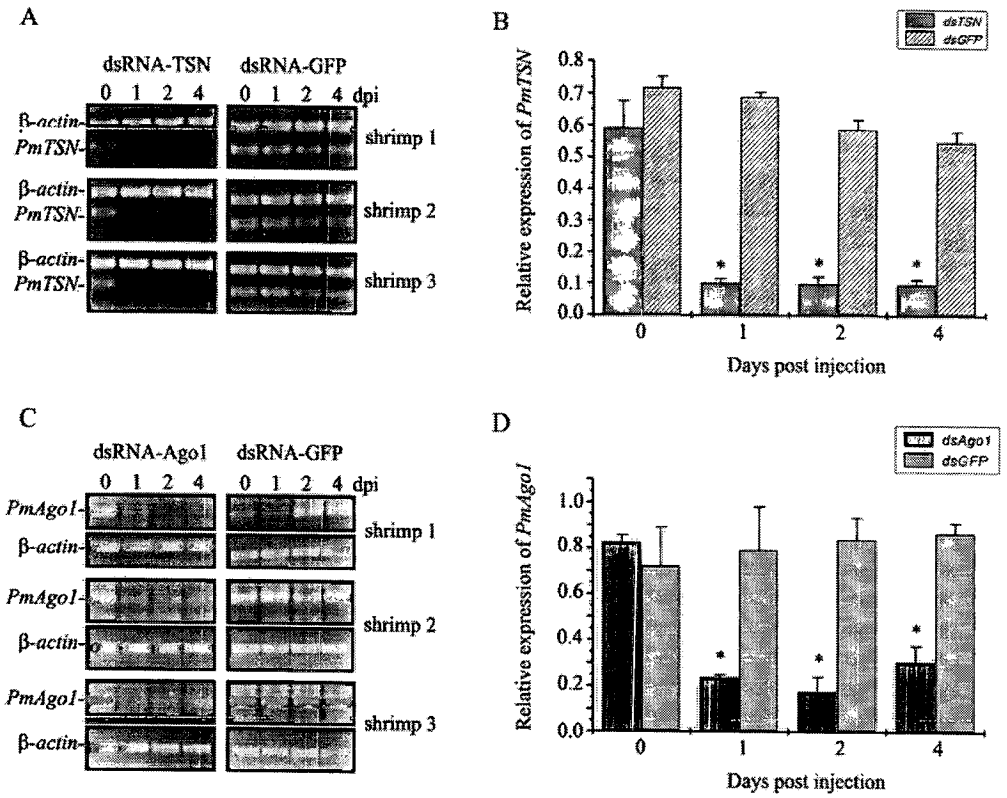

Fig. S1 Time-course analysis of *PmTSN* and *PmAgo1* knockdown by dsRNA. Agarose gel electrophoresis of RT-PCR amplified *PmTSN*, *PmAgo1*, and *β-actin* mRNAs from hemolymph of (A) *PmTSN*- and (C) *PmAgo1*- knockdown shrimp. Injection of dsRNA-GFP was used as a control. Semi-quantitative RT-PCR was used to determine *PmTSN* (B) and *PmAgo1* (D) expression at 0, 1, 2, and 4 days after dsRNA injection. *β-actin* was used as an internal control. . The PCR products were resolved by using 1.5% agarose gel electrophoresis and visualized by ethidium bromide staining. M is 2-log DNA ladder. Bars represent mean ± SEM (n = 3). The asterisks (*) represent the significant difference ($P < 0.05$) between before and after 1, 2, or 4 days dsRNA injection.

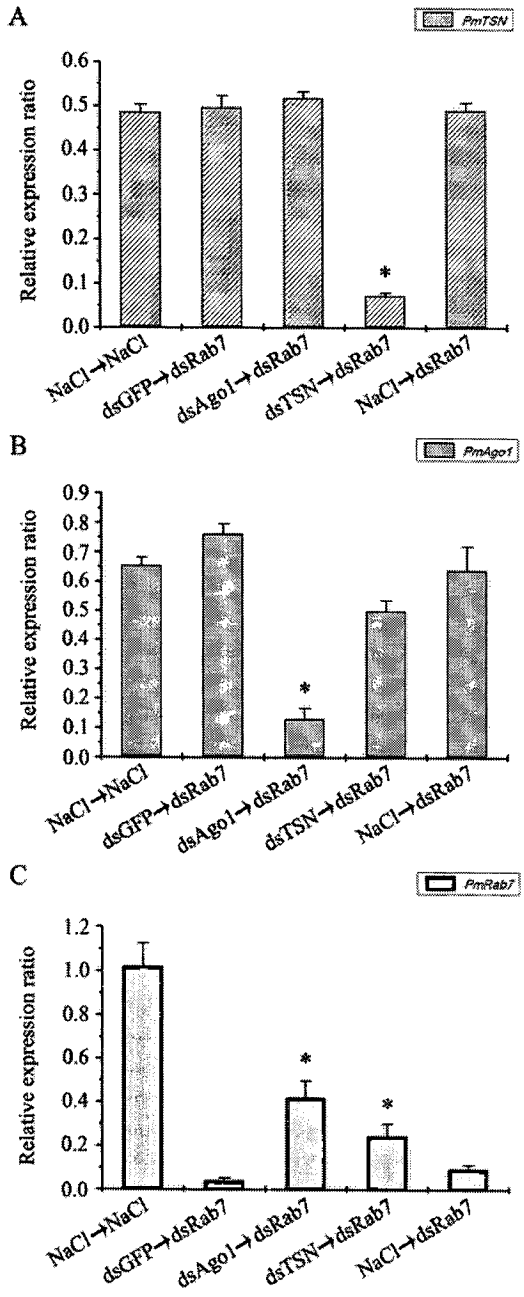

Fig. 6 Knockdown of *PmTSN* and *PmAgo1* diminished RNAi activity in shrimp. dsRNA-Rab7 was injected into control (NaCl→dsRab7 and dsGFP→dsRab7), *PmAgo1*-knockdown (dsAgo1→dsRab7), and *PmTSN*-knockdown shrimps (dsTSN→dsRab7), and qRT-PCR was used to determine the transcription levels of *PmRab7*. (A, B) Semi-quantitative analysis of *PmTSN* and *PmAgo1* expression. *β-actin* was used as an internal control for normalization. The asterisks (*) represent a significant difference ($P < 0.05$) in the relative transcription levels of *PmTSN* and *PmAgo1*, compared to control groups. (C) qRT-PCR analysis of *PmRab7* transcripts. *EF1-α* was used as an internal control for normalization. The relative transcription levels of *PmRab7* were calculated by comparative Ct method ($2^{-\Delta\Delta Ct}$). Bars represents means ± SEM ($n = 6$). Statistical analysis was performed by using one-way ANOVA. The asterisks (*) represent a significant difference ($P < 0.05$) in the relative

transcription levels of *PmRab7* in dsAgo1→dsRab7 or dsTSN→dsRab7 groups, compared to control groups.

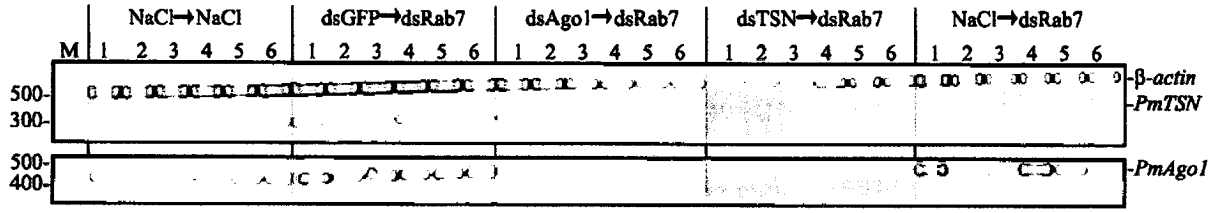

Fig. S2 Expression of *PmAgo1* and *PmTSN* in shrimps from *in vivo* RNAi assay. Each lane shows RT-PCR products of *PmAgo1*, *PmTSN* and *β-actin* from shrimps in each group. The PCR products were resolved by using 1.5% agarose gel electrophoresis and visualized by ethidium bromide staining. M is 2-log DNA ladder.

A

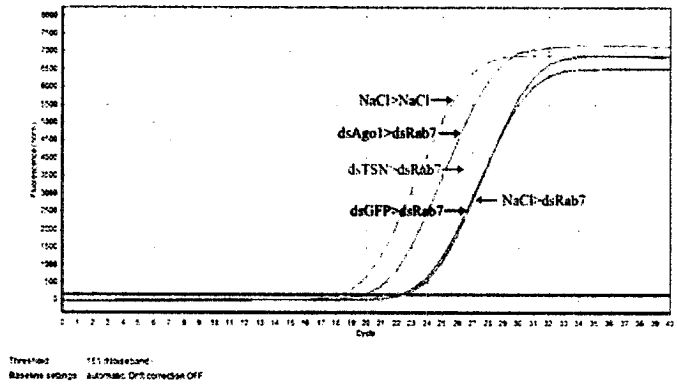

B

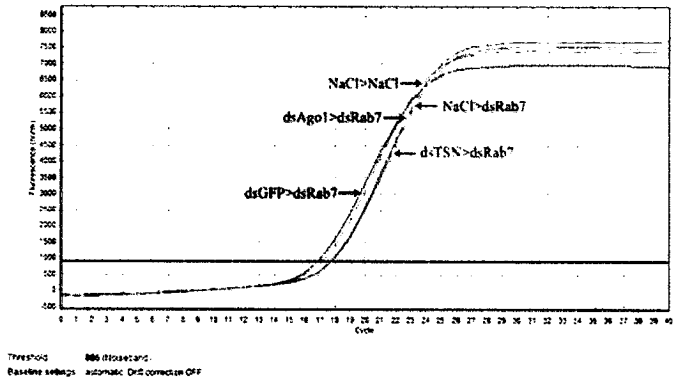

Fig. S3 Knockdown of *PmAgo1* and *PmTSN* diminished RNAi activity in shrimp. qRT-PCR was performed with specific primers for *PmRab7*. *EF1-α* was used as an internal control for normalization. The representative amplification plots of *PmRab7* (A) and *EF-1α* (B) are shown.

4. Discussion

In this study, the interaction between PmTSN and the core component of RISC, PmAgo was demonstrated. Three Ago proteins are identified in *P. monodon*. PmAgo1 or Pem-Ago1 is involved in dsRNA-mediated gene silencing [28], and is responded to yellow head virus infection [32]. Recent study in *Marsupenaeus japonicus* revealed that there are three Ago1 isoforms encoded by shrimp Ago1 gene. Two of the isoforms, including MjAgo1A and MjAgo1B contain an insert sequence in the PIWI domain and play key roles in host RNAi antiviral responses [33]. PmAgo2 is a germ cell-specific Ago protein which its function is not yet to be identified (Udomkit et al, unpublished data). PmAgo3 shares amino acid sequence similarity to *L. vannamei* Ago2 [34] and is expressed ubiquitously in various shrimp tissues (Phetrungnapha et al, unpublished data). Recently, Huang et al. (2012) demonstrated MjAgo2 (which showed 77% amino acid sequence identity with PmAgo3) is required for the function of viral-derived siRNA, suggesting its important role in shrimp RNAi pathway against an invasion of DNA virus [35]. By using Y2H and *in vitro* pull-down assay, it was found that PmTSN specifically interacts with PmAgo1, but not PmAgo2 or PmAgo3, suggesting that PmTSN is one of the components of PmAgo1-RISC. In *C. elegans* and *Drosophila*, the organisms that contain multiple Ago proteins, TSN resides in both RISC and miRNP complex, suggesting that it is a common factor in RISC [19]. Nevertheless, the specific interaction of PmTSN and PmAgo1 indicates that PmTSN is predominantly involved in some sub-class of the RNAi pathways in shrimp.

The mapping of the interaction between PmTSN and PmAgo1 showed unique domains that were required for their binding. PmTSN directly interacted with the N-terminal domain of PmAgo1 via SN1-2 domains, while SN3, SN4, Tudor and SN5 domains were not involved in this interaction. Previous evidences demonstrated that TSN used different domains to interact with different proteins. The four tandem repeats of SN domains interacted with several basal transcription machineries and activator proteins such as EBNA2, TFIIE [16], STAT5 [13], STAT6, RNA polymerase II [14], Pim-1 [15], CBP/p300 [36], and RNA helicase A [37], whereas Tudor-SN5 domains formed a hook to interact with symmetrical dimethylated arginine-containing proteins, SmB/B' and SmD1/D3, and involved in snRNP assembly [17, 38-39]. Intriguingly, recent study in mouse has revealed that Tudor-SN5 domains recognized Piwi, a germ-line-specific clade of Argonaute family proteins, in an arginine methylation-dependent manner, suggesting the role of TSN in Piwi-interacting RNA (piRNA) pathway [40]. In our case, analysis of amino acid sequences of three PmAgo proteins did not show the RG/RA-rich motif, the signature motif of arginine methylation [41]. We speculate that PmTSN uses different domains to interact with distinct PmAgo proteins in different manners. Identification and characterization of the Piwi protein in shrimp will clarify this point better.

TSN is the first RISC-associated protein to be identified. It contains recognizable nuclease domains [19]. Nuclease activity assay revealed that PmTSN possessed a calcium-dependent nuclease activity which was specific to ssRNA, but not dsRNA and DNA. The nuclease activity of TSN has been reported in *Drosophila*, parasites, human, and plants [18-19, 31]. The presence of RNase activity of TSN may involve in the degradation of the remaining mRNA after the site-specific cleavage by Ago [42-43]. Recently, Musiyenko et al. 2012 have demonstrated that, in parasite, *Toxoplasma gondii*, TSN interacted with a single Ago protein in an arginine methylation-dependent

manner, and functioned as a potent second slicer of the parasitic RISC [44]. Whether PmTSN functions as a second slicer in PmAgo1-RISC remains to be clarified.

Our previous study demonstrated that knockdown of *PmTSN* significantly affected the dsRNA-mediated gene silencing in shrimp [22]. According to the results of Y2H and *in vitro* pull-down showing that PmTSN was one of the components of PmAgo1-RISC, we hypothesized that PmAgo1-RISC involved in dsRNA-mediated gene silencing in shrimp. To address this question, the knockdown effects of *PmAgo1* and *PmTSN* on the ability of dsRNA-Rab7 in *PmRab7* silencing were analyzed. Knockdown of *PmAgo1* significantly diminished the ability of dsRNA-Rab7 to inhibit *PmRab7* expression in shrimp. Similarly, the ability of dsRNA-5HT receptor to inhibit *5HT receptor gene* expression in Oka cells was also diminished in *PmAgo1*-knockdown [28]. These results suggest the crucial role of PmAgo1 in shrimp RNAi pathway. Diminishing of the RNAi activity in *PmTSN*-knockdown shrimps can be demonstrated by targeting either an endogenous PmRab7 or an exogenous protease gene of YHV [22]. A reduction in the efficiency of dsRNA-YHV to inhibit YHV replication was shown in *PmTSN*-knockdown shrimps [22]. Even though TSN was reported to function in various aspects of gene expression such as transcription and RNA splicing, expression of β-actin was not changed in *PmTSN*-knockdown shrimp (Fig. S1A). The results implied that an indirect effect of the *PmTSN*-knockdown on other endogenous shrimp gene expression could be excluded. The silencing effect of *PmTSN*-knockdown was less than that observed in *PmAgo1*-knockdown, suggesting that PmTSN is a minor component in PmAgo1-RISC. Recent study has revealed that TSN acted as a scaffold protein which recruited Astrocyte-elevated gene-1 (AEG-1), another RISC-associated factor, to Ago2-RISC, and was essential for the RISC activity in hepatocyte cells [20]. We hypothesized that PmTSN may also function as a bridging or scaffold protein in PmAgo1-RISC. Therefore, knockdown of PmTSN may disrupt the recruitment of other RISC-associated factors to PmAgo1-RISC, resulted in diminishing the RNAi activity in shrimp.

In conclusion, our study demonstrated that PmTSN was a component of PmAgo1-RISC, but not PmAgo2 and PmAgo3. The PmAgo1-PmTSN interaction was mediated through the N-terminal domain of PmAgo1 and SN1-2 domains of PmTSN. To our knowledge, this study is the first study that maps TSN and Ago interacting domains. We also demonstrated that PmTSN possessed a calcium-dependent single-stranded RNase activity, and PmTSN and PmAgo1 were important for dsRNA-mediated gene silencing in shrimp. Our study provided new insights in RISC in shrimp RNAi pathway, expanding the understanding of RNAi-based mechanisms in this economically important species.

Acknowledgements

The authors would like to thank Dr. Apinunt Udomkit for plasmids pGEM-T-PemAgo1, pGEM-T-PemAgo2, pET-17b-stAgo1, and primers for *PmAgo1* amplification, Dr. Witoon Tirasophon for plasmid pET-3a-stGFP, Dr. Saengchan Senapin for plasmid pGBKT7, pGADT7, and yeasts strains AH109 and Y187, and Ms. Chaweewan Chimwai for technical assistance. This work is supported by grants from the Thailand Research Fund (RSA5480002 to C.O.), the Office of the Higher Education Commission and Mahidol University under the National Research University Initiatives. A student fellowship granted to A.P. by the Royal Golden Jubilee Ph.D. Program.

References

[1] Sabin LR, Hanna SL, Cherry S. Innate antiviral immunity in *Drosophila*. Curr Opin Immunol. 2010 22:4-9.

[2] Kemp C, Imler JL. Antiviral immunity in *Drosophila*. Curr Opin Immunol. 2009 21:3-9.

[3] Aliyari R, Wu Q, Li HW, Wang XH, Li F, Green LD, et al. Mechanism of induction and suppression of antiviral immunity directed by virus-derived small RNAs in *Drosophila*. Cell Host Microbe. 2008 4:387-97.

[4] Galiana-Arnoux D, Dostert C, Schneemann A, Hoffmann JA, Imler J-L. Essential function *in vivo* for Dicer-2 in host defense against RNA viruses in *Drosophila*. Nat Immunol. 2006 7:590-7.

[5] van Rij RP, Saleh M-C, Berry B, Foo C, Houk A, Antoniewski C, et al. The RNA silencing endonuclease Argonaute 2 mediates specific antiviral immunity in *Drosophila melanogaster*. Genes & Development. 2006 20:2985-95.

[6] Wang X-H, Aliyari R, Li W-X, Li H-W, Kim K, Carthew R, et al. RNA interference directs innate immunity against viruses in adult *Drosophila*. Science. 2006 312:452-4.

[7] Zambon RA, Vakharia VN, Wu LP. RNAi is an antiviral immune response against a dsRNA virus in *Drosophila melanogaster*. Cell Microbiol. 2006 8:880-9.

[8] Robalino J, Browdy CL, Prior S, Metz A, Parnell P, Gross P, et al. Induction of antiviral immunity by double-stranded RNA in a marine invertebrate. J Virol. 2004 78:10442-8.

[9] Assavalapsakul W, Chinnirunvong W, Panyim S. Application of YHV-protease dsRNA for protection and therapeutic treatment against yellow head virus infection in *Litopenaeus vannamei*. Dis Aquat Organ. 2009 84:167-71.

[10] Tirasophon W, Yodmuang S, Chinnirunvong W, Plongthongkum N, Panyim S. Therapeutic inhibition of yellow head virus multiplication in infected shrimps by YHV-protease dsRNA. Antiviral Res. 2007 74:150-5.

[11] Tirasophon W, Roshorm Y, Panyim S. Silencing of yellow head virus replication in penaeid shrimp cells by dsRNA. Biochem Biophys Res Commun. 2005 334:102-7.

[12] Robalino J, Bartlett T, Shepard E, Prior S, Jaramillo G, Scura E, et al. Double-stranded RNA induces sequence-specific antiviral silencing in addition to nonspecific immunity in a marine shrimp: convergence of RNA interference and innate immunity in the invertebrate antiviral response? J Virol. 2005 79:13561-71.

[13] Paukku K, Yang J, Silvennoinen O. Tudor and nuclease-like domains containing protein p100 function as coactivators for signal transducer and activator of transcription 5. Mol Endocrinol. 2003 17:1805-14.

[14] Yang J, Aittomaki S, Pesu M, Carter K, Saarinen J, Kalkkinen N, et al. Identification of p100 as a coactivator for STAT6 that bridges STAT6 with RNA polymerase II. EMBO J. 2002 21:4950-8.

[15] Leverson JD, Koskinen PJ, Orrico FC, Rainio EM, Jalkanen KJ, Dash AB, et al. Pim-1 kinase and p100 cooperate to enhance c-Myb activity. Mol Cell. 1998 2:417-25.

[16] Tong X, Drapkin R, Yalamanchili R, Mosialos G, Kieff E. The Epstein-Barr virus nuclear protein 2 acidic domain forms a complex with a novel cellular coactivator that can interact with TFIIE. Mol Cell Biol. 1995 15:4735-44.

[17] Gao X, Zhao X, Zhu Y, He J, Shao J, Su C, et al. Tudor staphylococcal nuclease (Tudor-SN) participates in small ribonucleoprotein (snRNP) assembly via interacting with symmetrically dimethylated Sm proteins. J Biol Chem. 2012 287:18130-41.
[18] Sundstrom JF, Vaculova A, Smertenko AP, Savenkov EI, Golovko A, Minina E, et al. Tudor staphylococcal nuclease is an evolutionarily conserved component of the programmed cell death degradome. Nat Cell Biol. 2009 11:1347-54.
[19] Caudy AA, Ketting RF, Hammond SM, Denli AM, Bathoorn AM, Tops BB, et al. A micrococcal nuclease homologue in RNAi effector complexes. Nature. 2003 425:411-4.
[20] Yoo BK, Santhekadur PK, Gredler R, Chen D, Emdad L, Bhutia S, et al. Increased RNA-induced silencing complex (RISC) activity contributes to hepatocellular carcinoma. Hepatology. 2011 53:1538-48.
[21] Grishok A, Sinskey JL, Sharp PA. Transcriptional silencing of a transgene by RNAi in the soma of *C. elegans*. Genes Dev. 2005 19:683-96.
[22] Phetrungnapha A, Panyim S, Ongvarrasopone C. A Tudor staphylococcal nuclease from *Penaeus monodon*: cDNA cloning and its involvement in RNA interference. Fish Shellfish Immunol. 2011 31:373-80.
[23] Studier FW. Protein production by auto-induction in high density shaking cultures. Protein Expr Purif. 2005 41:207-34.
[24] Adachi M, Hamazaki Y, Kobayashi Y, Itoh M, Tsukita S, Furuse M. Similar and distinct properties of MUPP1 and Patj, two homologous PDZ domain-containing tight-junction proteins. Mol Cell Biol. 2009 29:2372-89.
[25] Ongvarrasopone C, Saejia P, Chanasakulniyom M, Panyim S. Inhibition of Taura syndrome virus replication in *Litopenaeus vannamei* through silencing the LvRab7 gene using double-stranded RNA. Arch Virol. 2011 156:1117-23.
[26] Ongvarrasopone C, Roshorm Y, Panyim S. A simple and cost effective method to generate dsRNA for RNAi studies in invertebrates. ScienceAsia. 2007 33:35-9.
[27] Ongvarrasopone C, Chanasakulniyom M, Sritunyalucksana K, Panyim S. Suppression of PmRab7 by dsRNA inhibits WSSV or YHV infection in shrimp. Mar Biotechnol (NY). 2008 10:374-81.
[28] Dechklar M, Udomkit A, Panyim S. Characterization of Argonaute cDNA from *Penaeus monodon* and implication of its role in RNA interference. Biochem Biophys Res Commun. 2008 367:768-74.
[29] Pfaffl MW. A new mathematical model for relative quantification in real-time RT-PCR. Nucleic Acids Res. 2001 29:e45.
[30] Pham JW, Pellino JL, Lee YS, Carthew RW, Sontheimer EJ. A Dicer-2-dependent 80S complex cleaves targeted mRNAs during RNAi in *Drosophila*. Cell. 2004 117:83-94.
[31] Hossain MJ, Korde R, Singh S, Mohmmed A, Dasaradhi PV, Chauhan VS, et al. Tudor domain proteins in protozoan parasites and characterization of *Plasmodium falciparum* tudor staphylococcal nuclease. Int J Parasitol. 2008 38:513-26.
[32] Unajak S, Boonsaeng V, Jitrapakdee S. Isolation and characterization of cDNA encoding Argonaute, a component of RNA silencing in shrimp (*Penaeus monodon*). Comp Biochem Physiol B Biochem Mol Biol. 2006 145:179-87.
[33] Huang T, Zhang X. Contribution of the argonaute-1 isoforms to invertebrate antiviral defense. PLoS One. 2012 7:e50581.
[34] Labreuche Y, Veloso A, de la Vega E, Gross PS, Chapman RW, Browdy CL, et al. Non- specific activation of antiviral immunity and induction of RNA

interference may engage the same pathway in the Pacific white leg shrimp *Litopenaeus vannamei*. Dev Comp Immunol. 2010 34:1209-1218.

[35] Huang T, Zhang X. Host defense against DNA virus infection in shrimp is mediated by the siRNA pathway. Eur J Immunol. 2012 43:1-10.

[36] Valineva T, Yang J, Palovuori R, Silvennoinen O. The transcriptional co-activator protein p100 recruits histone acetyltransferase activity to STAT6 and mediates interaction between the CREB-binding protein and STAT6. J Biol Chem. 2005 280:14989-96.

[37] Valineva T, Yang J, Silvennoinen O. Characterization of RNA helicase A as component of STAT6-dependent enhanceosome. Nucl Acids Res. 2006 34:3938-46.

[38] Yang J, Valineva T, Hong , Bu T, Yao Z, Jensen ON, et al. Transcriptional co-activator protein p100 interacts with snRNP proteins and facilitates the assembly of the spliceosome. Nucleic Acids Res. 2007 35:4485-94.

[39] Shaw N, Zhao M, Cheng C, Xu H, Saarikettu J, Li Y, et al. The multifunctional human p100 protein 'hooks' methylated ligands. Nat Struct Mol Biol. 2007 14:779-84.

[40] Liu K, Chen C, Guo Y, Lam R, Bian C, Xu C, et al. Structural basis for recognition of arginine methylated Piwi proteins by the extended Tudor domain. Proc Natl Acad Sci U S A. 2010 107:18398-403.

[41] Chen C, Jin J, James DA, Adams-Cioaba MA, Park JG, Guo Y, et al. Mouse Piwi interactome identifies binding mechanism of Tdrkh Tudor domain to arginine methylated Miwi. Proc Natl Acad Sci U S A. 2009 106:20336-41.

[42] Sontheimer EJ. Assembly and function of RNA silencing complexes. Nat Rev Mol Cell Biol. 2005 6:127-38.

[43] Schwarz DS, Tomari Y, Zamore PD. The RNA-Induced Silencing Complex Is a Mg2+-Dependent Endonuclease. Current biology : CB. 2004 14:787-91.

[44] Musiyenko A, Majumdar T, Andrews J, Adams B, Barik S. PRMT1 methylates the single Argonaute of *Toxoplasma gondii* and is important for the recruitment of Tudor nuclease for target RNA cleavage by antisense guide RNA. Cell Microbiol. 2012 14:882-901.

Part III: Transcriptional profiling of *Marsupenaeus japonicus* in response to MjTSN and MjArgonaute-1 knockdown

Results

1 Transcriptional profiling of the transcripts affected by MjAgo1 and MjTSN knockdown

Previous data demonstrated that PmTSN was a component of PmAgo1-RISC. Therefore, in order to gain more insights in the role of Ago1-RISC in shrimp RNAi pathway, the transcripts which were regulated by Ago1-RISC components were identified. Microarray was employed to study the expression profiles of the transcripts affected by *MjAgo1* and *MjTSN* knockdown in kuruma shrimps. In this study, the dsRNA-SN3 and dsRNA-Ago1 designed from *PmTSN* and *PmAgo1* sequences were used to knockdown the expression of *MjTSN* and *MjAgo1 in vivo*. RT-PCR analysis demonstrated that injection of dsRNA-SN3 and dsRNA-Ago1 could specifically knockdown the expression of *MjTSN* and *MjAgo1*, respectively. In addition, injection of dsRNA-GFP had no effect on the expression of *MjTSN* and *MjAgo1*, indicating the specificity of dsRNA-SN3 and dsRNA-Ago1 (Fig. 1).

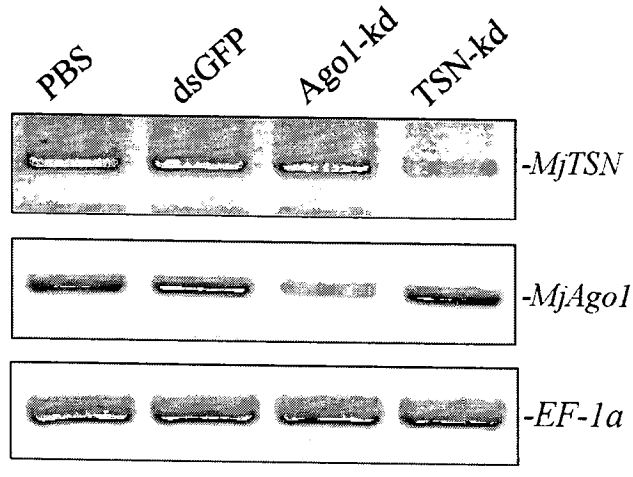

Fig. 1 *In vivo* gene knockdown of *MjTSN* and *MjAgo1* in kuruma shrimps. Representative gels showing RT-PCR analysis of *MjTSN* and *MjAgo1* expression. The dsRNA-SN3 and dsRNA-Ago1 designed from *PmTSN* and *PmAgo1* sequences were used to knockdown *MjTSN* and *MjAgo1 in vivo*. Fifty micrograms each of dsRNA-SN3, dsRNA-Ago1, or dsRNA-GFP were injected into shrimps, and hemolymph was collected after 3 days-post dsRNA injection. *MjEF-1α* was used as an internal control gene. Lane M, 100-bp DNA ladder. PBS, PBS-injected; dsGFP, dsRNA-GFP-injected; Ago-kd, *MjAgo1*-knockdown; *MjTSN*-knockdown shrimps.

To perform microarray analysis, the 8 x 15K custom microarray slides with 14411 probes were designed from GenBank and EST sequences of the kuruma shrimp. One-color microarray hybridization was performed with total RNA from PBS-injected (PBS), dsRNA-GFP-injected (dsGFP), *MjAgo1*-knockdown (Ago1-kd), and *MjTSN*-knockdown shrimps (TSN-kd). Normalization was performed based on the median of

the PBS-injected group. One-way ANOVA unequal variance with Benjamini-Hochberg's multiple correcting test was used for statistical analysis. An overview of the microarray results is shown in Table 1. A total of 2393 transcripts with ≥ 2-fold change ($p < 0.05$) in at least one of the four treatment groups were observed. These transcripts were subsequently clustered by using hierarchical clustering algorithm. The hierarchically-clustered heat map is shown in Fig. 2. The clustering data revealed similar expression profiles of all dsRNA-injected shrimps. Nevertheless, the expression profile of TSN-kd is more similar to dsGFP, as they are in the same cluster, while Ago1-kd is unique and localized to a separated branch.

The transcripts with ≥ 2-fold change ($p < 0.05$) in each treatment group are shown in Table 1. Ago1-kd contains 663 up-regulated and 1027 down-regulated, while TSN-kd contains 424 up-regulated and 863 down-regulated transcripts. dsGFP contains 433 up-regulated and 571 down-regulated transcripts. The distribution of these transcripts among Ago1-kd, TSN-kd, and dsGFP groups were represented in Venn diagram (Fig. 3). The result showed that injection of dsRNA dramatically altered gene expression in shrimp, as 263 up-regulated and 285 down-regulated transcripts were observed in all dsRNA-injected groups. Among these, the genes involved in RNAi pathway were found to be up-regulated upon dsRNA injection, including *MjAgo2*, *MjDicer-2*, *Mjsid-1* and *Mjmov-10* genes (Table 2). In addition, within the down-regulated genes, *MjAgo1* and *MjTSN* were found to be down-regulated for 2.8 and 4.8 folds, respectively, confirming the effectiveness of dsRNA in *MjAgo1* and *MjTSN* knockdown.

For more comprehensive understanding of the differentially expressed genes, they were classified according to their predicted function. Functional classification of the differentially expressed genes is shown in Fig. 4. The functional classifications of the putative genes are: (1) cellular process–any process that is carried out at the cellular level; (2) enzyme and metabolism; (3) biological regulation–any process that modulates a measurable attribute of any biological process such as quality or function; (4) cellular response; (5) signaling pathway; (6) cell cycle and proliferation; (7) cell death; (8) differentiation and development; (9) cell structure and cellular compartment organization; and (10) unknown.

It has been shown that suppression of the core RNAi machineries led to general loss of RNAi mechanism. Therefore, the transcripts which were up-regulated upon knockdown of *MjAgo1*, the core component of shrimp Ago1-RISC, possibly represented the putative targets of miRNA or RNAi-mediated gene silencing in shrimp. From Venn diagram, a total of 294 transcripts which represent 274 unique genes were up-regulated exclusively in Ago1-kd (Fig. 3). Functional classification of these up-regulated transcripts revealed that knockdown of *MjAgo1* affected various biological processes in shrimp cells (Fig. 4A). Apart from unknown genes, the greatest number of up-regulated genes was related to cellular process (21.4%), while the lowest was related to cell death (1.4%) and differentiation and development (1.4%). Among these up-regulated genes, heat shock protein 70 (*hsp70*) was the most up-regulated gene (16.6 fold).

Interestingly, a common set of 58 up-regulated (58 unique genes) was observed in both Ago1-kd and TSN-kd (Fig. 3). Functional classification of these up-regulated transcripts indicated that with the exception of unknown genes, the greatest number of the up-regulated genes was related to enzyme and metabolism (22.4%), while the lowest was related to cell structure and cellular compartment organization (1.7%) and cell death (1.7%) (Fig. 4B). Among these up-regulated genes, glycine N-acyltransferase was the most up-regulated gene which was up-regulated 18.9 and 8.4 fold in Ago-kd

and TSN-kd shrimp, respectively. List of the top ten most up-regulated genes found in both Ago1-kd and TSN-kd is shown in Table 3. Genes related to shrimp innate immunity, including Kazal-type serine proteinase inhibitors 1 (KPI-1) and Persephone (PSH) were found to be up-regulated in both Ago1-kd and TSN-kd. In addition, the up-regulation of the genes involved in DNA repair, including Fanconi anemia group M protein and DNA cross-link repair 1a protein was observed.

A large number of transcripts were found to be down-regulated in TSN-kd shrimps (Fig. 4). Functional classification of 310 down-regulated transcripts revealed that knockdown of *MjTSN* affected various biological processes in shrimp cells. Apart from unknown genes, the greatest number of the up-regulated genes was related to enzyme and metabolism (12.58%), while the lowest was related to cell death (0.32%) (Fig. 4C). With the exception of the unknown genes, *MjTSN*, hexamethylene bisacetamide-inducible protein 1 (HEXIM1) was the most down-regulated gene (3.9 fold). The top ten most down-regulated genes are listed in Table 4. Interestingly, down-regulation of the genes related to signaling pathway, including dedicator of cytokinesis protein 7 (DOCK7) and serine/threonine-protein kinase 38 (STK38) was observed. Genes involved in mRNA splicing, including serine/arginine-rich splicing factor 18 (SR18) and heterogeneous nuclear ribonucleoprotein splicing factor Q (HRP-Q) were also found to be down-regulated in TSN-kd shrimps.

2. Validation of the microarray results by qRT-PCR

The microarray results were validated by using qRT-PCR. Four of the up-regulated genes found in both Ago1-kd and TSN-kd shrimps were selected for confirmation by qRT-PCR. PBS group was used as a control group for normalization. The relative expression ratio of the transcripts was calculated by comparative Ct method. The results showed that glycine N-acyltransferase (GNAT), carbonic anhydrase-related protein (CARP), tripartite motif-containing protein 3 (TRIM3), and Pirin-like protein were up-regulated in both Ago-kd and TSN-kd groups when compared to the PBS and GFP groups, confirming the microarray results (Fig. 5).

Table 1 Overview of gene expression profiles of the *MjAgo1*-knockdown, *MjTSN*-knockdown and dsRNA-GFP-injected shrimps

	Numbers of transcripts		
Probes	14411		
All entities	13935		
Filtered on flags (detected, not detected)	13935		
Filtered on expression (1.548 – 799248.188 in raw data)	13935		
Filtered on error (correlation of variation < 50%)	11931		
1-way ANOVA unequal variance with corrected p-value ($p < 0.05$)	5501		
Fold change ≥ 2.0 (total)	2393		
	Ago-kd	**TSN-kd**	**dsGFP**
Differentially expressed ≥ 2.0 fold	1690	1287	1004
- Up ≥ 2.0 fold	663	424	433
- Down ≥ 2.0 fold	1027	863	571

Table 2 List of the RNAi-related genes which found to be differentially expressed in dsRNA-injected shrimps

Probes	Fold change			RNAi-related genes
	Ago1-kd	TSN-kd	dsGFP	
CUST_6755_PI427842156	8.1	4.9	5.8	MjDicer2
CUST_9451_PI427842156	29.8	29.2	20.5	MjAgo2
CUST_7829_PI427842156	8.8	5.9	5.5	Mjsid-1
CUST_8967_PI427842156	15.1	14.1	15.9	Mjmov-10
CUST_6572_PI427842156	-2.8	-0.2	-0.07	MjAgo1
CUST_1064_PI427842156	-0.88	-4.8	-0.37	MjTSN

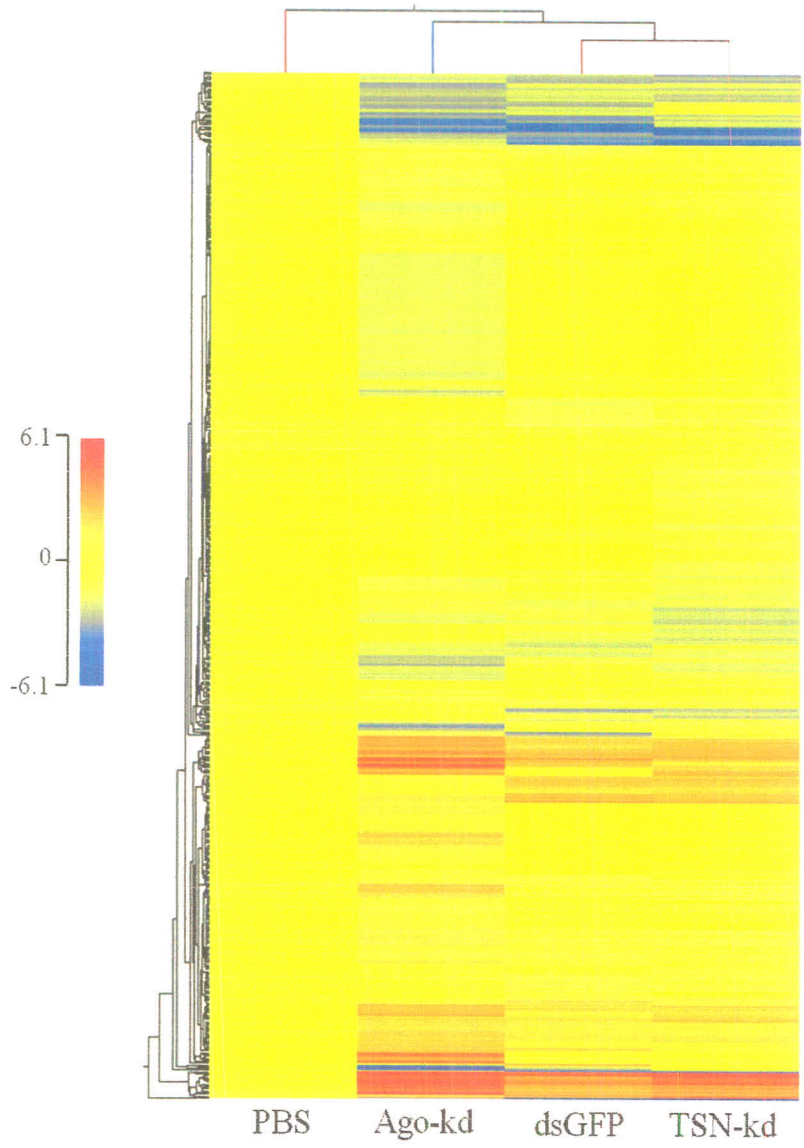

Fig. 2 Gene expression profiles of *MjAgo1*-, *MjTSN*-knockdown shrimps and dsRNA-GFP-injected shrimps comparing to PBS-injected shrimps

Hierarchically-clustered heat map showing the differentially expressed transcripts in all profiles. Normalization was performed based on the median of PBS-injected group. A total of 2393 differentially expressed transcripts were selected as at least 2-fold regulated ($p < 0.05$, one-way ANOVA) in at least one of four treatment groups. Transcripts shown in red are up-regulated and transcripts shown in blue are down-regulated relative to PBS-injected shrimp, while yellow indicates no change in expression. The intensity of the colors is shown in log 2 ratio. PBS, PBS-injected; dsGFP, dsRNA-GFP-injected; Ago-kd, *MjAgo1*-knockdown; *MjTSN*-knockdown shrimps.

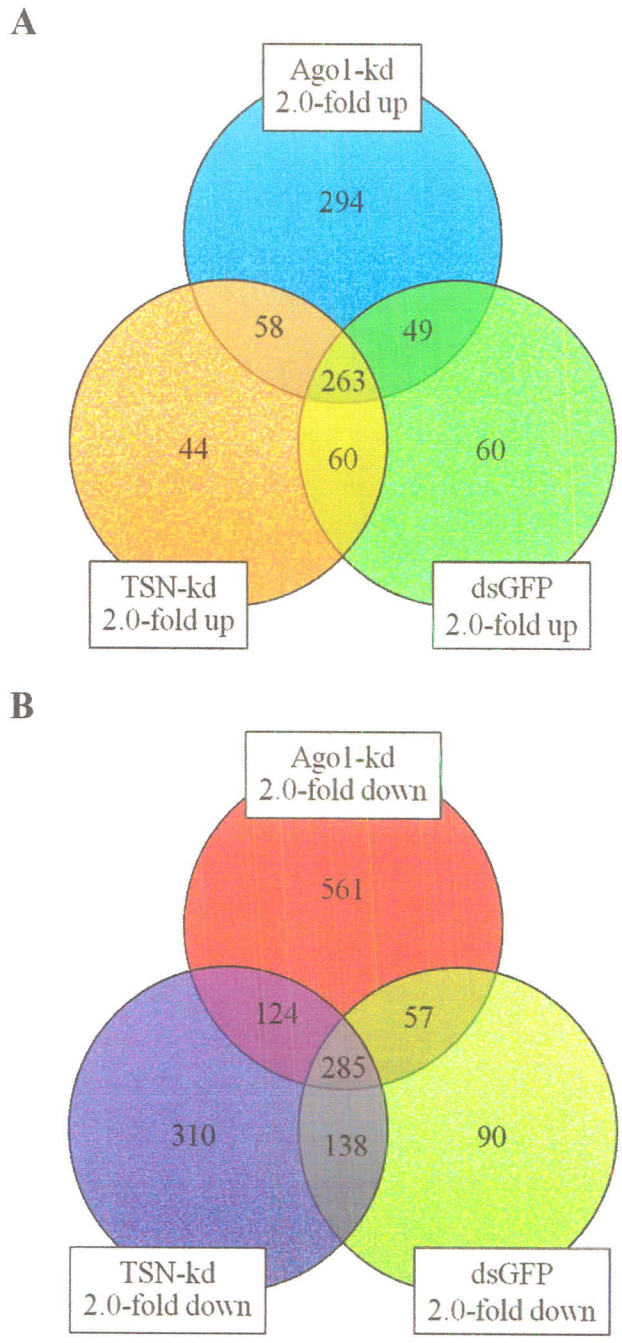

Fig. 3 Transcriptome changes upon *MjAgo1*- and *MjTSN*-knockdown in kuruma shrimps

Venn diagrams show the overlaps of differentially expressed transcripts with ≥ 2-fold change in *MjAgo1*-knockdown (Ago1-kd), *MjTSN*-knockdown (TSN-kd) and dsRNA-GFP-injected shrimps (dsGFP). (A) up-regulated transcripts (B) down-regulated transcripts.

A

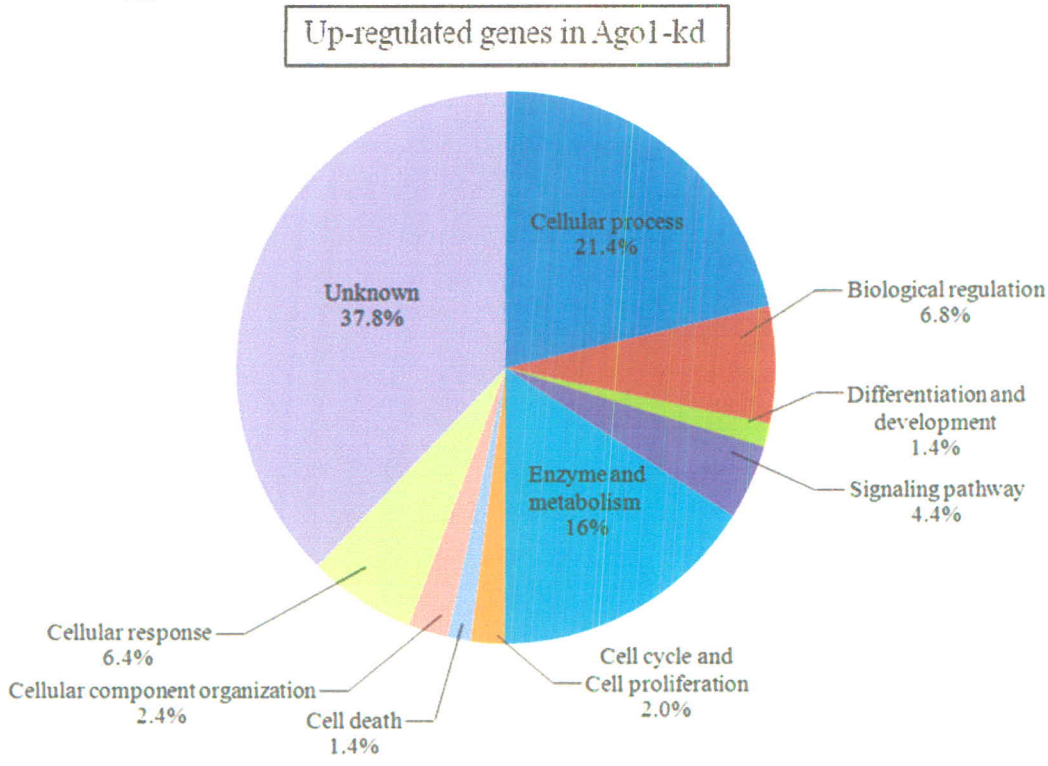
Up-regulated genes in Ago1-kd
Cellular process
21.4%
Biological regulation
6.8%
Differentiation and
development
1.4%
Signaling pathway
4.4%
Cell cycle and
Cell proliferation
2.0%
Cell death
1.4%
Cellular component organization
2.4%
Cellular response
6.4%
Unknown
37.8%
Enzyme and
metabolism
16%

B

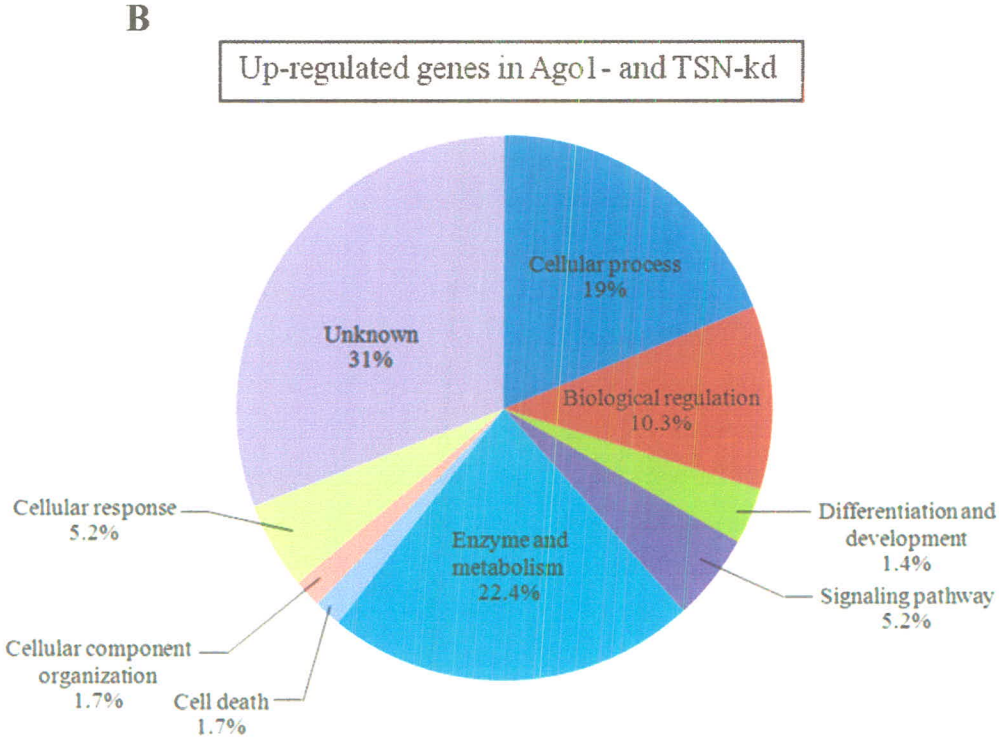
Up-regulated genes in Ago1- and TSN-kd
Cellular process
19%
Biological regulation
10.3%
Differentiation and
development
1.4%
Signaling pathway
5.2%
Cell death
1.7%
Cellular component
organization
1.7%
Cellular response
5.2%
Unknown
31%
Enzyme and
metabolism
22.4%

C

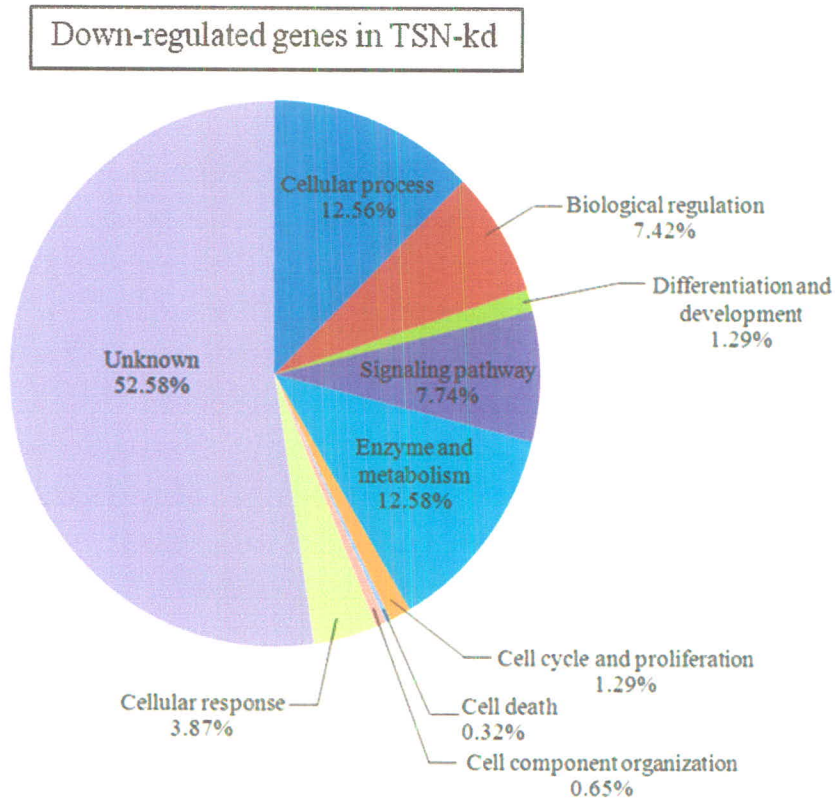

Fig. 4 Functional classification and distribution of the differentially expressed genes based on their functions

Pie diagrams depict the percentage of functional classification and distribution of the differentially expressed genes from microarray. The predicted functions of the putative genes were inferred from UniProt and FlyBase, or from BlastX against AmiGO. (A) up-regulated genes found exclusively in MjAgo1-knockdown shrimps (Ago1-kd). (B) up-regulated genes found in both MjAgo1- and MjTSN-knockdown shrimps (TSN-kd). (C) down-regulated genes found exclusively in MjTSN-knockdown shrimps.

Table 3 List of the top ten most up-regulated genes found in both *MjAgo1*- and *MjTSN*-knockdown shrimps

Probes	Fold change in Ago1-kd	Fold change in TSN-kd	Putative genes	Putative functions
CUST_4689_PI427842156	18.9	8.4	glycine N-acyltransferase	posttranslation modification of proteins
CUST_8566_PI427842156	18.0	7.9	carbonic anhydrase-related protein	a non-catalytic carbonic anhydrase which is predominantly expressed in brain
CUST_986_PI427842156	11.7	6.4	cuticle protein 72EA	a structural constituent of cuticle
CUST_451_PI427842156	10.4	5.8	Kazal-type serine protease inhibitor	an inhibitor of serine protease, immune defense response
CUST_12719_PI427842156	9.8	4.9	carboxypeptidase A2	proteolysis, protein metabolism
CUST_2203_PI427842156	6.6	4.4	tripartite motif-containing protein 3	a protein which composed of three zinc-binding domains, a RING, a B-box type 1 and 2, and a coiled-coil region; probably involved in myosin V-mediated cargo transport
CUST_4612_PI427842156	7.7	3.9	Pirin-like protein	a putative transcription coactivator
CUST_8862_PI427842156	4.2	3.2	Draper protein	phagocytosis of apoptotic cells
CUST_422_PI427909186	2.5	3.2	pigment-dispersing hormone peptides	a peptide hormone with an unknown function, probably involved in pigment granules transport
CUST_3877_PI427842156	2.0	3.1	Serpin	an inhibitor of serine protease, immune defense response

*Unknown genes and hypothetical proteins were excluded.

*Putative genes and their functions are ascribed by homology to already functionally annotated genes in the GenBank, UniProt and AmiGO databases.

Table 4 List of the top ten most down-regulated genes found exclusively in *MjTSN*-knockdown shrimp

Probes	Fold change	Putative genes	Putative functions
CUST_6880_PI427842156	-3.9	HEXIM1	inhibitor of the positive transcription elongation factor b
CUST_7137_PI427842156	-3.9	hemocyte protein-glutamine gamma-glutamyltransferase	posttranslational modification of proteins
CUST_4876_PI427842156	-3.8	fatty-acid amide hydrolase 2	fatty acid amides metabolism
CUST_12210_PI427842156	-3.3	galactoside 2-alpha-L-fucosyltransferase 2-like	posttranslational modification of proteins
CUST_6766_PI427842156	-3.3	enhancer of mRNA-decapping protein 4	mRNA destabilization via decapping process
CUST_362_PI426112206	-3.2	wsv367	unknown
CUST_8_PI427909186	-3.2	1,3-beta-D-glucan-binding protein	immune defense response
CUST_4233_PI427842156	-3.2	CTP synthase	synthesis of CTP
CUST_5122_PI427842156	-3.1	heat shock protein 67B2	heat stress response
CUST_2055_PI427842156	-3.1	solute carrier family 20 member 1	phosphate ion transport

*Unknown genes and hypothetical proteins were excluded.

*Putative genes and their functions are ascribed by homology to already functionally annotated genes in the GenBank, UniProt and AmiGO databases.

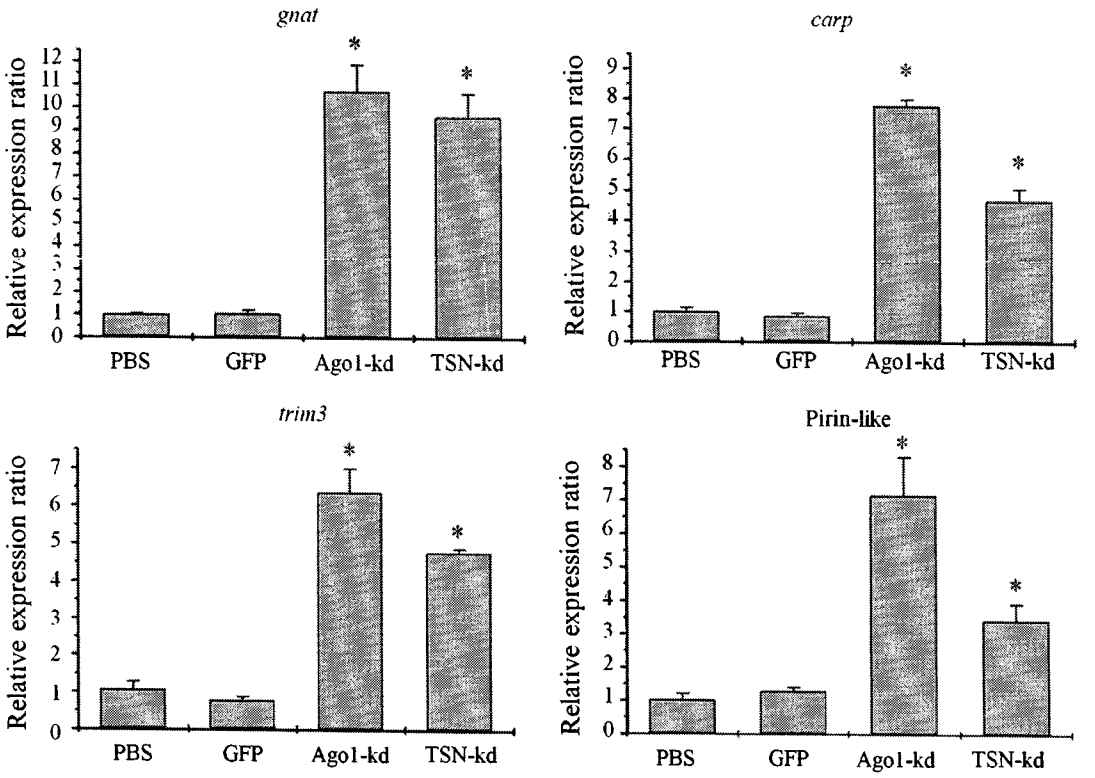

Fig. 5 Validation of microarray results by using qRT-PCR

Four of the transcripts which up-regulated in both *MjAgo1*- and *MjTSN*-knockdown shrimps were selected for qRT-PCR, including glycine N-acyltransferase (GNAT), carbonic anhydrase-related protein (CARP), tripartite motif-containing protein 3 (TRIM3), and Pirin-like protein. *EF-1α* was used as an internal control gene for normalization. Relative expression ratio of the transcripts was calculated by using comparative Ct method ($2^{-\Delta\Delta Ct}$). The asterisks represent significant difference ($p < 0.05$) between the experimental groups and PBS-injected. Bars represent means ± SEM (n = 3). PBS, PBS-injected; GFP, dsRNA-GFP-injected; Ago1-kd, *MjAgo1*-knockdown; TSN-kd, *MjTSN*-knockdown shrimps.

Discussion

TSN is a multifunctional protein involved in a variety of cellular processes [1-2]. Therefore, to further explore the role of TSN in shrimp, the genes differentially expressed in TSN-kd shrimps were analyzed. Notably, a large number of transcripts were found to be down-regulated exclusively in TSN-kd. Functional classification of 310 down-regulated genes suggested that TSN is involved in a variety of biological processes in shrimp. With the exception of the unknown genes, HEXIM1 was the most down-regulated gene. HEXIM1 is known as the inhibitor of positive transcription elongation factor b (p-TEFb), a cyclin-dependent kinase which plays an essential role in the regulation of transcription by RNA polymerase II (Pol II) [3]. Inhibition of p-TEFb activity by HEXIM1 blocks most Pol II transcription [4]. The role of TSN in the transcriptional activation was described by several studies [5-9]. However, there is no report about the role of TSN in the elongation step of the transcriptional process. Down-regulation of *hexim1* upon TSN knockdown in shrimp suggested the possible role of TSN in the regulation of the elongation step of the transcriptional process. Interestingly, the genes involved in intracellular signaling pathway were found to be down-regulated in TSN-kd shrimp, such as DOCK7 and STK38. DOCK7 is a guanine nucleotide exchange factor (GEF) which involved in an activation of Rho GTPase family protein, specifically, Rac [10]. In neuron cells, activation of Rac and Cdc42 by Dock7 resulted in an activation of the c-Jun N-terminus kinase (JNK) signaling pathway [11]. STK38 is a serine/threonine protein kinase belonging to the NDR family of the AGC kinases [12]. STK38 was shown to be a negative regulator of the mitogen-activated protein kinase (MAPK) signaling pathway by interacting with MEKK1/2 to inhibit its autophosphorylation [13]. Down-regulation of *dock7* and *stk38* in TSN-kd shrimp might imply the involvement of TSN in these signaling pathways. In addition, the genes related to mRNA splicing such as, SR18 [14] and HRP-Q [15] were also down-regulated in TSN-kd shrimp. The role of TSN in mRNA splicing was described by several studies [16-17]. Although down-regulation of these genes upon knockdown of TSN might be linked to the functions of TSN in the elongation step of the transcriptional process, signaling pathway, and mRNA splicing in shrimp, further studies are needed to clarify these scenarios better.

References

[1] Li CL, Yang WZ, Chen YP, Yuan HS. Structural and functional insights into human Tudor-SN, a key component linking RNA interference and editing. Nucleic Acids Res. 2008;36(11):3579-89.

[2] Tsuchiya N, Ochiai M, Nakashima K, Ubagai T, Sugimura T, Nakagama H. SND1, a component of RNA-induced silencing complex, is up-regulated in human colon cancers and implicated in early stage colon carcinogenesis. Cancer Res. 2007;67(19):9568-76.

[3] Michels AA, Fraldi A, Li Q, Adamson TE, Bonnet F, Nguyen VT, et al. Binding of the 7SK snRNA turns the HEXIM1 protein into a P-TEFb (CDK9/cyclin T) inhibitor. EMBO J. 2004;23(13):2608-19.

[4] Chao SH, Price DH. Flavopiridol inactivates P-TEFb and blocks most RNA polymerase II transcription in vivo. J Biol Chem. 2001;276(34):31793-9.

[5] Tong X, Drapkin R, Yalamanchili R, Mosialos G, Kieff E. The Epstein-Barr virus nuclear protein 2 acidic domain forms a complex with a novel cellular coactivator that can interact with TFIIE. Mol Cell Biol. 1995;15(9):4735-44.

[6] Leverson JD, Koskinen PJ, Orrico FC, Rainio EM, Jalkanen KJ, Dash AB, et al. Pim-1 kinase and p100 cooperate to enhance c-Myb activity. Mol Cell. 1998;2(4):417-25.

[7] Valineva T, Yang J, Palovuori R, Silvennoinen O. The transcriptional co-activator protein p100 recruits histone acetyltransferase activity to STAT6 and mediates interaction between the CREB-binding protein and STAT6. J Biol Chem. 2005;280(15):14989-96.

[8] Yang J, Aittomaki S, Pesu M, Carter K, Saarinen J, Kalkkinen N, et al. Identification of p100 as a coactivator for STAT6 that bridges STAT6 with RNA polymerase II. EMBO J. 2002;21(18):4950-8.

[9] Paukku K, Yang J, Silvennoinen O. Tudor and nuclease-like domains containing protein p100 function as coactivators for signal transducer and activator of transcription 5. Mol Endocrinol. 2003;17(9):1805-14.

[10] Watabe-Uchida M, John KA, Janas JA, Newey SE, Van Aelst L. The Rac activator DOCK7 regulates neuronal polarity through local phosphorylation of stathmin/Op18. Neuron. 2006;51(6):727-39.

[11] Yamauchi J, Miyamoto Y, Chan JR, Tanoue A. ErbB2 directly activates the exchange factor Dock7 to promote Schwann cell migration. J Cell Biol. 2008;181(2):351-65.

[12] Tamaskovic R, Bichsel SJ, Hemmings BA. NDR family of AGC kinases--essential regulators of the cell cycle and morphogenesis. FEBS Lett. 2003;546(1):73-80.

[13] Enomoto A, Kido N, Ito M, Morita A, Matsumoto Y, Takamatsu N, et al. Negative regulation of MEKK1/2 signaling by serine-threonine kinase 38 (STK38). Oncogene. 2008;27(13):1930-8.

[14] Fu XD. The superfamily of arginine/serine-rich splicing factors. RNA. 1995;1(7):663-80.

[16] Kabat JL, Barberan-Soler S, Zahler AM. HRP-2, the Caenorhabditis elegans homolog of mammalian heterogeneous nuclear ribonucleoproteins Q and R, is an alternative splicing factor that binds to UCUAUC splicing regulatory elements. J Biol Chem. 2009;284(42):28490-7.

[16] Yang J, Valineva T, Hong J, Bu T, Yao Z, Jensen ON, et al. Transcriptional co-activator protein p100 interacts with snRNP proteins and facilitates the assembly of the spliceosome. Nucleic Acids Res. 2007;35(13):4485-94.

[17] Gao X, Zhao X, Zhu Y, He J, Shao J, Su C, et al. Tudor staphylococcal nuclease (Tudor-SN) participates in small ribonucleoprotein (snRNP) assembly via interacting with symmetrically dimethylated Sm proteins. J Biol Chem. 2012;287(22):18130-41.

Part IV: Identification and characterization of *Penaeus monodon* Tudor staphylococcal nuclease interacting protein, laminin receptor

Abstract

Penaeus monodon Tudor staphylococcal nuclease (PmTSN) is a multifunctional protein involved in many biological processes and also acts as one of the components in the RNA-induced silencing complexes (RISC) in shrimp. To identify the interacting proteins of PmTSN, yeast two-hybrid screening on white spot syndrome virus (WSSV)-infected shrimp hemocyte cDNA library was performed by mating approach. By screening 1.38 million clones (6.57% mating efficiency), 10 diploids showed the positive results. After sequence analysis by using Blastx, the results showed that five clones were Laminin receptor (40S Ribosomal protein SA or Lamr), one was histone H2A, and four were unknown. Previous data showed that LamR was identified as a binding protein for capsid protein (VP1) of taura syndrome virus (TSV) and envelope protein gp116 of yellow head virus (YHV). To elucidate the involvement of the interaction between PmTSN and laminin receptor upon YHV and TSV infection, an *in vitro* pull down assay was performed. The interaction of PmTSN and PmLamr cannot form a complex with viral binding proteins gp116 of YHV or VP1 of TSV. These results suggested that the effect of the interaction between PmTSN and Lamr may not play a significant role during viral infection.

KEY WORDS: TUDOR STAPHYLOCOCAL NUCLEASE/ LAMININ RECEPTOR/ VP1/ GP116

Results

1. Y2H screening of shrimp hemocyte cDNA library

Yeast two-hybrid screening was performed to identify the interacting proteins of PmTSN. Yeast strain Y187 harboring pGBKT7 was used to screen WSSV-infected shrimp hemocyte cDNA library in yeast strain AH109 by using mating approach. By screening 1.38 million clones (6.57% mating efficiency), 77 positive diploids were observed on the triple dropout medium (SD/-W/-L/-H). After confirming, 10 diploids showed the positive results observed on the quadruple dropout medium containing 40 mg/ml of X-α-Gal (SD/-W/-L/-H/-A/X-α-gal) (Fig. 1). Plasmids were then extracted from positive diploids, transformed to *E. coli* DH5α, and subjected for DNA sequencing. After sequence analysis by using Blastx, the results showed that five clones were Laminin receptor (40S Ribosomal protein SA or Lamr), one was histone H2A, and four were unknown.

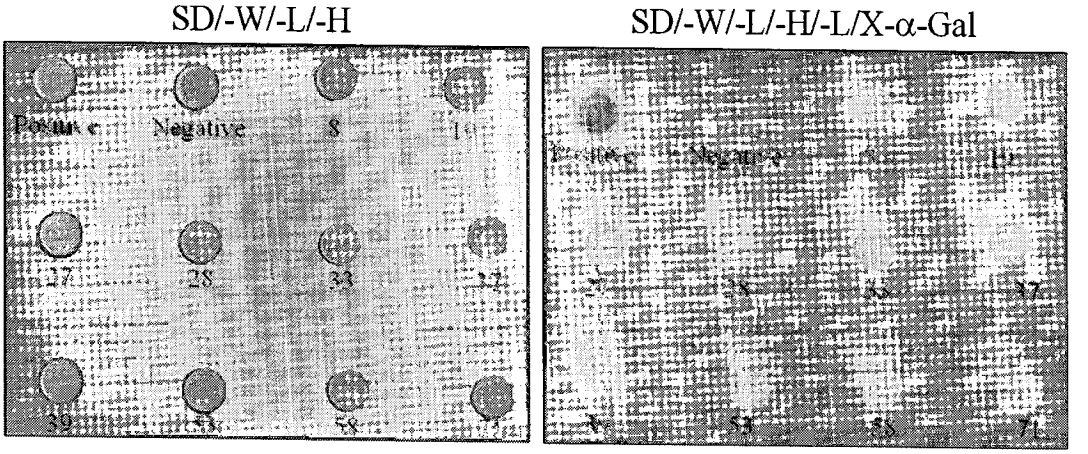

Fig. 1 Confirmation of the positive diploids obtained from Y2H screening of shrimp hemocyte cDNA library

Yeast strain Y187 harboring pGBKT7-TSN was used to screen WSSV-infected shrimp hemocyte cDNA library in AH109 by mating approach. After screening on SD/-W/-L/-H, 77 diploids were obtained. They were cultured on the SD/-W/-L/-H/-A/X-α-Gal medium to confirm the positive interaction. The numbers indicate ten diploids showing positive results after confirmation. Positive control (+), diploids harboring pGBKT7-p53/pGADT7-T; Negative control (-), diploids harboring empty pGBKT7/pGADT7-T; 8, 27, 28, 58 and 71, Lamr; 39, Histone H2A; 19, unknown 1; 33, unknown 2; 37, unknown 3; 53, unknown 4.

2. *In vitro* pull-down assay to study the interaction of *PmTSN*, laminin receptor and TSV capsid protein

An *in vitro* pull-down assay was conducted to study the interaction of GST-TSN, His-Lamr and His-VP1 and -VP3. Purified GST-TSN bound to Glutathione agarose beads was incubated with His-tagged Lamr and His-tagged VP1 or VP3, respectively, Following the elution step, western blot analysis using anti-his monoclonal antibody and HRP-conjugated goat-α-mouse antibody were used to detect His-Lamr, -VP1 or -VP3. The results showed that GST-TSN bound to His-Lamr whereas TSN-Lamr complex cannot form a complex with His-VP1 or His-VP3 (Fig. 2). In addition, GST-TSN alone cannot form the complex with His-VP1 or His-VP3. In contrast, none of these fusion proteins; His-Lamr, -VP1 or -VP3 was found to form a complex with GST protein alone. The result of an *in vitro* pull-down assay revealed that the interaction between GST-TSN and His-tagged Lamr cannot form a complex with His-tagged VP1.

3. YHV lysate from shrimp tissues

YHV lysate was extracted from shrimp tissue. The concentration of YHV lysate protein was determined by Bradford's protein assay and confirmed by western blot analysis using anti-gp116 and anti-gp64 of YHV. The result showed that anti-gp116 and anti-gp64 of YHV can be used to detect YHV envelope protein gp116 and gp64 of the YHV lysate, respectively (Fig. 3).

4. *In vitro* pull-down assay to study the interaction of *PmTSN*, *PmLamr* and YHV envelope protein

An *in vitro* pull-down assay was conducted to study the interaction of GST-TSN, His-Lamr and gp116. The purified GST-TSN bound to Glutathione agarose beads was incubated with His-Lamr and YHV lysate, respectively. Following an elution, western blot analysis using anti-His monoclonal antibody and HRP-conjugated goat-α-mouse antibody were used to detect His-Lamr while anti-GST antibody and HRP-conjugated goat-α-rabbit antibody were used to detect GST-TSN. In addition, anti-gp116 and anti-gp64 antibodies were used to detect YHV envelope protein gp116 and gp64, respectively. The result showed that GST-TSN bound to His-Lamr whereas TSN-Lamr complex cannot bound with gp116 or gp64 (Fig. 4). In addition, gp116 and gp64 have no direct interaction with GST-TSN. In contrast, none of these fusion proteins; His-Lamr, gp116 and gp64 was found to form a complex with GST protein alone. The result of *in vitro* pull-down assays revealed that the interaction between GST-TSN and His- Lamr cannot form a complex with YHV envelope protein gp116.

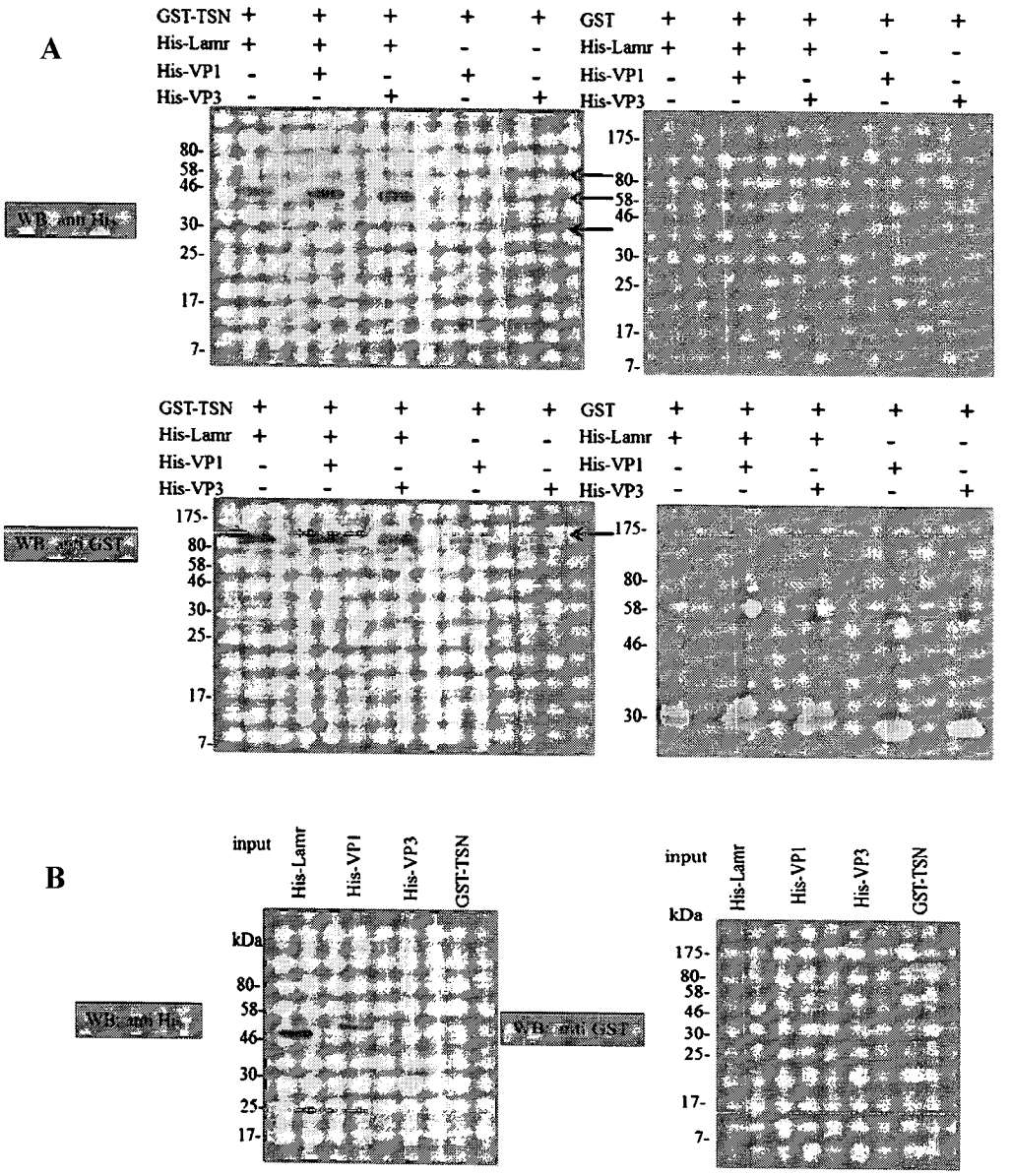

Fig. 2 Mapping of the PmTSN-Lamr-VP1 interaction by *in vitro* pull down assay

(A) Western blot analysis of *in vitro* pull-down assay using anti-His antibody to detect His-Lamr, -VP1 and -VP3 and anti-GST antibody to detect GST-TSN. GST-TSN was immobilized on Glutathione-agarose beads and subsequently mixed with bacterial cells lysate containing His-Lamr, followed by cell lysate containing His-VP1 or -VP3. The protein complexes were analyzed by using western blot. (B) The input of the bacterial lysate containing His-lamr, -VP1, -VP3. (+) and (-) represent the presence and absence of the added components.

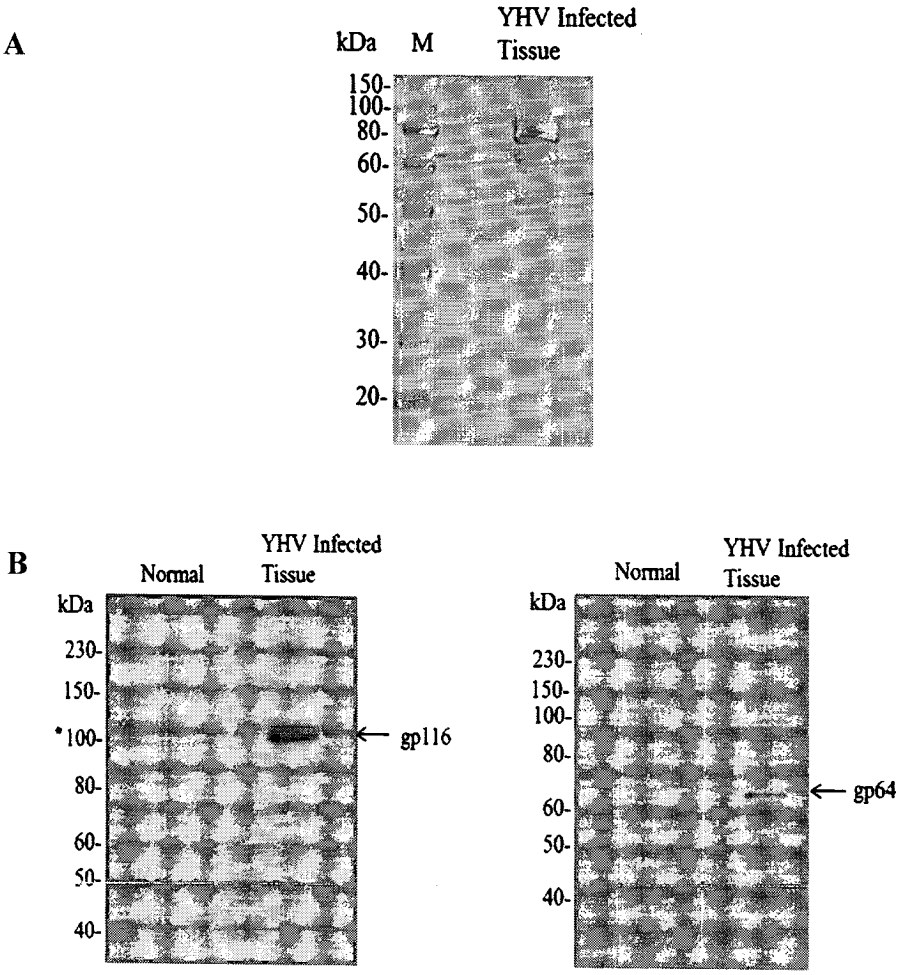

Fig. 3 SDS-PAGE and western blot analysis of YHV infected tissue

(A) YHV lysate was extracted from YHV infected shrimp tissue and analyzed on 12% SDS-PAGE. (B) Western blot analysis of using anti gp-116 (left panel) and anti- gp64 antibodies to detect gp116 and gp64 of the YHV infected tissue.

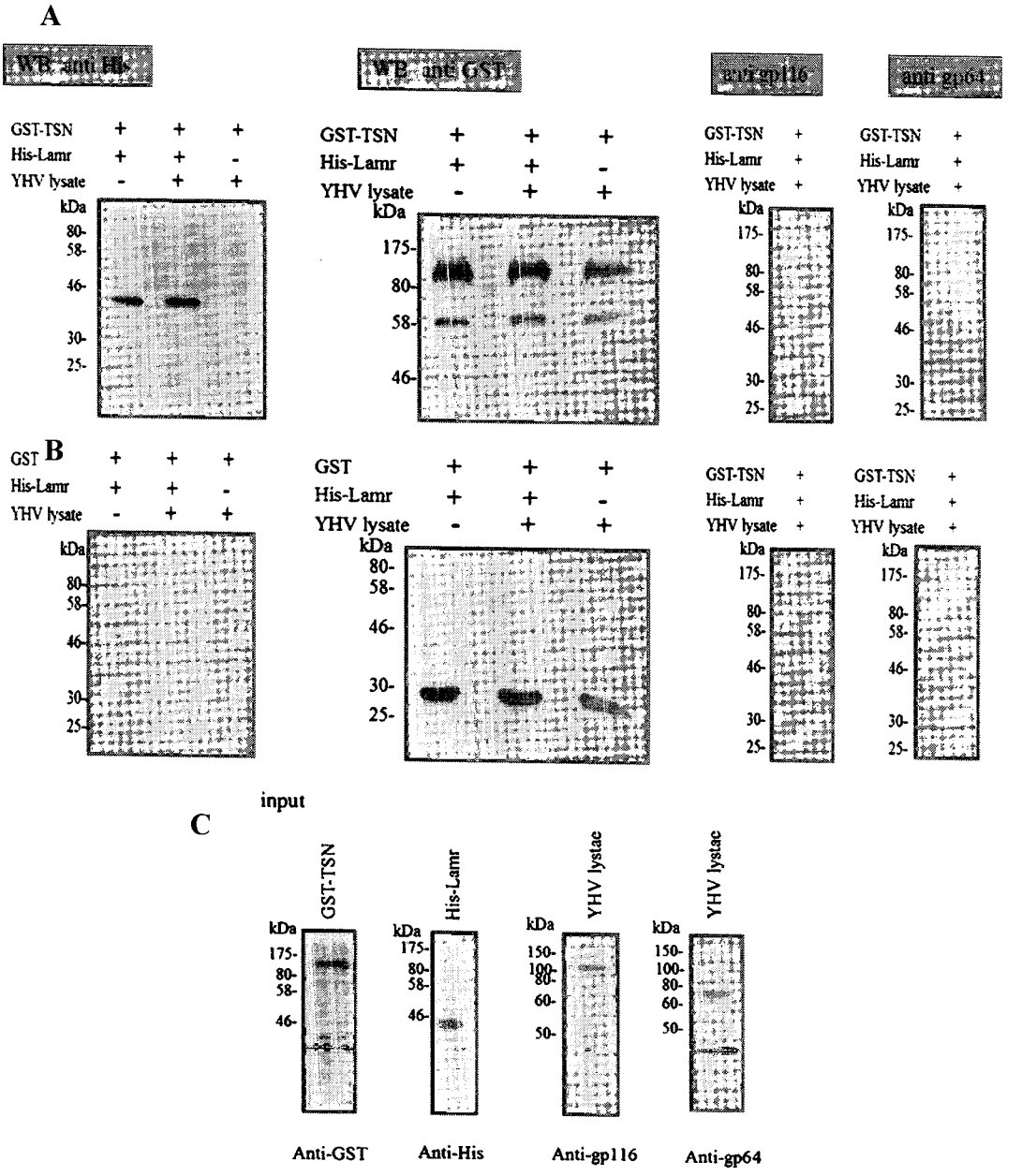

Fig. 4 Mapping of the PmTSN-Lamr-gp116 interaction by *in vitro* pull down assay

(A) Western blot analysis of *in vitro* pull-down assay using anti-His antibody to detect His-Lamr, anti-GST antibody to detect GST-TSN, anti gp116 and gp64 to detect viral protein gp116 and gp64. GST-TSN was immobilized on Glutathione-agarose beads and subsequently mixed with bacterial cell lysate containing His-Lamr, followed by YHV lysate. The protein complexes were analyzed by using western blot (B). The protein GST was used as a negative control showing no direct interaction with His-Lamr and YHV lysate. (C) The input of the bacterial lysate containing His-Lamr, -VP1, -VP3. (+) and (-) represent the presence and absence of the added components.

Discussion

Tudor staphylococcal nuclease (TSN) is a multifunctional protein involved in many biological processes. In order to study the function of PmTSN, TSN-interacting proteins were identified by yeast-two-hybrid (Y2H) screening with hemocyte cDNA library from WSSV-infected *P. monodon*. Y2H screening demonstrated that PmTSN interacted with laminin receptor (Lamr, also known as 40S ribosomal protein SA), histone H2A, and four other unknown proteins. Lamr is a protein which functions as a cell surface receptor of laminin, and involved in cell adhesion, cell migration, and signal transduction [1]. Lamr also serves as a cell surface receptor for prion and several viruses, such as Sindbis virus, Venezuelan equine encephalitis virus, and Dengue virus [2-5]. Besides functions as a cell surface receptor, Lamr acts as an integral component of 40S ribosomal subunit which required for 20S rRNA processing [6]. In shrimp, Lamr also acts as a cell surface receptor for shrimp viruses, including TSV, YHV, and infectious myonecrosis virus (IMNV) [7-9]. It was also found that PmTSN interacted with histone H2A. Similarly, screening of *Plasmodium falciparum* cDNA library by bacterial two-hybrid assay demonstrated that histone H2A is one of the PfTudor-SN interacting proteins [9], suggesting that the interaction between TSN and histone H2A is evolutionarily conserved. The interaction between PmTSN and histone H2A may be involved in the regulation of chromatin structure via post-translational modification of histone H2A. The involvement of TSN in histone modification was elucidated by Valineva et al. (2005). Recruitment of the histone acetyltransferase, CBP/p300 to STAT6 promoter by TSN resulted in the activation of the transcription of *Igε* [10].

By using an *in vitro* pull down assay, it was found that PmTSN specifically interacted with Lamr whereas TSN-Lamr complex cannot interact with VP1 of TSV. In addition, PmTSN was not directly interacted with VP1. According to the study of Y2H and *in vitro* pull down assay of TSV binding protein by Senapin et al (2006) [8], the result confirmed that Lamr was interacted with VP1. The VP1 and Lamr clones in this study were obtained from their lab. Eventhough, the *in vitro* pull down reaction containing TSN and Lamr, the complex of TSN-Lamr-VP1 was not observed in this study. This is indicated that the interaction of PmTSN and Lamr may not involve in the TSV infection although Lamr was reported as a binding protein of viral capsid protein VP1 of TSV.

The interaction of PmTSN and laminin receptor during YHV infection was studied by an *in vitro* pull down assay. However, the interaction of PmTSN and PmLamr has no direct interaction with YHV envelope protein gp64 or gp116. In addition, no direct interaction of PmTSN and gp116 or gp64. Previous study of shrimp laminin receptor showed that Lamr interacted with YHV envelope protein gp116 [7]. Taken together, the results revealed that the interaction of PmTSN and Lamr may not involve in the YHV infection although Lamr has been reported to interact with gp116 of YHV.

In both experiments, the order to add each protein in the interaction mixture of an *in vitro* pull down assay had no effect in forming the binding complex. These results confirmed that the interaction of PmTSN and Lamr cannot form the viral protein complex with capsid protein VP1 of TSV and gp116 of YHV. The results suggested that the interaction of PmTSN and Lamr was not involved in viral infection and may function in other biological processes.

References

[1] Nelson J, McFerran NV, Pivato G, Chambers E, Doherty C, Steele D, et al. The 67 kDa laminin receptor: structure, function and role in disease. Biosci Rep. 2008;28(1):33-48.

[2] Wang KS, Kuhn RJ, Strauss EG, Ou S, Strauss JH. High-affinity laminin receptor is a receptor for Sindbis virus in mammalian cells. J Virol. 1992;66(8):4992-5001.

[3] Ludwig GV, Kondig JP, Smith JF. A putative receptor for Venezuelan equine encephalitis virus from mosquito cells. J Virol. 1996;70(8):5592-9.

[4] Gauczynski S, Peyrin JM, Haik S, Leucht C, Hundt C, Rieger R, et al. The 37-kDa/67-kDa laminin receptor acts as the cell-surface receptor for the cellular prion protein. EMBO J. 2001;20(21):5863-75.

[5] Tio PH, Jong WW, Cardosa MJ. Two dimensional VOPBA reveals laminin receptor (LAMR1) interaction with dengue virus serotypes 1, 2 and 3. Virol J. 2005;2:25.

[6] Ford CL, Randal-Whitis L, Ellis SR. Yeast proteins related to the p40/laminin receptor precursor are required for 20S ribosomal RNA processing and the maturation of 40S ribosomal subunits. Cancer Res. 1999;59(3):704-10.

[7] Busayarat N, Senapin S, Tonganunt M, Phiwsaiya K, Meemetta W, Unajak S, et al. Shrimp laminin receptor binds with capsid proteins of two additional shrimp RNA viruses YHV and IMNV. Fish Shellfish Immunol. 2011;31(1):66-72.

[8] Senapin S, Phongdara A. Binding of shrimp cellular proteins to Taura syndrome viral capsid proteins VP1, VP2 and VP3. Virus Res. 2006;122(1-2):69-77.

[9] Hossain MJ, Korde R, Singh PK, Kanodia S, Ranjan R, Ram G, et al. *Plasmodium falciparum* Tudor staphylococcal nuclease interacting proteins suggest its role in nuclear as well as splicing processes. Gene. 2010;468(1-2):48-57.

[10] Valineva T, Yang J, Palovuori R, Silvennoinen O. The transcriptional co-activator protein p100 recruits histone acetyltransferase activity to STAT6 and mediates interaction between the CREB-binding protein and STAT6. J Biol Chem. 2005;280(15):14989-96.

Part V: Molecular cloning and characterization of *Penaeus monodon* Argonaute-3

Please see the attached paper.

ผลงานวิจัยที่ได้

ผลงานวิจัยที่ตีพิมพ์ในวารสารวิชาการระดับนานาชาติ

1. Phetrungnapa, A., Ho T., Udomkit A., Panyim, S. **Ongvarrasopone, C.** (2013) Molecular cloning and functional characterization of Argonaute-3 gene from *Penaeus monodon*. Fish & Shellfish Immunol. 35(3);874-882.

2. Phetrungnapa, A., Panyim, S. **Ongvarrasopone, C.** (2013) *Penaeus monodon* Tudor staphylococcal nuclease preferentially interacts with N-terminal domain of Argonaute-1. Fish & Shellfish Immunol. 34;875-884.

3. Phetrungnapa, A., Panyim, S. **Ongvarrasopone, C.** (2011) A tudor staphylococcal nuclease from *Penaeusmonodon*: cDNA cloning and its involvement in RNA interference. Fish & Shellfish Immunol. 31:373-380.

กิจกรรมอื่น ๆที่เกี่ยวข้อง

การนำเสนอผลงานวิจัยในที่ประชุมวิชาการ

1. Phetrungnapha, A., Panyim, S.,and **Ongvarrasopone, C.** Suppression of tudor staphylococcal nuclease gene of *Penaeus monodon* through dsRNA targeting SN-like domain. The 36th Congress on Science and Technology of Thailand: "Toward a Better Society through Science and Technology" 26-28 October 2010 Bitec, Bangna (Proceeding, poster presentation).

2. Patpol, P., Panyim, S., and **Ongvarrasopone, C.** Expression of *Penaeus monodon* tudor staphylococcal nuclease protein for polyclonal antibody production. Proceeding of The 39th Congress on Science and Technology of Thailand: "Innovative Science for a Better Life" 21-23 October 2013 Bitec, Bangna p641-643 (Proceeding, poster presentation).

ผลงานอื่น ๆ

1. ผลิตนักศึกษาปริญญาเอก หลักสูตรวิทยาศาสตรดุษฎีบัณฑิต สาขาอณูพันธุศาสตร์และพันธุวิศวกรรมศาสตร์ นายอำนาจ เพชรรุ่งนภา (5137141 MBMG/D) วิทยานิพนธ์เรื่อง Tudor staphyloccal nuclease and its functions in penaeid shrimp RNAi pathway (บทบาทหน้าที่ของโปรตีนทูดอร์สแตฟฟิโลคอกคอลนิวคลีเอสในกระบวนการอาร์เอ็นเอไอของกุ้งพีเนียด) สำเร็จการศึกษาเมื่อ 25 เมษายน 2556

2. ผลิตนักศึกษาปริญญาโท หลักสูตรวิทยาศาสตรมหาบัณฑิต สาขาพันธุศาสตร์ระดับโมเลกุลและพันธุวิศวกรรมศาสตร์ นางสาว พริมรตา แพทย์ผล (5436475 MBMG/M) วิทยานิพนธ์เรื่อง Functional roles of the interaction between PmTSN and laminin receptor

(บทบาทหน้าที่การปฏิสัมพันธ์ของโปรตีนทูดอร์สแตฟฟิโลคอกคอลนิวคลีเอสและตัวรับของลามินิน) สำเร็จการศึกษาเมื่อ 22 เมษายน 2557

การเชื่อมโยงกับต่างประเทศ

งานวิจัยทางด้าน Microarray ได้ทำงานวิจัยร่วมกับ Prof. Ikuo Hirono ที่ Laboratory of Genome Science, Tokyo University of Marine Science and Technology, Tokyo Japan,